Frequency regulation for power systems with renewable energy sources

Regulación en frecuencia para sistemas de potencia con fuentes renovables de energía

Julián Alberto Patiño Murillo

Universidad Nacional de Colombia
Facultad de Ingeniería y Arquitectura, Departmento de Ingeniería Eléctrica
Manizales, Colombia
2018

Frequency regulation for power systems with renewable energy sources

Regulación en frecuencia para sistemas de potencia con fuentes renovables de energía

Julián Alberto Patiño Murillo

Tesis o trabajo de grado presentada(o) como requisito parcial para optar al título de:
Doctor en Ingeniería - Automática

Director(a):
Ph.D., Prof., Ing. Jairo José Espinosa Oviedo

Línea de Investigación:
Modelamiento, Simulación y Control de Sistemas Dinámicos
Grupo de Investigación:
Grupo de Automática de la Universidad Nacional - GAUNAL

Universidad Nacional de Colombia
Facultad de Ingeniería y Arquitectura, Departmento de Ingeniería Eléctrica
Manizales, Colombia
2018

Dedicatory

To my beloved ones, my Mother Aracelly and my Brother Alejo, because they are the strength that makes me get up every day and their support is always there for me...

To my Granny Consuelo, who taught me to have faith and to know that good things happens when you believe...and by extension to all the Murillo's ...

And to Paula...you inspire me to be better, babe, please keep letting my soul come to you!

Dedicatoria

A mis seres más queridos, mi Madre Aracelly y mi hermano Alejo, porque ellos son la fuerza que me hace levantarme cada día y su apoyo siempre está disponible para mí...

A mi mamita Consuelo, quien me enseñó a tener fe y a saber que cosas buenas pasan cuando creemos...y por extensión a toda la familia Murillo Otálvaro...

Y a Paula...tu me inspiras a ser mejor cada día, linda, sigue permitiendo que mi alma llegue a ti!

Acknowledgements

I could have written a thesis composed solely of thanks for so many lessons learned... however, space is short, and though being brief it's not my strongest suit, here I go. Thanks to:

First, to Professor Jairo Espinosa for the confidence and patience to letting me to develop the required skills at my own pace. He has always believed in me, sometimes more than myself, and he has taught me to trust my abilities to exercise my research and teaching vocation.

To Colciencias, for funding this work through the call "528 - Convocatoria Nacional para Estudios de Doctorados en Colombia año 2011", allowing my doctoral training at Universidad Nacional, my alma mater, and my second home.

To my "brothers in arms": Alejo, Pablo, José David, Felipe, and Jarol. We shared a world full of coffee, laughter, beer, soccer, rumba, and academics. I am proud to consider myself their friend, and I hope that the feeling is reciprocal. Also, I can not help but especially thank José David, who between hours of football and in his role as Professor José David López of Universidad de Antioquia, disinterestedly played a crucial role in the methodological structuring and elaboration of this document.

To the members of the GAUNAL group: César, Richard, Semaria, Roviro, Pipe Happy, Magda, Anna, and those that I'm not naming in my (long!) trajectory in the group, for all the memories. To my colleagues at Delft University: Graziana, Tomás, Farid and Roviro himself, for helping me to see the world with different eyes.

To my people at I. U. Pascual Bravo, where more than co-workers I found friends who have made me feel part of a family, even without being working there. To the Tecnoparque team, who "suffered"the final stretch of this process. To my undergraduate friends in Control Engineering, another of those families that life gave me. Special mention for Saudith and her husband Pablo, who opened the doors of their home and made more pleasant the greatest adventure of my life.

To my big family, my biggest fans, who are always there to support me no matter what. To my mother and my brother, whom I hope to make proud with every step I take.

Finally, to Paula, *for giving me the desire, size and measure, healing the wounds that time gave me, for giving my hours reasons for life* and, above all, *for letting our love grow.*

Thank you!

Agradecimientos

Me he pasado tanto tiempo en el doctorado, que siento que podrÃa haber escrito una tesis compuesta única y exclusivamente de agradecimientos por tantas experiencias y aprendizajes vividos en este proceso...sin embargo, el espacio es corto y haré un esfuerzo por ser breve, característica que no suele ser mi fuerte, pero aquí voy. Agradezco a:

En primer lugar, al profesor Jairo Espinosa por la confianza y la paciencia para permitirme desarrollar las competencias requeridas a mi propio ritmo; siempre ha creído en mí, a veces más que yo mismo, y me ha enseñado a confiar en mis habilidades para ejercer la vocación investigadora y docente.

A Colciencias, por financiar este trabajo a través de la convocatoria "528 - Convocatoria Nacional para Estudios de Doctorados en Colombia año 2011", permitiendo mi formación doctoral en la Universidad Nacional, mi alma mater, y mi segundo hogar.

A mis "hermanos de armas": Alejo, Pablo, José David, Felipe, y Jarol. Compartimos aventuras, desventuras y un mundo de vivencias de tinto, risas, cerveza, fútbol, rumba y academia. Estoy orgulloso de poder considerarme su amigo, y espero que el sentimiento sea recíproco. Además, no puedo dejar de agradecer especialmente a José David, quien entre horas de fútbol americano y en su rol como el profesor José David López de la Universidad de Antioquia, de manera desinteresada jugó un papel fundamental en la estructuración metodológica y la elaboración del hilo conductor en las fases finales de este documento.

Al resto de los integrantes del grupo GAUNAL: César, Richard, Semaria, Roviro, Pipe Happy, Magda, Anna, y aquellos que se me escapa nombrar en mi (larga) trayectoria en el grupo, por las conversaciones y las historias compartidas. A mis compañeros en la Universidad de Delft: Graziana, Tomás, Farid y el mismo Roviro, por ayudarme a ver el mundo con otros ojos.

A mi gente de la Institución Universitaria Pascual Bravo, donde más que compañeros de trabajo encontré amigos que me han hecho sentir parte de una familia, aún sin estar directamente allí. Al equipo de Tecnoparque, quienes *padecieron* conmigo la recta final de este proceso. A mis compañeros de pregrado de Ingeniería de Control, otra de esas familias que me ha dado la vida. Mención especial para Saudith y su esposo Pablo, quienes me abrieron las puertas de su hogar e hicieron más grata la mayor aventura de mi vida.

A mi gran familia, mi mejor hinchada, quienes siempre están ahí para apoyarme y sostenerme sin importar nada más.

A mi madre y a mi hermano, mis motores, y a quienes espero llenar de orgullo con cada paso que doy.

Por último, a Paula, *por darme las ganas, tamaño y medida, sanar las heridas que el tiempo me dio, por darle a mis horas razones de vida* y, sobre todo, *por dejar crecer el amor.*

Gracias!

Resumen

Tanto la creciente penetración de fuentes renovables de energía como su participacón en el despacho de suministro energético en el sistema de potencia requiere un análisis completo del comportamiento dinámico de la estructura de regulación de frecuencia. En este sentido, esta tesis presenta el uso de las Funciones de Sensibilidad de Control para describir las caracteríticas dinámicas de los lazos primario y secundario de regulación de frecuencia en sistemas de potencia, utilizando diagramas de Bode como herramienta de visualización y análisis. Estas funciones de sensibilidad se aplican en el estudio del comportamiento dinámico de la regulación en frecuencia con contribuciones de turbinas eólicas a través de las técnicas de emulación inercial. Bajo este escenario, los efectos de las incertidumbres o variaciones en la inercia son estudiados desde la integración de las turbinas eólicas en la estructura de control. Partiendo de una representacón lineal del sistema, se proponen las formulaciones matemáticas necesarias para analizar la sensibilidad y la estabilidad del sistema con respecto a los cambios en la inercia. Estas expresiones se verifican a través de simulación de varios casos bajo diferentes condiciones de estabilidad y perturbaciones en la velocidad del viento y en la carga del sistema.

Palabras clave: Fuentes Renovables de Energía, Control de Frecuencia, Análisis Dinámico, Funciones de Sensibilidad, Inercia, Turbinas eólicas.

Abstract

Both the increasing penetration of renewable sources and their participation in the production of power in the electrical system require a more comprehensive analysis of the dynamic behavior of the grid frequency regulation structure. In this sense, this work presents the use of Control Sensitivity Functions to describe the dynamical characteristics of both primary and secondary control loops in frequency regulation. Bode plots are employed as a visualization and analysis tool. These sensitivity functions are applied to study the behavior of the power system with the contribution of wind turbines through the inertia emulation techniques. In this regard, the effects of inertia variations in frequency control are addressed for power systems under the integration of wind units. The transfer functions of the system are obtained starting from a linearized wind turbine model. The mathematical relationships are formulated to analyze the sensitivity and stability regarding inertia coefficient H. These expressions are then verified through simulation of several cases under different stability conditions and disturbances in wind speed and load.

Keywords: Renewable Energy Sources, Frequency Regulation, Dynamic Analysis, Sensitivity Functions, Inertia, Wind Turbines

List of Acronyms

Abbreviation	Term
AC	AlternativeCurrent
ACE	Area Control Error
AGC	Automatic Generation Control
APF	Area Participation Factors
AVR	Automatic Voltage Regulators
DC	Direct Current
$DFIG$	Doubly-Fed Induction Generator
ECS	Energy Storage Systems
ESS	Energy Storage Systems
GSC	Generator Side Converter
LFC	Load Frequency Control
LQR	Linear Quadratic Regulator
$MISO$	Multiple Input Single Output
PI	Proportional Integral
PID	Proportional Integral Derivative
PFC	Primary Frequency Control
PV	Photo-Voltaic
RES	Renewable Energy Sources
$ROCOF$	Rate Of Change Of Frequency
RSC	Rotor Side Converter
SFC	Secondary Frequency Control
SFR	System Frequency Response
$SISO$	Single-Input Single-Output
$SMES$	Superconducting Magnetic Energy Storage
$VSWT$	Variable-Speed Wind Turbines
$VSWTG$	Variable-Speed Wind Turbines Generators
$WSCC$	Western System Coordination Council
WT	Wind Turbine
WTG	Wind Turbine Generators

Contents

List of Figures

List of Tables

1 Introduction

The generation of electrical energy from non-traditional Renewable Energy Sources (RES) is increasing worldwide, both in the number of units installed and in the levels of production [66, 71]. Discussions on how to measure penetration and the appropriate characterization of the generation quota corresponding to RES are still open questions [66, 1, 16]. However, different reports suggest that the participation of this type of units (mainly wind turbines) can represent more than half of the production of electricity in some regions [19]. Although the installed capacity of electric power generation from solar energy is still not as high as that of wind energy, its usage is also increasing worldwide. Factors such as cost reduction and advances in several solar generation projects (especially from photovoltaic panels) raise the possibility for solar energy reaching a significant level of penetration in a not too distant future.

The generation of electrical energy from solar and wind sources presents a wide variety of new challenges, as they become a significant fraction of the set of power generation systems. Large traditional synchronous generators powered by steam, water or gas turbines have traditionally dominated the production of electricity worldwide, and in many aspects, their characteristics have implicitly dictated the development of philosophies for active power and frequency regulation schemes in power systems in general. Based on such conventional control methodologies, the impact of the potentially different characteristics of new energy production technologies based on non-traditional RES must be considered. The determination of these impacts can help to know to what extent the current practices correspond to the actual control needs of the electrical network, or if they are the exclusive response to the practical implementation of a specific technology and classic actuators such as the units of conventional generation. In general, a desirable aspect is the characterization of control objectives independently of the type of technology to be used, to determine whether such goals can be met from non-traditional renewable generation, or to what level of compliance they can arrive. For this, it is necessary to establish metrics from which to determine the performance of the control, and then consider the specific capabilities of the different actuators of the system to achieve the desired response.

From the control systems theory, the increase in the penetration of non-traditional renewable generation can be seen as the integration of a new class of actuators within the power system.

In the same way, the development of new measurement and monitoring systems in the power network, under the Smart Grid paradigm, can be seen as the availability of more information and data about the system. Despite some difficulties related to the necessary communication infrastructure (latency, reliability, security and the cost of transmission systems, among others), the abundance of data makes the alternative of using multivariate control schemes, and with shared information among themselves, an increasingly viable strategy for power systems.

Although significant advances have been made in the literature on these questions, many of the existing approaches to the application of control technologies for power systems are somewhat outdated. Specifically for the regulation of grid frequency and active power, most of the strategies discard the possible contribution of unconventional renewable generation or force the new units to behave in a similar way to traditional systems as much as possible. While it is fair to recognize that these types of proposals are framed within the context of existing technical and regulatory standards, it is a widely explored philosophy in the literature. For example, in the case of wind turbines, many works consider additional control loops for replicating the inertial characteristics that are inherent to the physical conditions of traditional synchronous machines [53, 52, 15, 21]. In this sense, the use of dynamic systems analysis tools applied to the frequency control system of the power network represents a valuable contribution to the integration of RES. A dynamic analysis could lead to the development of strategies and alternatives allowing the necessary control action on the part of the time more significant non-conventional renewable generation so that the objectives of stable and secure operation of the grid are maintained, taking advantage of the characteristics of these new elements in the system.

1.1. State of the Art

Below is a brief review of the literature on the proposed studies in for grid frequency control with renewable sources. The review has centered about wind and photovoltaic generation systems. Currently, those are the non-conventional renewable sources with more significant development and penetration.

1.1.1. Inertial response with RES

Since the inertia of the synchronous machines is the first parameter of opposition to the fluctuations of the frequency of the power system, it has been sought that the renewable generation units emulate, in some way, the role of the same in their generation systems.

For photovoltaic units, this means operating below the maximum power extraction and maintaining a "virtual inertia"from the active power reserve [11].

Wind turbine systems of variable speed capabilities such as those of doubly-fed induction generators (DFIG), use electronic converters to achieve an effective decoupling between the generator rotor and the rotor of the blades. In consequence, the natural inertia of the turbine blades cannot be used, decreasing the capacity of these kind of turbines for providing active frequency contributions during a generation loss event. It has been shown that the inertial response can be emulated for turbines of type DFIG through secondary control [19, 38, 94]. Also, the work in [53] demonstrated that the inertial response of this type of units is highly conditioned by the bandwidth of the rotor current controller. Despite these developments, the increasing penetration of renewable sources with electronic network decoupling, and the subsequent reduction of conventional generation leads to a diminution of the physical inertia available in the network.

Conversely, a gearbox is coupling the generator and the wind turbine rotor for fixed-speed systems. This configuration allows the provision of some rotational inertia to the grid, using the kinetic energy stored in the turbine blades [6]. The work in [53] suggests that an adequate mix of variable and fixed speed wind turbines could be helpful for the frequency and voltage of the power system.

1.1.2. Primary Control with RES

The impacts of wind generation and other renewable sources on the development and operation of electrical systems of several countries have been reported. Studies have discussed the cases of the United Kingdom [86], Belgium [45] and Ireland [57]. The impacts of the components of the wind generation systems and their variations in the frequency control of the power systems were reported in [43, 5]. The effects on frequency regulation occur mainly in a temporary space ranging from seconds to a few minutes; therefore, an adequate definition of the timescales is essential when comparing the different studies carried out on the integration of wind generation [19].

The latest generation of wind turbines with high capacity and variable speed and more inertia can reduce power variations in the wind farms; such fluctuations cause deviations in the nominal frequency of the system [21, 63]. In [52], a system for storing kinetic energy (through the blades and the inertia of the machine) is described to contribute to the control of primary frequency, through inertial emulation. The capacity to contribute to the production of active power for a short time by wind farms has been discussed in [89]. For contributions to primary control for longer times, several techniques such as the combination of wind

units along with fuel cells [85] and other energy storage systems such as flywheels [18] were proposed. The use of fuzzy-based supervisors for wind turbines was explored to ensure the availability of an initial energy reserve, even for operation under nominal speed [50]. This supervisor kept a primary reserve and simultaneously controlled turbine angle of attack and generator torque.

Some studies have used dynamic analysis tools looking to determine the effects of wind generation on the grid frequency regulation. In [46], Bode diagrams are used to approximate a system transfer function and quantify the amount of wind power fluctuations that can be supported for maximum frequency deviation, in a system composed of conventional thermal generators. The dynamic impacts of wind generation on primary regulation was explored in [74] using modal analysis, demonstrating that wind turbines excite the electromechanical modes of the power system.

Several works explored the integration of Energy Storage Systems (ESS) or Energy Capacitor Systems (ECS) with the wind and photo-voltaic generation units to reduce their effects in power system frequency [54, 28, 56, 15, 82, 78]. In [44], a filtering algorithm for wind power based on the combination of batteries is presented. Furthermore, research community also studied other energy storage techniques such as double layer capacitors[54, 56], magnetic superconductors (SMES, Superconducting Magnetic Energy Storage) [82] and energy saving systems [28, 15, 78].

1.1.3. Secondary Control with RES

Several studies have analyzed the impact of renewable energy sources on the operation of the energy market and secondary frequency control [16, 43, 15, 82, 75, 17]. References [19, 84] discuss initiatives to determine the interaction of wind generation in the energy market and its role in the resource portfolio, offering auxiliary services such as frequency regulation and reserve balance. According to these results, each variation in wind power production should not be compensated by corresponding variations of different value from other generation units. Also, the standards for frequency regulation must be intended for the aggregate model of the system instead of each individual unit.

Many works studied the effects of the fluctuation of renewable energies in the structure of frequency control [43, 44, 54, 15]. An AGC scheme for variable speed turbines was presented using supervisory and a machine level control [73]. The requirements and necessary conditions to develop power system performance studies for large-scale wind participation were analyzed with real data [48]. The effects of wind generation on transferred power between areas, manifested in the form of low-frequency electromechanical oscillations, are analyzed in [35,

20]. An AGC scheme in the presence of distributed generation for intelligent networks is shown in [39], to attenuate the deviation in power flows exchanged between areas due to renewable sources.

Regarding the power reserve for frequency regulation with renewable energy, several studies have been carried out. Since the compensation of the effects of the additional power variations in the system reduces the operational availability of conventional units, the increasing penetration of renewable sources will reduce the reserves for frequency support tasks. Several approaches have been proposed to overcome this problem. Demand-based control structures have been studied to support frequency control when the conventional reserve is not enough or is not available [2]. Some characteristics of smart grids, such as demand management, have also been explored to determine the load system characteristics most affected by renewable energies [14].

The influence of photovoltaic systems (PV) on frequency control is discussed in [11], as a complement to the inertial response of conventional units. The use of batteries for the control and maintenance of the quality of the power in the presence of distributed generation and solar units is analyzed in [12]. The response of batteries in frequency control tasks can be up to 10 times greater than fossil-based systems. The role of capacitors in combination with photovoltaic panels for frequency support is studied in [37]. Given the variability of power production from RES at every moment, these sources are not considered as the power reserve for grid frequency support tasks. The storage of the kinetic energy from wind turbines consists solely of supporting the secondary regulation during the first seconds of synchronous machines initialization.

Regarding the modeling of the secondary control response, the model in [11] considers the effects of PV installations on the economic and operational aspects of large-scale power systems. The study in [96] proposes modifications to the maximum power extraction algorithms of the photovoltaic panels for contribution to auxiliary tasks such as frequency control. Other works establish that the large time constants of conventional units can filter the rapid variations the individual RES based units [5]. Also, the combination of wind generation with demand variations only adds significant power fluctuations when a determined penetration threshold is surpassed [30]. An adequate dispersion of the wind generation through an extensive geographical area would reduce the variability, increase the predictability of the resource, and decrease the periods of low energy production. Typically, the energy required by the secondary control is determined by the error in the prediction of the wind resource (the difference between the predicted power and the active power generated from the wind) [35]. The fluctuation of the aggregated power of wind is considered as constant for short periods. According to [40], the amount of reserve needed decreases (by almost 50 %) when the entire control area compensates for the variability of renewable units.

1.1.4. Comments on state of the art

In general terms, these systems of inertial emulation seek that renewable sources behave like conventional sources, even in their intrinsic qualities dictated by the physics of their components. More studies are required to determine the validity of these strategies, and their effects on the power system parameters when integrated into frequency regulation.

In this aspect, the strategies proposed to quantify the effects of alternative sources to primary control are focused on maintaining the constant active power contribution despite RES power fluctuations: hence the support with different storage units, and the proposition of some coordination schemes. However, few studies seek to improve the response characteristics of the actuators or the bandwidth of the systems participating in the control. More studies are needed from this point of view.

In secondary control, the research emphasis has been predominantly the management of operational reserves. The compensation of the variation of the renewable sources requires additional efforts from the conventional units, affecting the required active power injections for correcting the frequency deviations and maintain the exchange flows. If the problem is addressed beyond the paradigm of conventional units, solutions arise that can benefit from the action of other elements. These strategies emerge from the same coordination of renewable sources, or even from dispatch actions made possible from the paradigm of smart grids such as demand management. Although there is no single and exclusive solution, the coordinated action of all these different actors may be more effective. This also opens the door to consider another type of controllers for the secondary loop, different from the PI of the classic schemes. Advances in computer systems and the availability of better computing resources open the door to the use of optimal control tools that were considered as unfeasible, and whose validity for frequency regulation tasks deserves to be studied.

1.2. Problem Formulation

Despite the continuous interest in the integration of RES to the electrical power system, and especially for participation in frequency regulation, more efforts are required in the development of effective compensation strategies. Further research is needed in the process of understanding how frequency regulation schemes should be designed so that RES can be integrated, and even another type of distributed generators in an increasingly liberalized and competitive market.

In this sense, both the increasing penetration of renewable sources and their participation in the production of power in the electrical system require a more comprehensive analysis of the

dynamic behavior of the grid frequency regulation structure. In general, the characteristics of the system must be known to ensure reliable operation in maintaining the frequency. For example, the additional variability from renewable sources coupled with the uncertainties of demand prediction and generation availability become critical factors in reserve planning for frequency regulation. The conventional power system operates under the assumption that the frequency control system works correctly, with which the impacts of renewable sources need to be studied in greater detail, and with the help of strategies supported in the analysis of dynamic systems, given their difference with the traditional behavior of the system.

Another aspect to consider lies in the change from the classic operational paradigm of the power system, from a system governed by a few sizable synchronous generation plants to a network with many plants of lower capacity. These changes also imply a change in the traditional concepts of control of a typically centralized scheme towards a more distributed one. These changes require an infrastructure of the new frequency regulation schemes allowing the provision of these services by different resources than the large conventional power plants. In this sense, the development of control schemes taking advantage of the dynamic characteristics of the new types of sources is paramount. At the same time, these new control structures require the interaction with the existing conventional infrastructure to ensure a reliable and effective frequency regulation. The use of dynamic analysis tools and multi-variable control arises as the fundamental way to address those challenges.

In general, it can be said that a frequency regulation scheme under renewable generation penetration must take advantage of the control characteristics of this type of units, as well as the contribution of new technologies and strategies (storage, demand management, among others), instead of emulating the radically different operating conditions of the standard synchronous units. For this, it is essential to know the dynamic characteristics and contribution capabilities of the new elements, to formulate strategies that efficiently take advantage of the bandwidths of the different actuators, and maintain coordination schemes that allow joint operation.

1.3. Objectives

1.3.1. Main objective

To analyze the dynamic characteristics of frequency regulation structure of power systems including renewable energy sources such as wind generation, starting from the knowledge of the dynamic characteristics and action margins of both conventional and non-traditional energy sources.

1.3.2. Specific objectives

- To determine the particular dynamic characteristics of frequency regulation in power systems.
- To determine the effects of renewable generation sources in frequency regulation loops for power systems.
- To propose frequency regulation strategies for power systems taking into account the dynamic characteristics of renewable generation sources.
- To implement a simulation scheme for the performance evaluation of the proposed frequency regulation strategies.

1.4. Thesis Outline

- **Chapter 2**. In this chapter, we briefly present the main theoretical elements used in this thesis. We begin presenting the operation of the Load Frequency Control (LFC) for power systems through the description and representation of its different components. For the timescales of the analysis presented here and the large-scale point of view, the classical model with first-order representations of the power system elements offers enough detail for frequency regulation tasks [42]. A brief explanation of this model is condensed from classical power system analysis books [42, 4, 79], with the notation suggested in [6, 68]. As the emerging Renewable Energy Sources are affecting the traditional control structure widely deployed worldwide, the chapter additionally includes models for representing wind generation systems for frequency regulation tasks. Finally, an illustrative example of the LFC behavior and some introductory analysis are presented.
- **Chapter 3**. Traditional Load Frequency Control schemes constitute a regulation structure extensively applied in power systems. This chapter presents the use of Control Sensitivity Functions to describe the dynamical characteristics of both primary and secondary control loops in frequency regulation. Bode plots are employed as a visualization and analysis tool. Results of frequency-domain analysis illustrate the role of Load Frequency Control and allow determining load disturbance effects on the system output.
- **Chapter 4**. This chapter explores the integration of the renewable sources to LFC. Starting with the consideration of RES units as disturbances to frequency regulation

tasks, the effects on system inertia are highlighted. The expressions from the studied model show the consequences of the reduced inertia in frequency control. The analysis through Control Sensitivity Functions and the time-response of the system has shown the need for some inertia contribution from the RES-based units to maintain the operational conditions of the power system. In this sense, we also study the performance of variable-speed wind turbines integration to the LFC structure of power systems. Using the inertial response emulation methodology, DFIG-WT are included in the primary regulation stage of the LFC.

- **Chapter 5**. This chapter addresses the effects of inertia variations for power system under the integration of wind units. The transfer functions of the system are obtained starting from a linearized wind turbine model. The mathematical relationships are formulated to analyze the sensitivity and stability regarding inertia coefficient H. These expressions are then verified through simulation of several cases under different stability conditions and disturbances in wind speed and load.

- **Chapter 6**. This section presents the main conclusions and contributions from this thesis. At last, some further research directions and recommendations of future work are proposed.

1.5. Main Contributions

From the dynamic analysis of the Load Frequency Regulation structure in Power Systems, the following contributions are shown through this thesis work:

- The application of Control Sensitivity Functions for Frequency-Domain Analysis of Frequency Regulation in Power Systems. These sensitivities arise as useful tools for the assessment of dynamical characteristics of the LFC system through Bode plots.

- The assessment of the impacts of renewable units in frequency regulation systems through both analytic expressions and Bode plots. Wind generation is considered as the RES of interest, given its worldwide growth and implementation in power systems.

- The determination of the effects of RES units in system inertia, under the consideration of these sources as disturbances to frequency regulation. The expressions obtained from dynamic studies show the consequences of the reduced inertia in frequency control. The analysis through Control Sensitivity Functions and the time-response of the system punctuates the need for some form of inertia contribution from the RES-based units to maintain the operational conditions of frequency regulation.

- This work also explores the integration of wind turbines into frequency regulation tasks through inertial emulation techniques. In this regard, the consequences of the inaccurate calculation of the generator inertia coefficient are demonstrated using both the derived analytic expressions and computational simulation studies.

1.6. Publications

The research of this thesis has led directly to two published works in SJR indexed peer-reviewed journals [63, 77]. Besides, the chapter titled "Sensitivity Analysis of Frequency Regulation Parameters in Power Systems with Wind Generation"makes part of the Springer Nature book **Advanced Control and Optimization Paradigms for Wind Energy Systems** [61]. Several parts from this research have been presented in five international conferences with published conference proceedings [91, 31, 76, 62, 60]. Related contributions in the areas of power systems and renewable energy systems have been published in indexed journals [22, 78], non-indexed publications [23, 24] or presented in conferences [92, 47, 64]. Also, a book chapter was published as a co-author [90].

2 Modeling of Frequency Regulation in Power Systems with Renewable Energy

In this Chapter, we briefly present the main theoretical elements used in this thesis. We begin presenting the operation of the Load Frequency Control (LFC) for power systems through the description and representation of its different components. For the timescales of the analysis presented here and the large-scale point of view, the classical model of Figure **2-1** with first-order representations of the power system elements offers enough detail for frequency regulation tasks [42]. A brief explanation of this model is condensed from the classical power system analysis books [42, 4, 79], with the notation suggested in [6, 68]. As the emerging Renewable Energy Sources are affecting the traditional control structure widely deployed worldwide, the chapter additionally includes models for representing wind generation systems for frequency regulation tasks. Finally, an illustrative example of the LFC behavior and some introductory analysis are presented.

2.1. Frequency Regulation in Power Systems

The frequency of an electrical system depends on the balance among active powers. Power from the generation systems ($P_{\text{Generated}}$) is either consumed by loads (P_{Demanded}) or dissipated by transmission losses (P_{Loss}) [42]:

$$P_{\text{Generated}} = P_{\text{Demanded}} + P_{\text{Loss}}. \tag{2-1}$$

In permanent regime, all synchronous generators of an electrical network work in synchronism; that is, the rotation frequency of any of them multiplied by the number of Pole pairs is precisely the electrical system frequency. If there is a variation of active power on demand, this will be reflected in the system frequency. Energy stored in the rotating masses of the turbines and generators will flow towards or from the network in function of the power deficit or surplus. If the contribution of mechanical energy is insufficient, the rotation speed of the

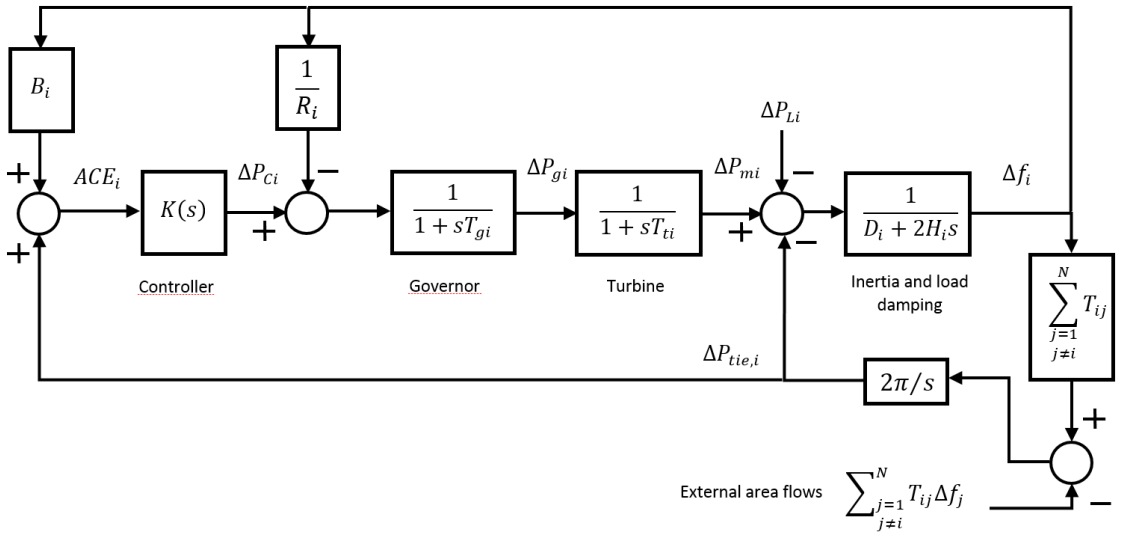

Figure 2-1: Frequency regulation system with one generation unit for a given area i (based on [6]). This system is the subject of study in this thesis and covers the most representative topics of this chapter.(ΔP_L) are load variations, ΔP_{mi} the change in mechanical power of the generator k, ΔP_{gi} the change in the generator power output, ΔP_L the load perturbation, Δf_i the frequency change, D_i the damping coefficient. H_i the equivalent inertia, ΔP_{ci} the control action of the LFC, T_{ij} the power exchange coefficient between area i and area j, $\Delta P_{tie,i}$ the total change in the power exchanged between area i and other areas and Δf_j the change in the frequency of area j connected to area i. Also, B_i denotes the bias factor for modulation of the error signal in secondary regulation, $K_i(s)$ is the transfer function of the secondary controller.

machines (under-frequency) will be reduced, or if the energy input mechanics is higher it will be increased (over-frequency). In consequence, it is necessary to match the differences in active power of the generators to keep the grid frequency in range.

Grid frequency constitutes a global parameter of the interconnected system. In this way, any power mismatch or load disturbance will have effects through the complete system (see figure **2-2**). Frequency regulation structures are in place to achieve the power balance proposed in equation (2-1), commonly referred as Load Frequency Control (LFC). LFC is usually organized at different levels depending on each country. Figure **2-3** shows the operational timescale for the different types of control in frequency regulation structure. Each stage operates in a time frame and involves a set of variables coming from a more or less extended part of the electrical system. The inertial response and the frequency controls associated with the response times shown in Figure **2-3** are described below.

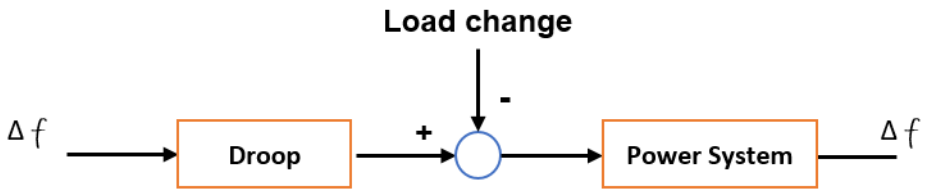

Figure 2-2: The basic representation of incidence of load changes in system frequency.

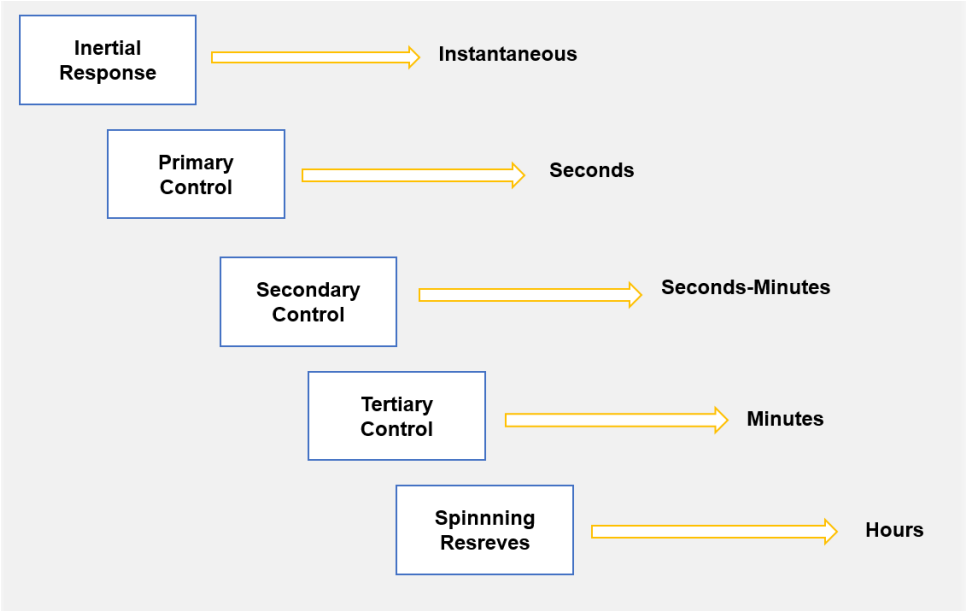

Figure 2-3: Timescale of power system frequency regulation stages [4].

We must highlight that the time constants of the excitation system or the Automatic Voltage Regulators (AVR) in generation units are significantly smaller than those of turbine governors. In consequence, variations in the excitation system are markedly faster than governor response and therefore will not have tangible effects on LFC. Then, voltage regulation loops and frequency control actions can be considered as decoupled phenomena, which is a common practice to study each problem independent from the other [42].

2.1.1. Inertial Response

In conventional generators, the immediate response to changes in the system frequency is to increase or decrease the speed of the rotating masses until the rate of change of the frequency is zero. If the balance proposed in equation (2-1) is altered, the electric frequency changes from its original value. For example, if the active power generated is lower than the active

power demanded plus losses, there will be a drop in the system frequency. During the first few seconds after the imbalance, the lack of energy in the system is compensated from the energy stored in the rotors of the generators to limit the load-generation disequilibrium, leading to a decrease in their speed with the corresponding fall in frequency below the nominal value. After a short period, the Primary Frequency Control (PFC) exerts its action through the controllers of conventional generators, increasing the power output to restore the load-generation balance. The activation of the PFC marks the end of the system's inertial response.

This action is denominated inertial response because the inertia of the power system (calculated as the sum of the individual inertia of each generating unit) is the variable that limits the rate of change of the frequency (ROCOF) of the system during the first seconds. The lower the inertia of the system, the higher the frequency fall due to a disturbance and vice versa. In consequence, a reduction of the system inertia causes steeper frequency falls. Depending on the operating conditions, these drops could lead to critical situations jeopardizing the stability of the system. Inertia reduction could occur due to the replacement of conventional to non-conventional generators. In power systems with low inertia, large frequency deviations could lead to [42] [6]:

- Activation of the low-frequency relays associated with the automatic load disconnection schemes, resulting in a massive disconnection of subsystems with the associated socio-economic consequences entailed.

- Reduction of the PFC performance due to lack of active power reserves. Usually, power reserves are provided by conventional machines with large inertial constants, and high generation. In low inertia systems, power reserves are reduced affecting the recovery capabilities after grid frequency disturbances.

The inertial response of the system is incapable of compensating frequency variations after disturbance events. The inertial response only relates to the depth of the frequency deviation. For this reason, more regulation layers are necessary to restore the frequency to operational values. The next layer is the so-called primary frequency control.

2.1.2. Primary Frequency Control

The primary frequency control (also known as *droop control* is the automatic action performed by the speed governors of the generators to correct instantaneous imbalances between generation and load, thus controlling the variations in the frequency of the system. In case of a power imbalance, the main objective of the PFC is to stabilize the system frequency close to its nominal value. PFC operates in a time range of 2 – 30 s (depending on the type

of generator) after a fault has occurred [80]. This control is directly related to the power reserves automatically activated in the initial seconds after a change in the system frequency (either due to usual demand variations or caused by a contingency). PFC relays on instantaneous contributions of the generator units according to their primary reserve, on the technical characteristics of the stator, and on the dead bands of the speed control systems.

After a disturbance, the generators that remain connected to the network are unable to instantaneously deliver the power deficit existing in the system due to the time constants of the machines involved, which produce delays. In case of over-generation, the excess energy is stored in the form of kinetic energy in the rotor of the generators, accelerating them and therefore increasing the system frequency. After the inertial response, the turbine speed regulators react by performing a proportional control on the gates or valves of the units depending on the type of plant (hydraulic or thermal). With this action the mechanical power increases and therefore the electrical power generated increases. On the other hand, the demand (sensitive to frequency) decreases the consumption at the same rate that the frequency decreases. As this process progresses, the generation equals the demand stabilizing the frequency of the system until reaching a new equilibrium.

Once the process of PFC has been completed, the system manages to reach a balance between the generated and the consumed active power. However, there is still a deviation of the electrical frequency of the system from its nominal value requiring another step in the frequency control. This new layer is the secondary frequency control (SFC), which is detailed below.

2.1.3. Secondary Frequency Control

The main function of the SFC is to compensate the frequency error remaining after the PFC action and to restore the primary reserves. SFC operates in a time interval ranging from seconds to several minutes after a contingency and the corresponding PFC action. The SFC is assigned to a group of units that must be able to perform this regulation. These units must operate under their maximum available power by allocating part of their capacity in reserve. The control action modifies the active power set-points of the units assigned to the SFC within the control area in which the imbalance occurred. The SFC is denominated Automatic Generation Control (AGC) when works in automatic mode. If the SFC is unable to return the frequency to its nominal value, it is necessary to use auxiliary reserve resources or to apply load disconnection procedures (emergency conditions).

The SFC action is commonly triggered by the Area Control Error (ACE). The ACE represents the mismatch between generated and demanded power for a given control area [6].

Other useful components of the SFC are the Area Participation Factors (APF). The APF are parameters regulating the power contribution of secondary control actions from each unit assigned to SFC. Performing as weighting factors, the sum of all participation factors for a given control area must be equal to one [6]. Figure **2-4** shows the power contribution strategy in AGC, starting from the ACE signal and using the area participation factors for the set-points of corresponding generators.

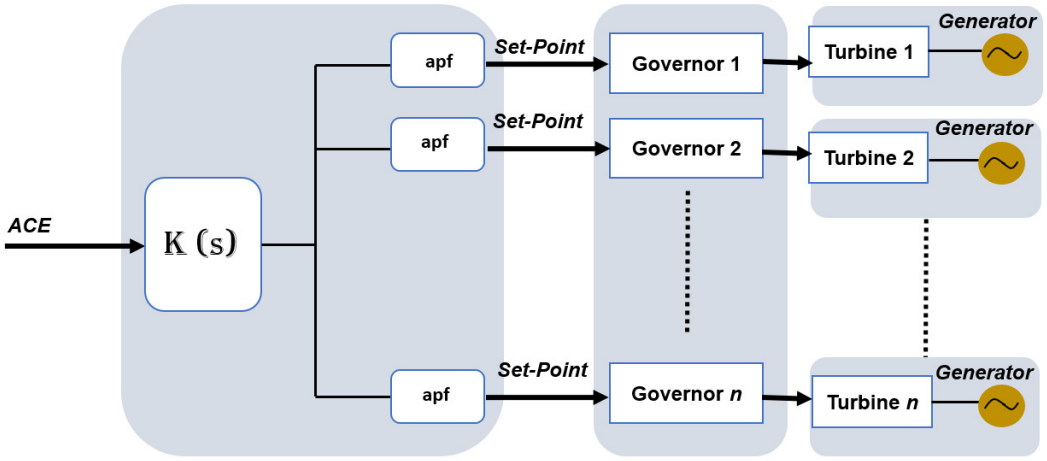

Figure 2-4: Power contributions to AGC from generators assigned to SFC [6]. Participation factors are weighting the control action of secondary regulation.

2.1.4. Additional stages

Tertiary control, another stage consisting of the release of control reserves after a disturbance, is not considered a specific part of the frequency regulation [4]. This is because the use of those control reserves, after a manually activated process, is more related to the energy production process according to the generation scheduling (dispatch). Another superior stage is the Emergency Condition operation and contingency management [6]. These stages are beyond the scope of this work and their action is not being considered in the models.

2.2. Mathematical Model for Dynamic Analysis of LFC

This section introduces the mathematical description of LFC in an interconnected power system. The description begins with the derivation of the swing equation describing the relationship between power balance and frequency in power systems. This also involves the representation of the load-generator dynamics and the modeling of the generation units.

The model is completed with the description of the control actions and the influence of the different interconnected systems in the local control area.

2.2.1. Modeling of Generator-Load dynamics

As frequency in an electric power system is directly related with rotational speed of generation units, frequency regulation can be transformed into a speed control issue for generators. This representation is based on the so-called swing-equation of synchronous generators [42]. The energy stored (W_{ke}^0) in the mechanical components of a generating unit can be expressed as:

$$W_{ke}^0 = H \cdot S_b. \tag{2-2}$$

where H is a constant value denominated as the inertia and S_b is the rated power in [MW]. As kinetic energy changes with the squared value of the fundamental frequency or angular speed, the corresponding variation in energy due to a frequency variation (Δf) can be expressed as [42]:

$$\frac{d}{dt}(W_{ke}) = \frac{2HS_b}{f_0}\frac{d}{dt}(\Delta f). \tag{2-3}$$

with f_0 being the standard operational frequency. Variations in W_{ke} can also be expressed as the difference between generated power ΔP_g and power demanded by load (ΔP_L). In consequence, the equation representing the power balance between generation and load would be:

$$\Delta P_g - \Delta P_L = \frac{2HS_b}{f_0}\frac{d}{dt}(\Delta f) \qquad \Rightarrow \qquad \frac{\Delta P_g}{S_b} - \frac{\Delta P_L}{S_b} = 2H\frac{d}{dt}\left(\frac{\Delta f}{f_0}\right) \tag{2-4}$$

In per unit representation (denoted as $[p.u]$), frequency variation Δf is the same as angular speed variation $\Delta\omega$, so:

$$\Delta P_g[p.u] - \Delta P_L[p.u] = 2H\frac{d}{dt}\Delta\omega. \tag{2-5}$$

When performing a dynamic analysis of frequency stability, generated power is directly related to the frequency [42]. However, the damping effect in equation (2-5) is mostly related with load sensitivity to frequency changes D_f [$p.u$/Hz]. D_f is defined as the sensitivity of the load change when there is a 1 % of frequency variation, expressed as:

$$\frac{\partial P_L}{\partial f} = D_f \Delta f \tag{2-6}$$

Load sensitivity D_f could be expressed in per-unit values as:

$$D[p.u] = D_{\text{unit}}[p.u] = \frac{P_{\text{G,unit}}}{S_{\text{base,unit}}}[p.u] \tag{2-7}$$

$$D_f[p.u] = D_{\text{unit}}[p.u] f_0 \left[\frac{p.u}{\text{Hz}}\right]$$

consequently, the complete swing equation including the damping effects in $[p.u]$ is:

$$\Delta P_g[p.u] - \Delta P_L[p.u] = 2H\frac{d}{dt}\Delta\omega[p.u] + D[p.u]\Delta\omega[p.u] \tag{2-8}$$

Having into account that $\Delta f[p.u] = \Delta\omega[p.u]$ in per-unit modeling, the swing equation can be represented in Laplace domain as:

$$\Delta f(s) = [\Delta P_g(s) - \Delta P_L(s)]\frac{1}{2Hs + D} \tag{2-9}$$

Figure **2-5** presents a block diagram of equation (2-9).

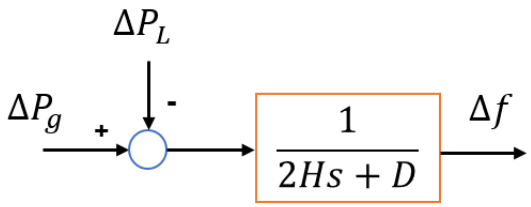

Figure 2-5: Block diagram model for the load and generation relationship in power systems [41].

2.2.2. Modeling of the Governor-Turbine group

Generator power output is regulated through the droop parameter of speed governor (R). There are several proposed models for representing turbine and generator dynamics in LFC analysis and control [3]. But low-order models can be applied after discarding the effects of fast generator dynamics and some slower thermal phenomena. Actually, first-order models could be enough for modeling governor and turbine behavior, as seen en equations (2-10) to (2-12) for thermal units without reheating:

$$\Delta P_g = \Delta P_{ref}\frac{1}{R}\Delta f \tag{2-10}$$

$$\Delta P_v = \frac{1}{1 + T_g s}\Delta P_g \tag{2-11}$$

$$\Delta P_m = \frac{1}{1 + T_t s}\Delta P_v \tag{2-12}$$

here, R is the speed droop, ΔP_g is the governor's input signal, and ΔP_{ref} is the change in power reference set-point. ΔP_v is the change in valve position, and T_g and T_t are generator-turbine time constants [6]. This model can be expanded depending on the system used (with reheat, or hydraulic). Figure **2-6** shows the commonly accepted block diagram descriptions of the governor-turbine group for thermal and hydraulic generation units, with T_{gt} are generator-turbine time constants.

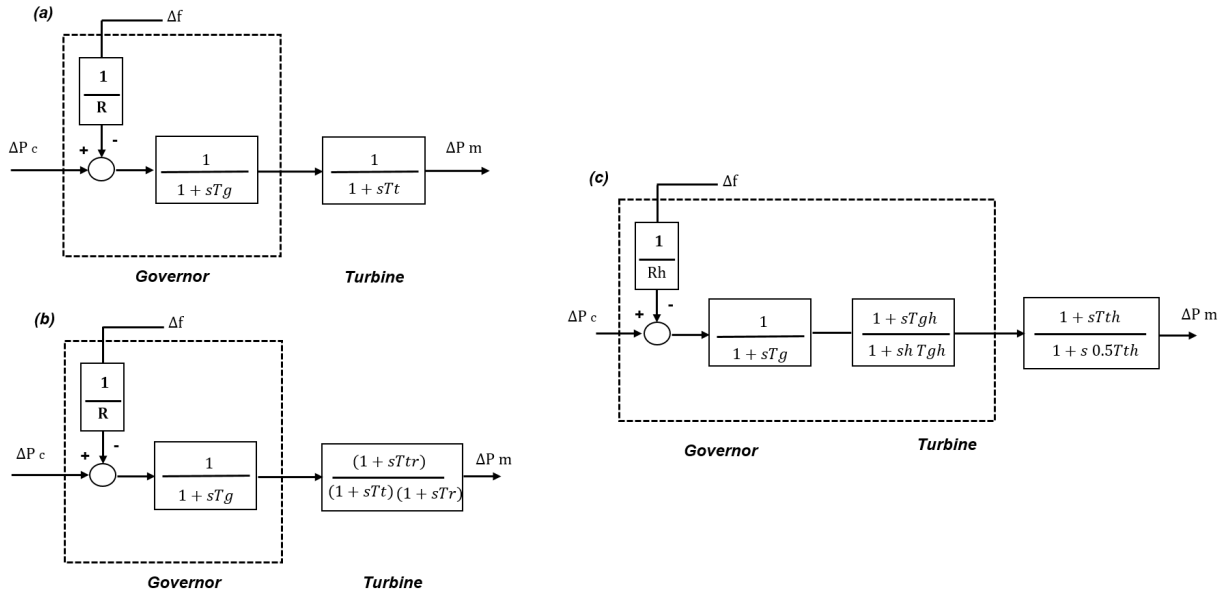

Figure 2-6: Block diagram of turbine-governor system; (a) non-reheat steam unit, (b) reheat steam unit, and (c) hydraulic unit [6].

2.2.3. Modeling of multi-area interconnected systems

Punctual frequency deviations would have effects in the whole system, as the frequency is a parameter of global incidence due to the interconnected nature of the power systems through multiple control areas and tie-line links. In consequence, frequency variations in external control areas and tie-line power deviations should be properly accounted for in the LFC regulation.

The secondary control action is adjusted to correct the frequency disturbance effects using the generation units of the affected area, aiming to minimize the consequences in other areas. However, the practical implementation of AGC strategies based on ACE present some effects on the closer areas under determined contingency conditions [6]. The generalized representation of AGC structure is shown in Figure **2-7**. According to this model, ACE signals will include the tie-line power flows reflecting the effects of the interconnected areas.

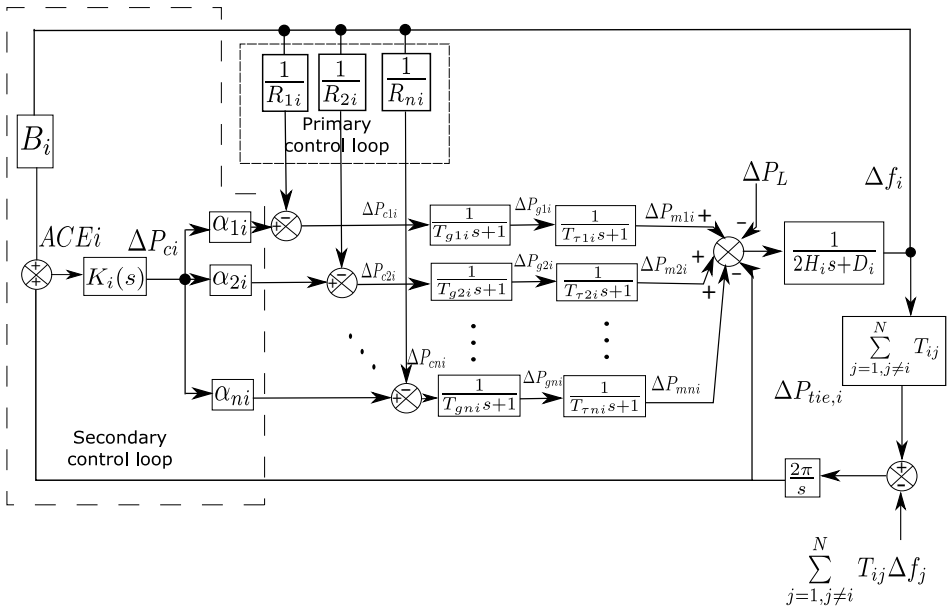

Figure 2-7: Frequency control strategy for dynamic analysis of interconnected systems [41].

In multi-area systems, the ACE control signal will perform complementary regulation services like the return of the system frequency to the reference value and the regulation of the interchanged power flow between the interconnected control areas. This ACE value for area i (ACE_i) is determined by variations in the inter-area exchanged power $\Delta P_{tie,ij}$ between areas i and j, and intra-area frequency deviations Δf_i,

$$ACE_i = \Delta P_{tie,ij} + \beta_i \Delta f_i \tag{2-13}$$

where $\beta_i = D_i + 1/R_i$ is denominated the frequency bias in the control area i. D_i is the load sensitivity damping constant and R_i is the droop value of the generators.

The scheduled power flow between areas is modeled through frequency deviations of the respective control areas. The tie-line power deviation needs to be included in the LFC model to represent the effects of the interconnections in a multi-area AGC on a system composed by N areas. The deviation between i-th area and the remaining connected areas can be calculated as [6]:

$$\Delta P_{tie,i} = \sum_{j=1,j\neq i}^{N} \Delta P_{tieA,ij} = \frac{2\pi}{s}\left[\sum_{j=1,j\neq i}^{N} T_{ij}\Delta f_i - \sum_{j=1,j\neq i}^{N} T_{ij}\Delta f_j\right] \tag{2-14}$$

$$\Delta P_{tieA,ji} = \varrho_{ij}\Delta P_{tieA,ij} \tag{2-15}$$

$$\varrho_{ij} = -\frac{P_{ri}}{P_{rj}}. \tag{2-16}$$

The term P_{ri} is the rated power of area i, P_{rj} is the rated power of area j and T_{ij} represents the synchronizing power coefficient between areas i and j.

2.2.4. Complete Model for LFC regulation in power system

Figure **2-1** depicts the frequency regulation structure with only one generation unit for a given control area i (from [6]). Besides of the already defined parameters, $K(s) = -k_I/s$ represents the secondary controller and $B_i = D_i + 1/R_i$ is the frequency bias of the area. Also, T_{gi} and T_{ti} denote the time-constants for the first-order representations of governor and turbine of the aggregated machine model for area i. T_{ij} is a constant defined as the synchronizing power coefficient [42], acting as a weighting factor for the power exchanged between area i through the interconnection area with j, from a total number of N areas in the system.

From figure **2-7**, it is easy to extract the following relationship expressing the frequency change for the area i:

$$\Delta f_i \left[\frac{1}{2H_i s + D_i} - \sum_{k=1}^{m} (B_i K(s) \alpha_k - \frac{1}{R_k}) M_k(s) + \frac{2\pi}{s} (\sum_{j=1, j\neq i}^{N} T_{ij}) (1 - K(s) \sum_{k=1}^{m} \alpha_k M_k(s)) \right]$$
$$= -\Delta P_{Li} + \frac{2\pi}{s} (\sum_{j=1, j\neq i}^{N} T_{ij} \Delta f_j) \left[1 - K(s) \sum_{k=1}^{m} \alpha_k M_k(s) \right] \quad (2\text{-}17)$$

From equation 2-17, the main relationships between the input and output signals for frequency regulation can be extracted. The term $M_k(s)$ denotes the k machine from a total of m in the area. Load disturbance ΔP_L and interconnected areas frequency variations Δf_j are considered as the input signals and Δf_i is the output. This forms a MISO (Multiple Input Single Output) system for frequency regulation. As both input disturbances can be considered as independent, each one should be analyzed separately.

2.3. Modeling of Renewable Energy Sources

2.3.1. Modeling of Variable-speed Wind Turbines

There are several types of wind turbines (WT) and a varied range of classifications for these. However, they are mostly divided between fixed-speed and variable-speed systems. Fixed-speed wind turbines are characterized by operating in a steady state at a constant rate independent of wind speed. Almost all fixed-speed WT use induction generators to convert wind kinetic energy into electrical energy. The WT could utilize the kinetic energy stored in

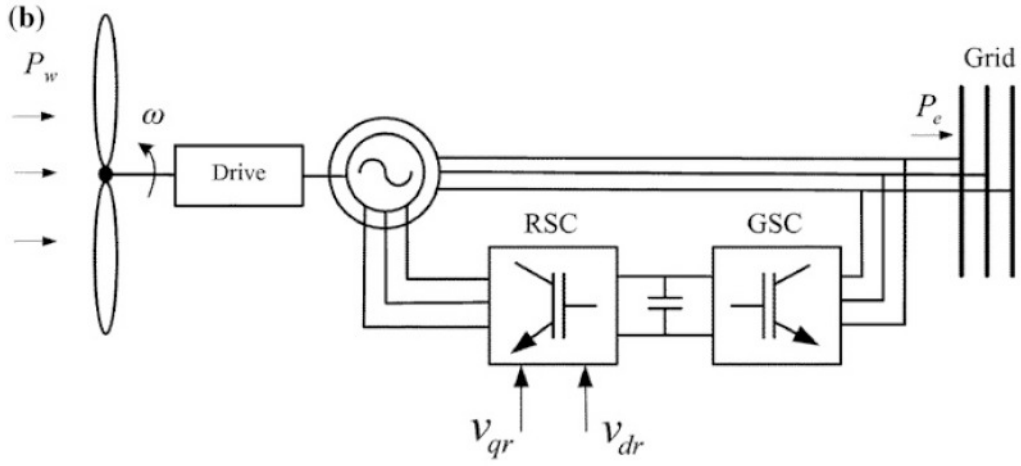

Figure 2-8: Variable speed wind turbine generator with doubly-fed induction generator (DFIG) [6].

the turbine blades and contribute to the system frequency stability by providing spinning inertia. However, as they cannot track wind speed fluctuations, the captured energy is not as efficient as in variable-speed systems [6].

Conversely, variable-speed wind turbines (VSWT) can use either induction or synchronous machines to obtain energy from the wind. Additionally, VSWT have the capability of maintaining an almost constant torque in the axis. The Doubly Feed Induction Generator (DFIG) is by far the most widely used double feeding machine and is one of the most common in the construction of WT; therefore, this type of machines are used in the modeling of wind farms for this thesis. The DFIG corresponds to an induction machine which feeds the stator and the rotor with alternating currents, unlike the machines of induction with squirrel cage rotor where only the stator can be supplied. This access to the rotor is made via flush rings and an AC/DC/AC inversion stage. A diagram for DFIG VSWT can be seen in Figure **2-8**, with RSC and GSC standing for Rotor Side Converter and Grid Side Converter, respectively.

DFIG VSWT can control the rotor reactive power allowing speed management in front of wind variations and electric system disturbances, offering a better quality of service. This control is exercised by acting on the part of the converter connected to the network, which allows absorbing or producing reactive power. However, the range of variation depends on the dimensions of the converter. It is also possible to control the frequency by acting on the part of the converter on the rotor side, which varies the torque and, consequently, the power delivered.

DFIG VSWT has some disadvantages. Its capacity to withstand voltage gaps is limited, leading even to disconnection from network in some cases. This kind of WT has also a higher cost due to the need of a power inverter. Additionally, access to the rotor introduces higher

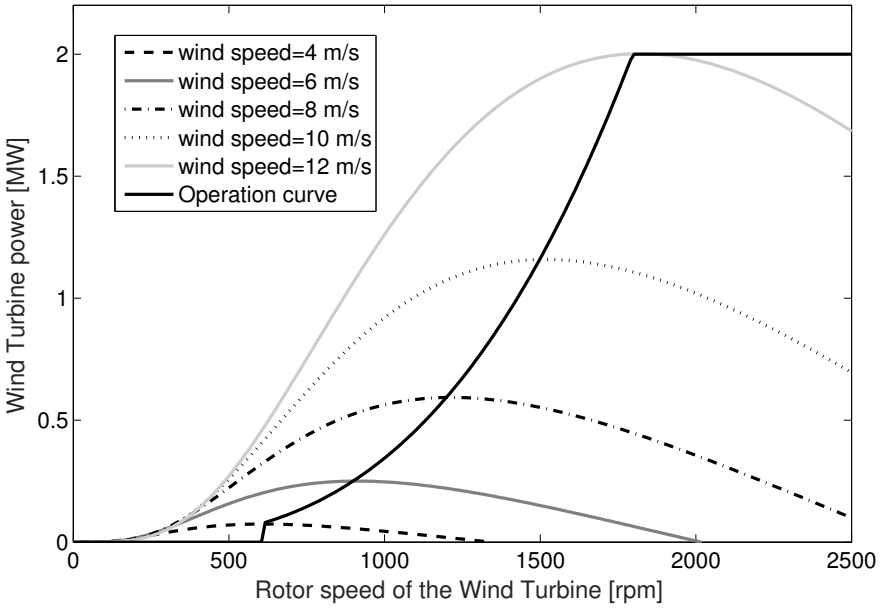

Figure 2-9: Wind turbine operational curve for different wind speeds.

maintenance costs. Finally, using an AC/DC/AC converter produces harmonic pollution in the network, which in the case of a massive increase in this technology, might damage the integrity of the interconnected system.

The mathematical expression relating mechanical power, wind speed, and the turbine rotor speed (as shown in the curves of Figure **2-9**) is described by equation (2-18) [87]:

$$P_m = \frac{1}{2}\rho\pi R^2 v^3 C_p(\lambda, \beta) \tag{2-18}$$

In the previous expression, wind speed is denoted by v, ρ = 1,225 kg/m^3 represents air density, and R = 45 m is the assumed length of the turbine blades. The so-called *power coefficient* of the wind turbine C_p denotes the fraction of available power in the wind that is being harvested. Usually, the performance coefficient C_p is found in look-up tables as the product of numerical calculations for the different models of wind turbines. However, there are some analytical approximations found in the literature, as the one suggested in [87]:

$$C_p = 0{,}22\left(\frac{116}{\lambda_t} - 0{,}4\beta - 5\right)e^{\frac{-12{,}5}{\lambda_t}}, \tag{2-19}$$

where β is the collective blade pitch angle [87] in degrees, and λ_t is represented by:

$$\lambda_t = \frac{1}{\frac{1}{\lambda + 0{,}08\beta} - \frac{0{,}035}{1+\beta^3}}. \tag{2-20}$$

This parameter is a function of the Tip-Speed Ratio (TSR) denoted by $\lambda = \frac{Rw_r}{v}$, with variable w_r denoting the DFIG angular speed.

As equations (2-19) and (2-20) indicate, the mechanical power of the DFIG is also influenced by the blade pitch-angle β. This variable is controlled when the power delivered is close to its nominal value. In order to operate the WT below its maximum power extraction point, the operation curve must cut the WT power curve in another point that necessarily will be located under the maximum value of the WT power curve for each wind speed. Usually, this would result in an operational curve slightly moved to the right from the one shown in Figure **2-9**. The selected operating point P_o for each power curve, which is lower than the maximum withdraw power, is given by the expression:

$$P_o = \frac{K_o v^2}{w_r} \tag{2-21}$$

In equation (2-21), the value of K_o is set as 0,3 [Ns$^2/m$]. Hence, the operating torque T_o [Nm] becomes $T_o = K_o v^2 = 0{,}3v^2$.

2.4. Illustration of LFC operation

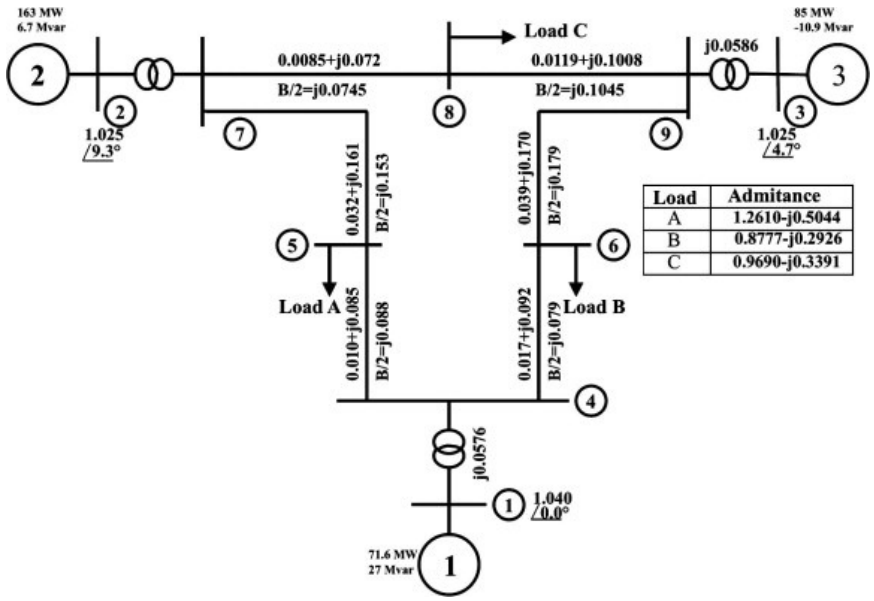

Figure 2-10: Standard three-machine nine-bus Western System Coordination Council (WSCC) power system [81].

Here, we illustrate the LFC model describing frequency dynamics with the three-machine nine-bus Western System Coordination Council (WSCC) power system of Figure **2-10**, which

contains three synchronous generating units in buses 1, 2 and 3, and load in buses 5, 6 and 8. The machine, network and load parameter values could be found in [3].

The system is modeled as a multi-machine isolated area system ($\Delta P_{tie} = 0$). A step change of 5 % in load is simulated using the representation of equation (2-17) for three different cases. Figure **2-11** shows the frequency variations of the system for inertial response, primary and secondary control actions. The inertial response delays the frequency drop but is unable to stop the disturbance effect. The proportional control action of primary regulation elevates generated power in the machines, stopping the frequency drop and stabilizing and compensating some of the impact. The integral action of secondary regulation is needed to fully return system frequency to nominal values in steady-state.

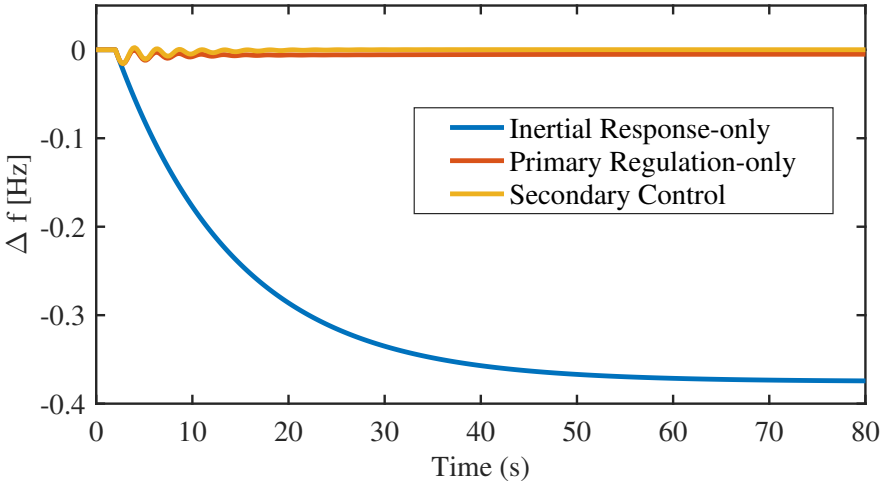

Figure 2-11: Illustrative example of the frequency behavior for the WSCC system: inertial response-only (blue), system with primary frequency regulation (red) and system with secondary control (yellow).

The increment in RES penetration is expected to reduce system inertia [6]. In this case, the WECC system is modified to simulate the effects of different penetration levels of renewable sources in LFC when facing a load disturbance. The same step change of the previous case is applied, and the results are being shown in Figure **2-12**. The magnitude of the deviation in frequency becomes more significant as RES penetration increases and inertia diminishes. The slope of the curve ($\Delta f/\Delta t$) grows indicating a higher rate of change in frequency. Besides, there is an increase in system oscillations before the frequency control loops can compensate for the disturbance effects. Some questions arise with this situation: how are the new energy sources affecting the parameters and behavior of the LFC? Do the RES need to contribute in the LFC loops? How? The following chapters will help to answer these questions.

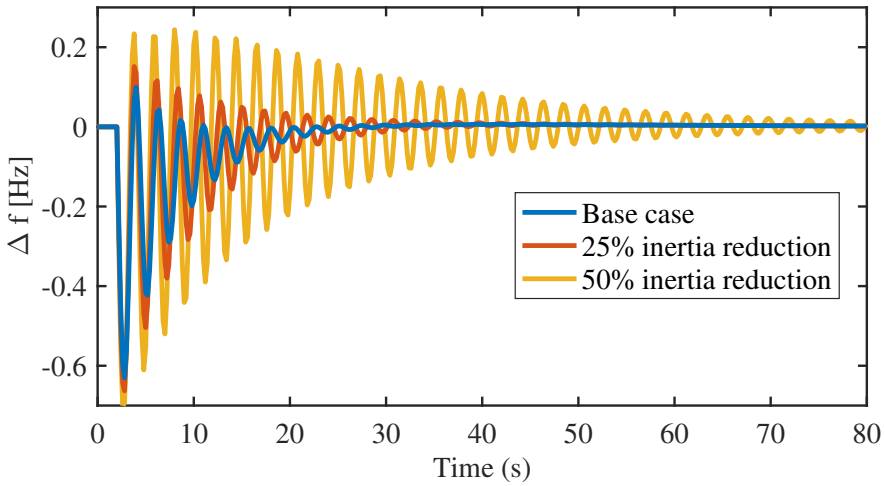

Figure 2-12: Frequency variations for the WSCC system with inertia reduction. LFC performance clearly degrades with the loss of inertia.

2.5. Summary

In this chapter, the frequency control characteristics in power systems and its dynamic performance were described; an overall frequency response model for the existing frequency control loops was presented; and the main relationships between a given control area frequency and its disturbances were extracted. Additionally, some issues regarding wind power and frequency regulation were presented. At first, the most widely employed technologies of Wind Turbines were reviewed, and a model for representing wind turbine power in frequency regulation analysis was presented. Basic performance of LFC and its expected behavior with renewable energy penetration were explored through a simulation illustrative example. These models and simulations are the basis of the analysis presented in subsequent sections.

3 Methodology for Frequency-Domain Analysis of Frequency Regulation in Power Systems

Traditional Load Frequency Control schemes constitute a regulation structure extensively applied in power systems. This chapter presents the use of Control Sensitivity Functions to describe the dynamical characteristics of both primary and secondary control loops in frequency regulation. Bode plots are employed as a visualization and analysis tool. Results of frequency-domain analysis illustrate the role of Load Frequency Control and allow determining load disturbance effects on the system output.

Maintaining the generation/load balance in a power system is a critical factor for frequency regulation. In recent years, controllable loads and renewable energy sources have been increasingly integrated to power grids. In practice, this may have substantial impact on the system frequency response (SFR). This chapter additionally investigates the effect of load-damping, generator inertia, and governor speed characteristics on system frequency using typical SFR model with hydraulic generation. Theoretic analysis based on transfer functions shows that the frequency deviation under variable load-damping, generator inertia and governor speed coefficients is relatively small and bounded when the power system is essentially stable; while the frequency deviation can be accelerated when a power system is unstable after disturbance. Multiple-machine cases are included in the analysis with validation via simulation studies. This analysis can be useful to system operators for decision-making of frequency regulation or load control.

3.1. Analysis of Frequency Regulation with Control Sensitivity Functions

The equilibrium between the power demanded by loads and the energy generated in the electrical system is indicated by *frequency*. Power system frequency is a characteristic parameter

determined by the rotational speed of the traditional synchronous generators. Frequency can deviate from the operational values due to changes in the mentioned balance of generation and demand, such as sudden load variations, power outages, transmission losses, or fluctuation in alternative energy sources [22]. These phenomena raised the need for control strategies capable of keeping system frequency inside the desired standard range. Frequency regulation structure is composed by machine inertia damping the speed changes of synchronous units, and by primary (LFC) and secondary (AGC) controllers restoring frequency to operational values in case of disturbances [6] [76].

Although frequency regulation for power systems has been widely studied [6, 59, 76, 63], this section focuses on the use of Control Sensitivity Functions [83] as the medium for extracting system information. The usage of Control Sensitivity Functions in power system has been studied previously. In [95], a robust H_∞ controller for an electric power steering system was developed using a mixed weighted sensitivity methodology to design complementary sensitivity functions. Complementary sensitivity functions are also employed to analyze model uncertainties in the design of robust decentralized power system stabilizers [13].

Some other variations of the sensitivity functions are also proposed and considered in robust control of power systems. In [8], a sensitivity-shaping function method is employed for the robust design of a digital control strategy for a wind turbine with a doubly-fed induction machine in variable-power operation. For the application of solar power generation systems operating in grid connect mode, a model-free mixed-sensitivity predictive H_∞ controller has been proposed [10]. Sensitivity analysis is also used to assess the small-signal stability of a given power system architecture designed with an optimization methodology [93].

For the specific application of sensitivity functions in frequency regulation, there are some applications from robust control theory, mainly in the design of H_∞ controllers [6]. Some related works using Bode plots as the analysis tool can be found to determine wind-power effects in power system frequency [44, 46]. Both [63] and [31] use Bode analysis for the assessment of the dynamic behavior of frequency regulation with renewable sources. Additionally, variations in the main parameters of the frequency regulation structure through the use of transfer functions and sensitivity-like expressions were developed in [33] and [34]. Amidst all these studies, this work focuses on the application of Control Sensitivity Functions to find dynamic information about the traditional frequency regulation structure of power systems. Bode plots are employed for analysis and visualization of the functions.

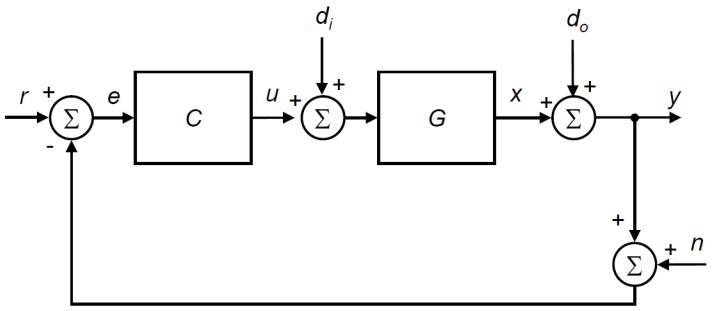

Figure 3-1: Feedback control system [83].

3.2. Sensitivity Functions in Control Systems

Consider the unit feedback control system shown in Figure **3-1**. Two blocks are representing the system: process G and controller C. Variable r is the reference, e represents the error signal that "activates" the controller, who in turn generates the control action u. y denotes the output signal of the process. There are three additional signals of interest in the system: input disturbance d_i (influencing the input of the process), output disturbance d_o, and measurement noise n (representing differences between the current value of y and the value measured by the sensor).

After applying some superposition properties and block algebra to the system of Figure **3-1**, the following relationships can be extracted:

$$Y = \frac{GC}{1+GC}R + \frac{G}{1+GC}D_i + \frac{1}{1+GC}D_o - \frac{GC}{1+GC}N \tag{3-1}$$
$$U = \frac{C}{1+GC}R - \frac{GC}{1+GC}D_i - \frac{C}{1+GC}D_o - \frac{C}{1+GC}N$$

For simplicity, Laplace variable s has been omitted in both Figure **3-1** and Equation (3-1). As several of the transfer functions repeat through Equation (3-1), all relationships can be described using just four of them. These are the so-called *Control Sensitivity Functions*, each denoted by its name, and described as:

- Sensitivity Function:

$$S(s) = \frac{1}{1+G(s)C(s)} \tag{3-2}$$

- Complementary Sensitivity Function:

$$T(s) = \frac{G(s)C(s)}{1+G(s)C(s)} \tag{3-3}$$

- Disturbance Sensitivity Function:

$$S_i(s) = \frac{G(s)}{1 + G(s)C(s)} \tag{3-4}$$

- Control Sensitivity Function:

$$S_o(s) = \frac{C(s)}{1 + G(s)C(s)} \tag{3-5}$$

Control Sensitivity Functions condense the essential information about the system performance, including reference tracking, disturbance effects, and dynamic behavior of the control action. All this information is useful for both static studies (low frequencies) and dynamic analysis (high frequencies). Moreover, Control Sensitivity Functions closely relate themselves through the following algebraic expressions:

$$S(s) + T(s) = 1 \tag{3-6}$$

$$S_i(s) = G(s)S(s) = \frac{T(s)}{C(s)} \tag{3-7}$$

$$S_o(s) = C(s)S(s) = \frac{T(s)}{G(s)} \tag{3-8}$$

Equations (3-6) to (3-8) show that the Control Sensitivity Functions are not "molded" through the arbitrary selection of a given controller $C(s)$. These restrictions imply the need of trade-off solutions compromising different control objectives, often requiring designer criteria for pondering the best control performance according to the desired conditions.

3.3. Control Sensitivity Functions for Frequency Regulation in Power Systems

3.3.1. Description of Frequency Control System

In electrical systems under normal operating conditions, the generators rotate in synchronism and together they generate the total demanded energy [3]. Since electrical energy can not be stored in large quantities, if the power consumed by the load increases but the mechanical power provided by the turbines remains constant, the increase in demand can only be

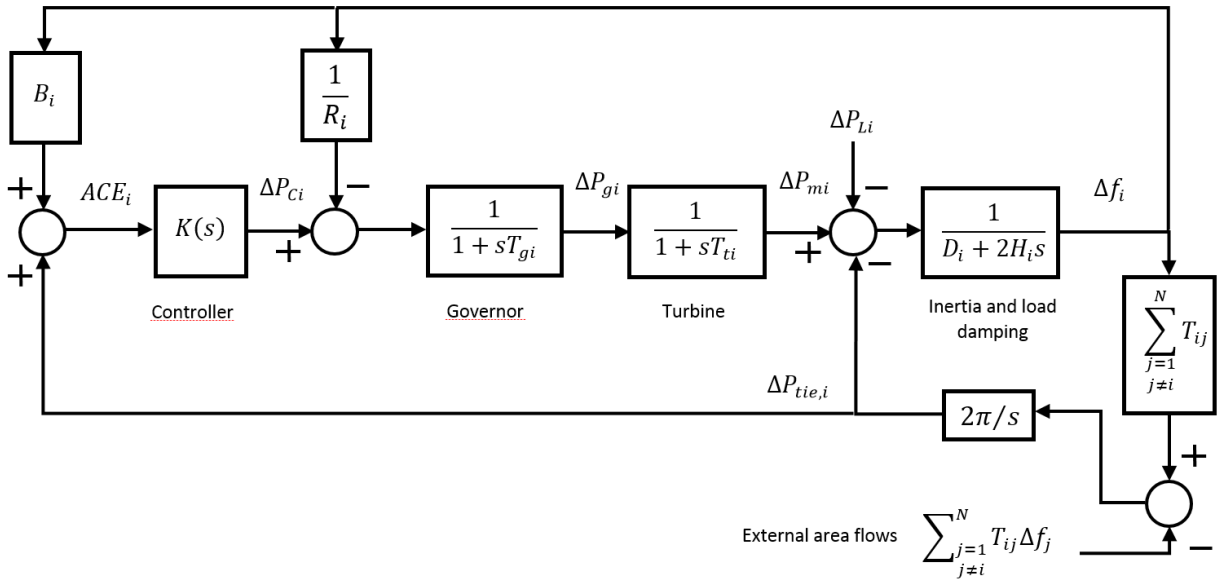

Figure 3-2: Block diagram for frequency control structure in power system including only one machine for a regulation area i (based on [6])

compensated by the stored kinetic energy [42]. This effect implies a decrease in the rotation speed of the generators and a frequency fall on the system, directly related to said speed. As the demand is variable, a control system is required to automatically adjusts the power generated in each generation unit while keeping the frequency within certain operational limits [79]. Frequency control scheme for power systems is conformed by the damping effects of speed variations of synchronous machines by the inertia, and by primary (Load Frequency Control –LFC) and secondary (Automatic Generation Control –AGC) control structures returning frequency to standard operating ranges in the presence of disturbance events [3]. A simple representation of the Frequency control for a single area power system is shown in Fig. **3-2**. The complete derivation of the system can be found in [6].

In Fig. **3-2**, $\Delta P_m(s)$ is the variation $[p.u]$ in the mechanical power of generating units, $\Delta P_l(s)$ represents the load changes $[p.u]$, $\Delta f(s)$ denotes the per-unit frequency deviation, H [s] is the adjusted inertia characteristic, and D is known as the load damping constant [6]. R is the speed drop of the machines, $K(s)$ is the secondary control block (usually, and for this work, $K(s) = -k_I/s$), and $B_i = D_i + 1/R_i$ is an adjusted gain denominated as frequency bias of the area. Finally, T_{ti} and T_{gi} denote the corresponding time constants of the turbine and governor first-order models, respectively.

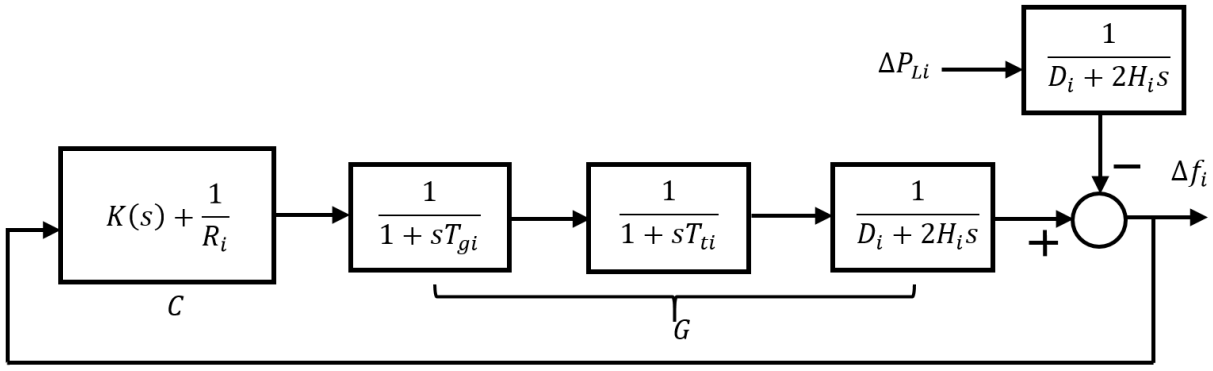

Figure 3-3: A single area power system frequency regulation scheme seen as a generalized feedback control system ([62])

3.3.2. Control Sensitivity Functions for Frequency Regulation Structure

The Frequency regulation structure in Fig. **3-2** can be expressed as the classic feedback control system of Fig. **3-1** after the application of certain block operations. Assuming the simplification $r = d_i = n = 0$, the system of Figure **3-3** is reached [62]. The system output y for this feedback control system is Δf_i, which is the variation in system frequency for an isolated (no interchanged power) area i.

From Figure **3-3**, the plant G is composed of the transfer functions of the machines and the total inertia and load damping for the area i. The controller C:

$$C = K(s) + \frac{1}{R_i} = \frac{-k_i B_i}{s} + \frac{1}{R_i}$$

combines the action of both primary and secondary control actions in the frequency regulation structure. Besides this, we can see how the output disturbance signal d_o:

$$d_o = -\Delta P_L \left(\frac{1}{D_i + 2H_i s} \right) \tag{3-9}$$

represents the load variations filtered by the transfer function of total inertia and load damping. The transfer function $G_f(s)$, representing the relationship between the process output $\Delta f(s)$ and the disturbance $\Delta P_L(s)$ is defined by equation (3-10):

$$G_f(s) = \frac{-\frac{1}{2H_i s + D_i}}{1 + \left(K(s) + \frac{1}{R_i} \right) \frac{1}{T_g s + 1} \frac{1}{T_t s + 1} \frac{1}{2H_i s + D_i}} \tag{3-10}$$

The control sensitivity functions, according to the frequency regulation structure of Figure **3-3**, are listed below:

$$S(s) = \frac{1}{1 + \left(K(s) + \frac{1}{R_i}\right)\left(\frac{1}{T_g s+1}\frac{1}{T_t s+1}\frac{1}{2H_i s+D_i}\right)} \tag{3-11}$$

$$T(s) = \frac{\left(K(s) + \frac{1}{R_i}\right)\left(\frac{1}{T_g s+1}\frac{1}{T_t s+1}\frac{1}{2H_i s+D_i}\right)}{1 + \left(K(s) + \frac{1}{R_i}\right)\left(\frac{1}{T_g s+1}\frac{1}{T_t s+1}\frac{1}{2H_i s+D_i}\right)} \tag{3-12}$$

$$S_i(s) = \frac{\frac{1}{T_g s+1}\frac{1}{T_t s+1}\frac{1}{2H_i s+D_i}}{1 + \left(K(s) + \frac{1}{R_i}\right)\left(\frac{1}{T_g s+1}\frac{1}{T_t s+1}\frac{1}{2H_i s+D_i}\right)} \tag{3-13}$$

$$S_o(s) = \frac{K(s) + \frac{1}{R_i}}{1 + \left(K(s) + \frac{1}{R_i}\right)\left(\frac{1}{T_g s+1}\frac{1}{T_t s+1}\frac{1}{2H_i s+D_i}\right)} \tag{3-14}$$

3.4. Analysis of Frequency Regulation Structure using Control Sensitivity Functions

We are interested in extracting information about the frequency control structure in power systems. for this purpose, the transfer functions of sensitivity functions and $G_f(s)$, as described in equations (3-10) to (3-14) are analyzed using Bode plots. Bode plots constitute a useful descriptive tool for linear control analysis, as they provide a visual representation of the system behavior.

As a proof of principle, an one-area frequency regulation structure, similar to the described in Figure **3-3**, is studied using the following parameter values (from [79]): $T_g = 0{,}2$ s, $T_t = 0{,}5$ s, $H = 5$ s, $R = 0{,}05$ $p.u$, $D = 0{,}8$ and $B_i k_i = 7$ for a configuration including the secondary control stage (AGC). The system with only a primary control is simulated by setting the secondary control gain to zero ($k_i = 0$).

Several scenarios are considered in the subsequent sections, all of them involving the extraction and analysis through Bode plots of the four control sensitivity functions S, T, S_i and S_u. The explored scenarios start with the study of the base case scenario (without disturbances over parameters), and then involve simulation and dynamic analysis of diverse conditions and variations of the LFC using the mentioned sensitivity functions. All magnitude Bode plots are presented in absolute units (abs), instead of the traditionally employed decibels

(dB); but results and conclusions are equivalent regardless of the measure scale. Step response is also employed in some cases for studying time-response of the transfer function between frequency and load-disturbance, when required.

3.4.1. Control Sensitivity Functions of frequency regulation system for the base case scenario

As previously mentioned, transfer function $G_f(s)$ represents the direct relationship between the area frequency Δf and the applied load disturbance ΔP_L, as shown in equation (3-10). This function expresses the overall performance of the LFC system, involving the control action of primary and secondary regulation structures (if available). The step response of Figure **3-4** represents the variation in the system output (electrical frequency) versus time when a step disturbance occurs in ΔP_L. The operation of the primary regulation is clear, with droop control acting and stopping the frequency decay, but failing to return the system to its original state. This limitation illustrates the need of a secondary regulation: the integral action of secondary control can compensate the steady-state error, even if there is a longer settling time.

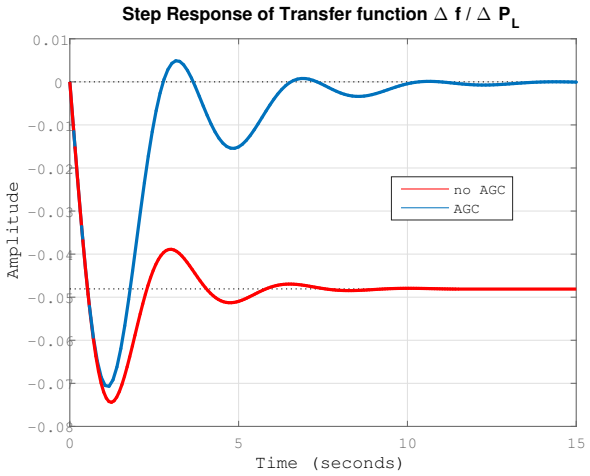

Figure 3-4: Step response of transfer function $G_f(s)$ with only a primary control (red), and with AGC (blue).

The dynamic performance of the step response is verified through the Bode plots of Figure **3-5**, which illustrate the four Control Sensitivity Functions for the base case scenario with and without secondary regulation. The Plots for Sensitivity S, Complementary Sensitivity T, and Control Sensitivity S_u present a similar behavior for the studied configurations, with

only larger magnitude peaks in the system with AGC. However, Disturbance Sensitivity S_u shows a notorious difference between configurations along the low-frequency region. This indicates how load variations in the low-frequency region are almost entirely attenuated by the secondary control (AGC), i.e., a demonstration of the steady-state error correction capabilities already mentioned in the time-domain analysis.

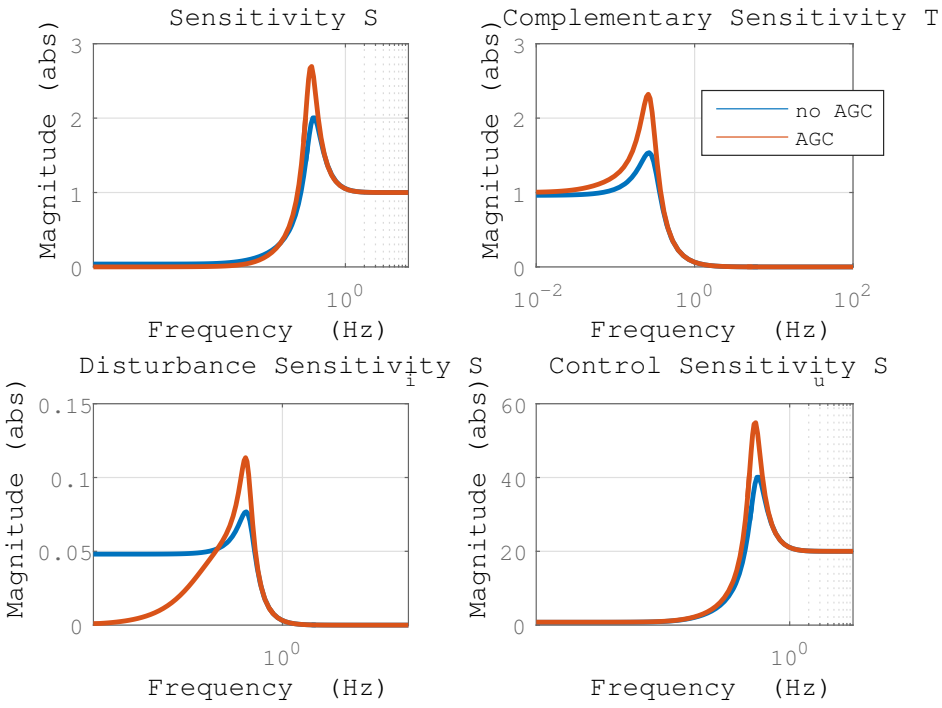

Figure 3-5: Bode plots of Sensitivity functions for the base case with primary-control-only (red), and with AGC (blue)

From Figure **3-5**, generator inertia is damping load fluctuations over 1 Hz in both cases for all Sensitivity functions. The response plots present maximum magnitude peaks around 0.3 Hz for both primary and secondary regulation cases. These phenomena indicate an amplifying effect for signals with spectral content around 0.3 Hz. Particularly for S_u, this means that a disturbance with spectral content at this frequency would cause the most significant impact on system output. The role of inertia in the damping of load disturbances should be highlighted, as the block involving the inertia parameter H in the control representation of Figure **3-3** is acting as a filter for the disturbance signal ΔP_L.

Performance of an optimally-tuned controller

Aiming to improve the dynamic response of the base case scenario, an optimally-tuned PID controller was designed using the optimal PID tuning rules of Padula and Visioli [58], which were developed to minimize the integrated absolute error while constraining the peak sensitivity of the system response. The system behavior including AGC was studied comparing both the base case integral controller and the optimally-tuned PID at the secondary regulation stage. However, the performance of the optimal controller in presence of a load step disturbance of 10 % was actually poor, as evidenced in Figure **3-6**.

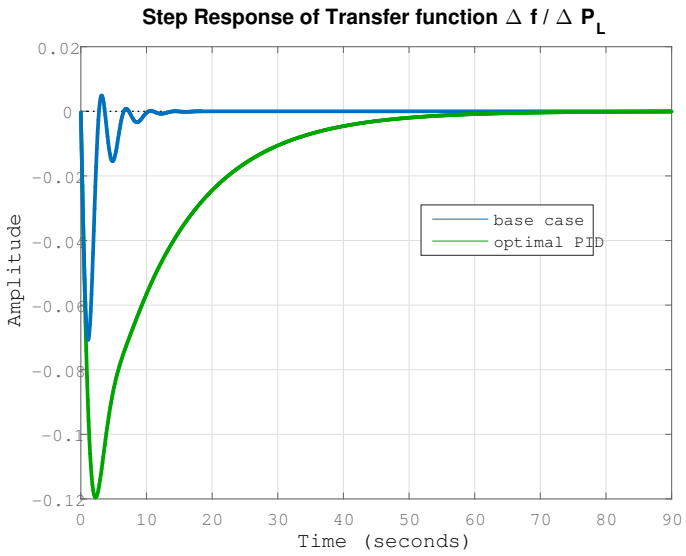

Figure 3-6: Step disturbance response for base case vs. optimally-tuned PID controller

This drop of performance can be explained with bode plots of Control Sensitivity Functions for frequency regulation. Figure **3-7** shows bode plots for both the base case scenario and the optimally-tuned controller. In the frequency domain, the performance of the system with optimal controller improved the behavior of the base case for each sensitivity function except for input disturbance sensitivity S_i. For the latter, the region of influence of the input disturbance actually was larger for the optimally-tuned controller, i.e. is more sensitive to load disturbances, as evidenced by the step disturbance response in Figure **3-6**. The smaller margin of execution of control actions shown in Control Sensitivity S_u suggests a worst frequency nadir and longer settling time for the optimally-tuned controller. This phenomena suggests that the design criteria focused excessively on improving the Sensitivity S and Complementary Sensitivity T responses for reference tracking, leaving the system more vulnerable to disturbance effects.

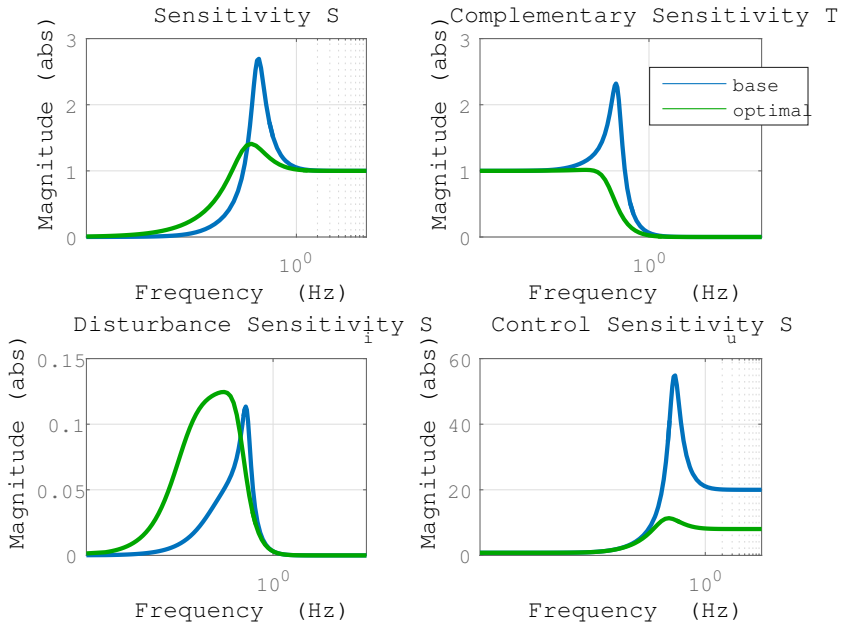

Figure 3-7: Sensitivities of base case vs. optimally-tuned controller

3.4.2. Effects of Parametric variations on Control Sensitivity Functions

We are also interested in analyzing the behavior of the sensitivity functions in the presence of changes in frequency regulation parameters and power system components. As we introduced in the previous chapter, the power system varies in time due to several reasons [63], such as the presence of renewable energy sources. In fact, a consequence of the growing penetration of renewable energy is a decrease in the system inertia [6]. In order to explore the sensitivities of the main components of the LFC in the regulation structure including a secondary control loop, we introduce variations respect to load damping D, turbine time-constant T_t, controller integral gain k_i, speed drop r, and system inertia H. Those parameters are changed once at a time and all the remaining parameters are left untouched. For each new value, the Control Sensitivity Functions are extracted and evaluated with Bode plots as illustrated in the following subsections.

Variations in load damping D

Load damping D is a parameter representing the impact of the frequency-dependent loads in the frequency regulation structure. The effects of changing it in the control sensitivity

functions are depicted in Figure **3-8**. The simulations show the minimal effect of D in the sensitivity functions. This behavior is due to the lack of frequency-dependent loads in the power systems, and evidences the limited value of load-damping for frequency regulation at these penetration levels.

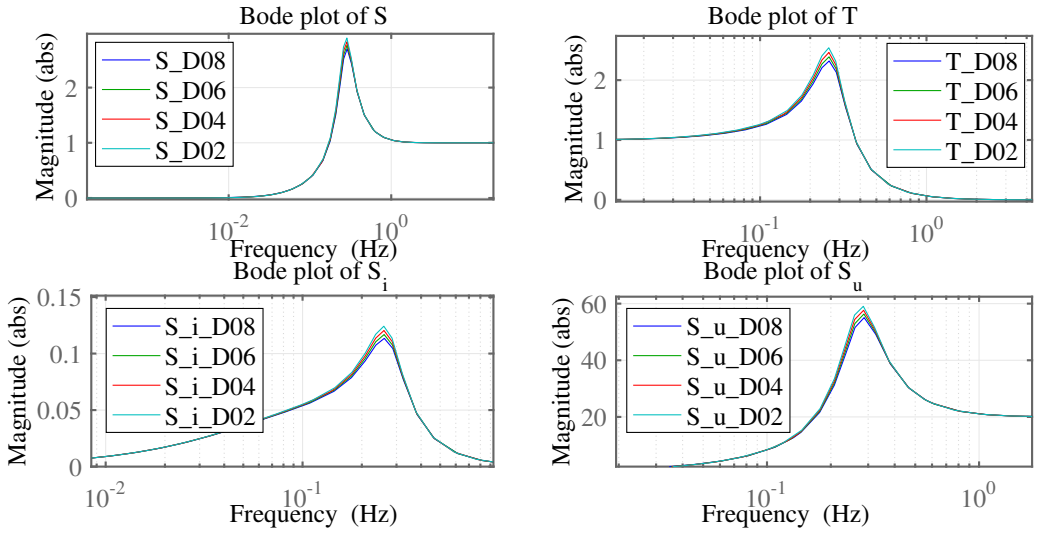

Figure 3-8: Effects of varying load damping D in the control sensitivity functions of frequency regulation system.

Variations in turbine time-constant T_t

The effects of changing the turbine time-constant T_t in the control sensitivity functions of the frequency regulation system are depicted in Figure **3-9**. The results show how the control sensitivity functions suffer a performance degradation when increasing T_t. This behavior causes an increased delay in the response of the system controllers caused by the slower action of the machines. However, we should acknowledge that this is not a parameter expected to change in the system, and these effects could be attributed more to parametric uncertainty rather than variations over time.

Variations in controller integral gain k_i

The effects of changing the controller integral gain k_i in the control sensitivity functions of the frequency regulation system are depicted in Figure **3-10**. As controller integral gain k_i increases, the only sensitivity function with significant change is S_i. As presented in

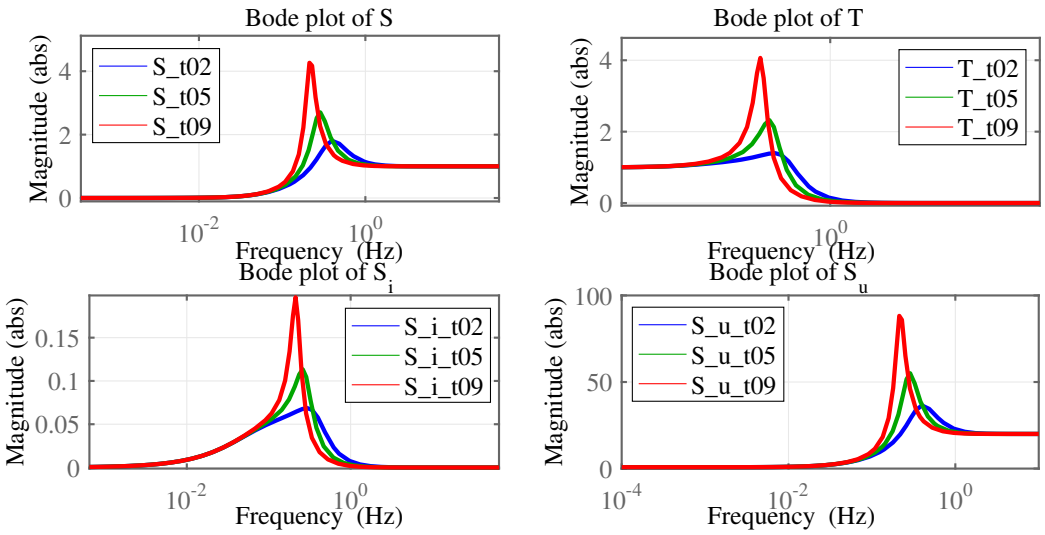

Figure 3-9: Effects of varying the turbine time-constant T_t in the control sensitivity functions of frequency regulation system.

section 3.4.1 for the optimally-tuned controller, this behavior of s_i makes sense because the disturbance rejection is improved with the adequate tuning of the secondary controllers for frequency regulation. Additionally, note that the input disturbance sensitivity S_i could behave as an adjustment indicator for tuning the integral gain of secondary regulation.

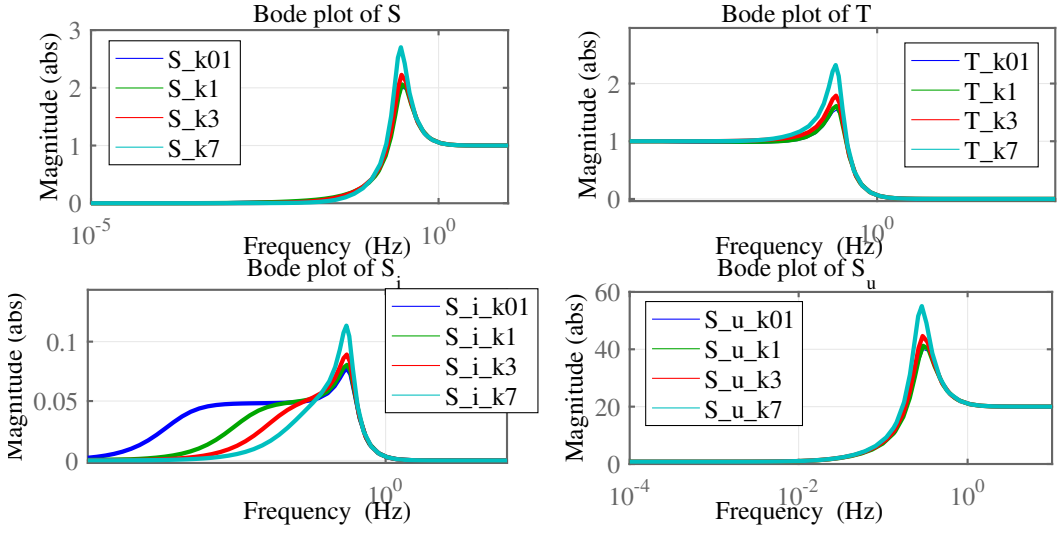

Figure 3-10: Effects of varying the controller integral gain k_i in the control sensitivity functions of frequency regulation system.

Variations in speed droop R

The parameter R represents the response capability of the machines, i.e, the operational margin for changing rotational speed and contributing to primary regulation. The effects of varying it are depicted in Figure **3-11**. As expected, the performance of the control system is directly related to this parameter. Sensitivity S and Complementary Sensitivity T present bigger peaks and an increased sensitivity region as R decays. Additionally, Control Sensitivity S_u is drastically augmented with small R values due to the lack of operational capability to perform the required control actions. However, input Disturbance Sensitivity actually worsens as R increases. This could reflect the effect of increasing the capabilities of primary regulation, but having a reduction of the control action of secondary regulation.

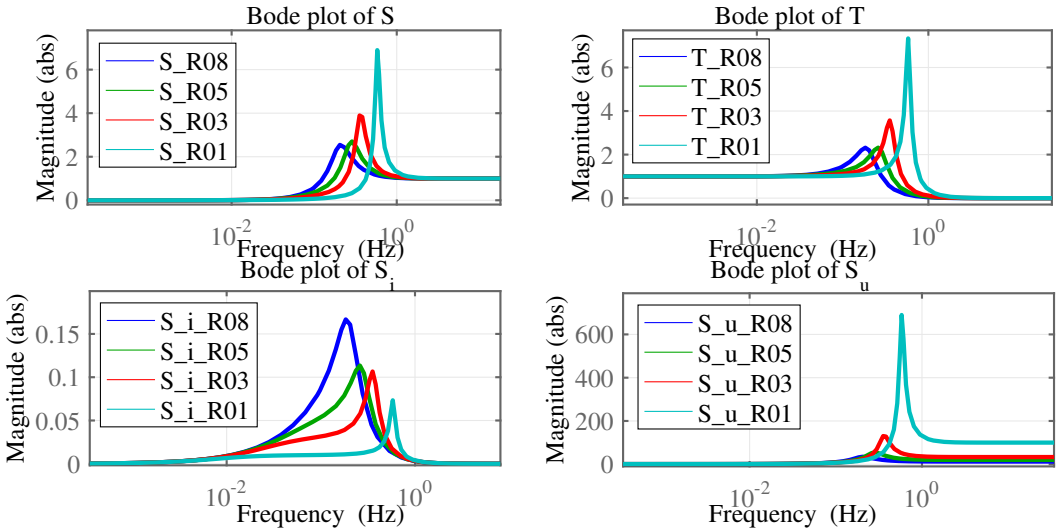

Figure 3-11: Effects of varying speed droop R in the control sensitivity functions of frequency regulation system.

Variations in inertia H

The effects of changing inertia H are depicted in Figure **3-12**. As the inertia is decreased gradually, the control sensitivity functions present more prominent peaks of magnitude. Figure **3-12** shows how the performance curve of the Control Sensitivity Functions maintains the same trends of the base case with AGC explored in Section 3.4.1. As inertia gets smaller, the same amplification region presents a growing trend in every one of the functions plots. This region is located between 0.1 and 1 Hz, the transition zone between the inertial response and the frequency regulation structure. As noted before, this behavior could lead to an

amplifying effect of disturbances with spectral content in that region. These effects evidence a performance degradation in the frequency regulation structure and highlight the importance of the inertia for frequency control purposes.

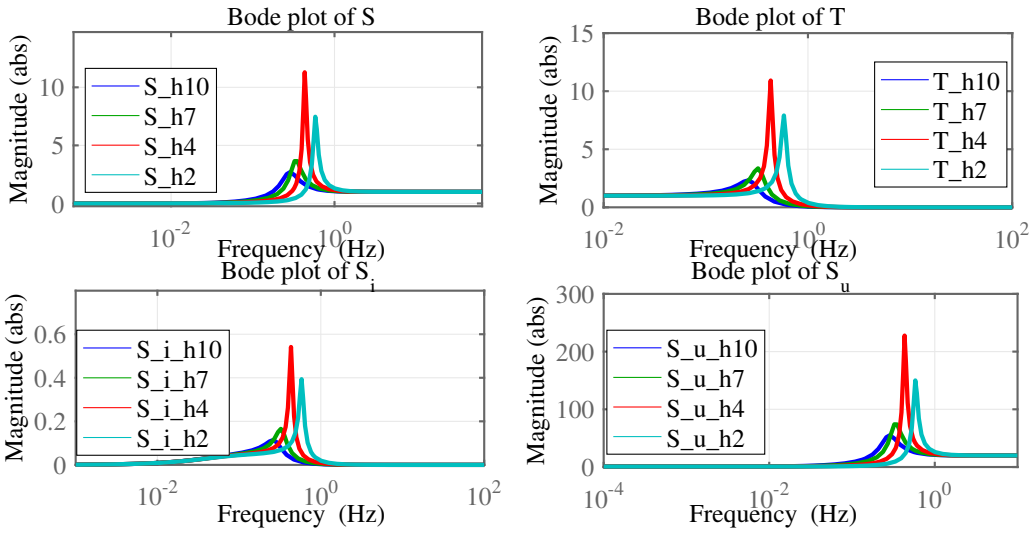

Figure 3-12: Effects of inertia variation in the control sensitivity functions of frequency regulation system.

3.4.3. Control Sensitivity Functions with an inertia-adjusted frequency regulation system

In Section 3.4.2, we showed the effects of parameter variations in frequency regulation structure. However, this performance comparison could be considered as unfair because the secondary controller was tuned using the parameter values of the base case. This is more important for the inertia, as the inertial response is the natural opposition of the system to frequency variations. If the inertia decreases, it makes sense to adjust the secondary controller to maintain the same control goals of the base case and to explore the performance of the Control Sensitivity Functions with the adjusted parameters. In other words, we expect to compensate the loss of inertia by tuning the Proportional-Integral controller of secondary frequency regulation.

Using the Gain and Phase Margin technique [29] as the tuning methodology, PI compensators were designed for each considered inertia value. Table **3-1** presents the controller parameters for each case. It shows how the performance indicators of Gain and Phase margins for each case were kept as close as possible to the base case with an inertia value of $H = 5$ s.

Parameter/Case	$2H = 10$	$2H = 8$	$2H = 6$	$2H = 4$
Gain Margin [dB]	9.04	9.08	9.18	9.09
Phase Margin [deg]	25.4	25.8	26.7	27.5
Compensator Gain	7	5.6111	4.2759	3.0382
Compensator Numerator	$1 + 2{,}9s$	$1 + 2{,}9s$	$1 + 2{,}9s$	$1 + 2{,}9s$

Table 3-1: Controller parameters for each inertia reduction case.

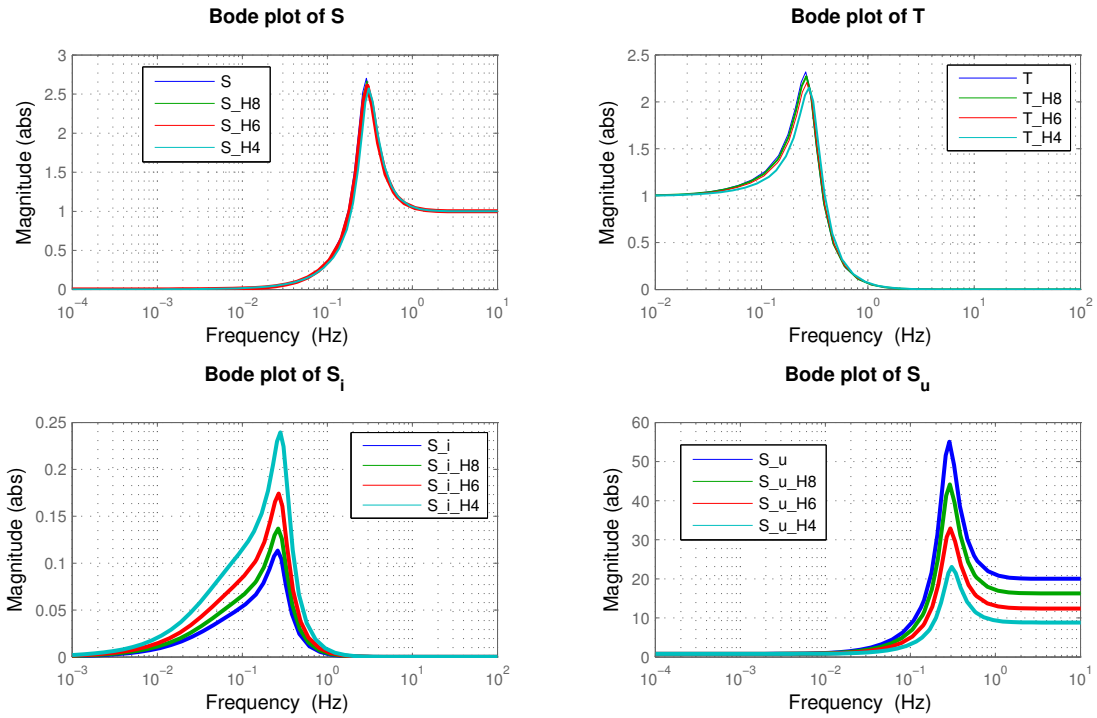

Figure 3-13: Sensitivity functions with variations in inertia H and adjusted controller.

The Bode plots of Control Sensitivity Functions of frequency regulation with inertia variations and adjusted PI controllers are shown in Figure **3-13**. Performances for Sensitivity S and Complementary Sensitivity T are almost identical for all the studied cases. This is expected due to the design requirements of the controller and the Gain and Phase margin technique employed. However, an increased region of influence to input disturbances can be observed from the plot of disturbance sensitivity S_i. Additionally, the performance curve for Control Sensitivity S_u indicates a reduced impact of the control actions when the inertia decreases. In consequence, Control Sensitivity Functions show that tunning the secondary controller is not enough to keep the same operational conditions of frequency regulation

structure when the system inertia is reduced.

The performance degradation of frequency regulation is also evident on the step response of the system. Figure **3-13** shows the performance of the regulation structure to a 10 % step disturbance in load for the different scenarios of inertia variations. The performance degradation in the case of the same secondary controller is significant and correlated with the inertia reduction. System performance is higher when secondary controllers are adjusted to compensate inertia variations. However, the frequency nadir (minimum peak of frequency deviation after disturbance) gets markedly lower as long as inertia decreases. Anyway, the performance of these inertia-adjusted controllers was better the response of the optimally-tuned PID controller studied in section 3.4.1, as evidenced in Figure **3-6**. These remarks the importance of the selected design criteria for the secondary controllers in Load Frequency Regulation.

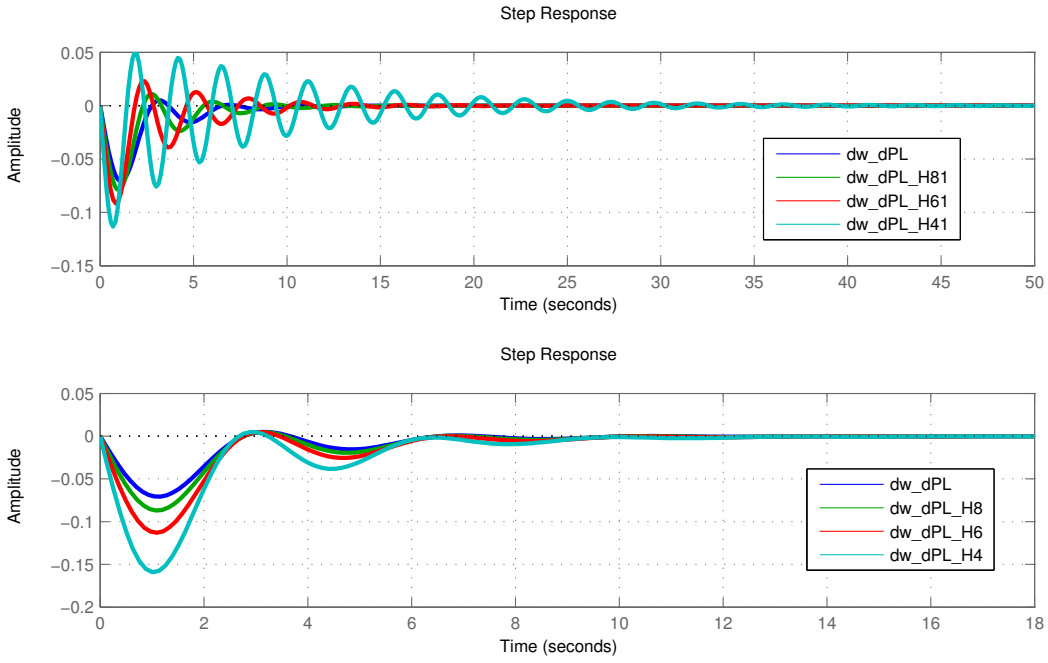

Figure 3-14: Step disturbance responses with variations in inertia H *(top)*, and variations in inertia H and adjusted controller *(bottom)*.

3.5. Summary

This chapter shows the use of the so-called Control Sensitivity Functions for extracting information about the dynamical characteristics of the traditional regulation structure for frequency control in power systems. Through the simulation of a one-area power system and using Bode plots for response visualization, the analysis of these sensitivities led to the description of some key features of control systems such as disturbance rejection, control action effects, and reference tracking. These analyses could be useful for assessing the effects of alternative energy systems such as renewable sources in power system frequency regulation.

Bode analysis also showed the behavior of the complete regulation structure when a step disturbance in load was applied. The role of both primary and secondary control in frequency regulation was also illustrated through simulation. Control sensitivity Functions showed how the inertia H makes the biggest impact over the performance of frequency control loops. Reduction of this parameter significantly diminishes the system opposition to frequency variations, even reaching an amplifying effect of power disturbances at maximum value. When there are inertia variations for the system, both the integral action and the proportional gain of the controller given by the machine speed *droop* need to be adjusted. Even when the control parameters are adjusted for the diminishing inertia, disturbance rejection performance decreases as evidenced by control sensitivities and the step response. There must be special attention to the required design considerations when using optimal tools for the tuning of control parameters. In this case, it is preferred a better disturbance rejection than reference tracking.

This chapter also analyzed the impacts of parametric variations in the Control Sensitivity Functions of frequency regulation in power systems. The negligible impact of load damping D suggests the lack of influence of this parameter in frequency regulation. Also, the increase in the time-constant T_t of the turbine represented a significant delay in the response of the control system. The variations in speed droop R and integral gain k_i showed that, even when the control parameters were adjusted for the diminishing inertia, disturbance rejection performance decreased as evidenced by control sensitivities. In this regard, the role of inertia as a filter for load disturbances needs to be highlighted. This effect is significant because an increased penetration of renewable energy sources in power systems could lead to a diminishing quantity of inertia, affecting the regulation structure and raising the possible need for new control strategies for frequency in power systems, as it will be shown in the next Chapter.

4 Frequency Regulation in Power Systems with Renewable Energy Sources

The expected increased penetration of non-dispatchable renewable energies (wind and solar) suggests that the operation of conventional plants will be more variable due to RES behavior, since the availability during the day of renewable resources will strongly condition the dispatch of the power plants attached to the ordinary regime. The massive integration of renewable energies will require a higher number of starts and stops of the conventional units with a smaller number of hours of operation. In consequence, operating costs and maintenance will increase while the performance is degraded. This effect, in turn, will increase the variable costs of conventional machines. Thus, with greater integration of renewable generation in electric systems, the conventional dispatchable generation must face at all times the so-called operational requirement: the expected demand minus the non-manageable generation [36].

Impacts of massive inflow from renewable sources will be notorious in the total installed power, especially to cover the demand at times of low availability of renewable resources; more use of adjustment mechanisms; and the inevitable spills of renewable energy to guarantee safe operation. These effects of RES are expected to affect the LFC structure and regulation capabilities. To analyze RES impacts in frequency control, renewable sources need to be considered in an aggregated way. However, with the increased integration and penetration levels, the active power production from RES power must be considered in the traditional LFC regulation.

4.1. LFC regulation in power system including RES

For the particular case of the LFC, the introduction of RES increases the production of active power for a given area. But this energy is commonly considered as a disturbance if the RES is not taking part of the frequency regulation control loops. This is shown in Figure **4-1**, with

many of the variables being as defined in Section 2.2.4. Usually, the inclusion of RES often implies the substitution of conventional generation, with the corresponding loss of inertia. As presented in Chapter 3, decreasing inertia will have a deep impact on the regulation capabilities of the LFC.

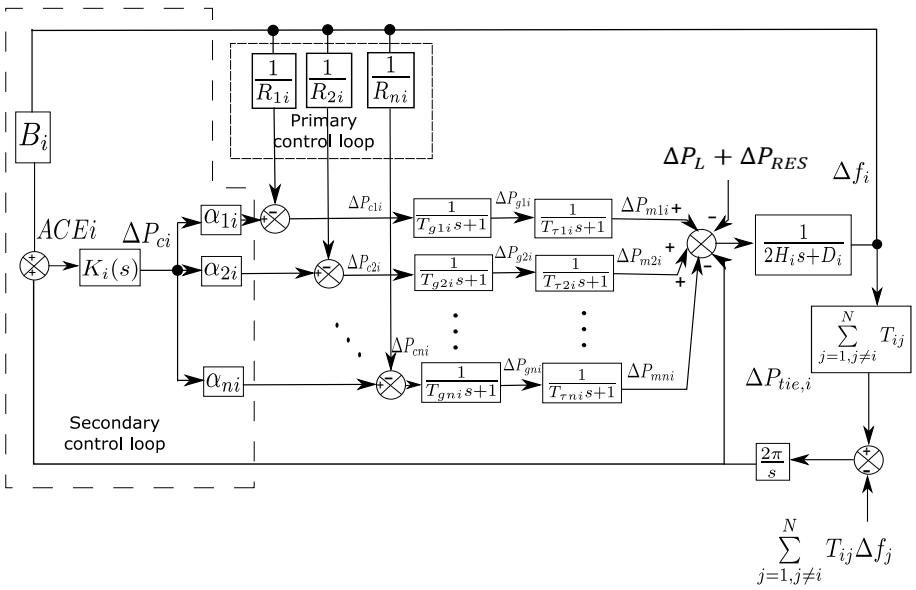

Figure 4-1: LFC scheme for a multi-area (N areas) power system, including primary and secondary control loops [6] and RES as disturbance.

4.1.1. Model for LFC regulation including RES

Let us assume that a given area i has m_1 conventional units and m_2 renewable generation sources. The total inertia H_{tot} can be calculated as the sum of the aggregated inertias $H_{conv,i}$ and $H_{RES,i}$ from conventional and renewable units respectively, then:

$$H_{tot,i} = H_{conv,i} + H_{RES,i} = \sum_{k=1}^{m_1} H_{conv,k} + \sum_{k=1}^{m_2} H_{RES,k} \tag{4-1}$$

From figure **4-1**, we can extract the following relationship expressing the frequency change for the area i with RES as disturbance:

$$G_i(s) = \frac{1}{2H_{tot,i}s + D_i}, \tag{4-2}$$

$$\Delta f_i(s) = G_i(s)\left[\sum_{k=1}^{m1}\left(B_i K(s)\alpha_k - \frac{1}{R_k}\right) M_k(s)\Delta f_i(s) - \Delta P_{tie,i}(s) - \Delta P_{RES}(s) - \Delta P_L(s)\right]$$

where

$$\sum_{k=1}^{m1} B_i K(s) \alpha_k \Delta f_i = \Delta P_{C_k}(s). \tag{4-3}$$

The term $\Delta P_{C_k}(s)$ is the control signals from secondary regulation. After some algebraic operations, equation (4-2) becomes:

$$\Delta f_i(s) = \frac{1}{z(s)} \left[\sum_{k=1}^{m1} \Delta P_{C_k}(s) M_k(s) - \Delta P_{tie,i}(s) - \Delta P_{RES}(s) - \Delta P_L(s) \right] \tag{4-4}$$

with

$$z(s) = 2H_{tot,i}s + D_i + \sum_{k=1}^{m1} \frac{M(k)}{R_k} \tag{4-5}$$

Equation (4-4) expresses the frequency variations of area i without RES participation in frequency regulation. In order to study the system response, let $\Delta P_L(s) = \dfrac{\Delta P_L}{s}$ represent a step load disturbance. This step disturbance is applied to area i, resulting in:

$$\Delta f_i(s) = \frac{1}{z(s)} \left[\sum_{k=1}^{m1} \Delta P_{C_k}(s) M_k(s) - \Delta P_{tie,i}(s) - \Delta P_{RES}(s) - \frac{\Delta P_L}{s} \right] \tag{4-6}$$

Assuming a simple first-order model for the turbine-governor group [42], machine dynamics can be represented as

$$M_k(s) = \frac{1}{(T_{g_k}s + 1)(T_{t_k}s + 1)}, \tag{4-7}$$

with T_{g_k} and T_{t_k} the governor and turbine time-constants, respectively. Replacing this expression in equation (4-6), and using the final value theorem, the steady-state frequency deviation $\Delta f_{ss,i}$ is:

$$\Delta f_{ss,i} = \lim_{s \to 0} s \Delta f_i(s) = \frac{R_{tot,i}(\Delta P_{C_k} - \Delta P_{tie,i}(0) - \Delta P_{RES} - \Delta P_L)}{DR_{tot,i} + 1} \tag{4-8}$$

The expression in equation (4-8) indicates the elimination of frequency deviations if secondary regulation can match the magnitude of load and RES disturbances (assuming $\Delta P_{tie,i}(0) \approx 0$). In this way, the lack of involvement of RES in frequency regulation can influence negatively on the frequency response characteristic of the system.

On the other hand, applying the inverse Laplace transformation to equation (4-4), we get:

$$2H_{tot,i}\frac{d\Delta f_i(t)}{dt} + D\Delta f_i(t) = \left[\sum_{k=1}^{m1} \Delta P_{C_k}(t) M_k(t) - \Delta P_{tie,i}(t) - \Delta P_{RES}(t) - \Delta P_L(t) \right] = \Delta P_{bal}(t)$$

(4-9)

Similar to equation (4-8), the term $\Delta P_{bal}(t)$ indicates that the equilibrium between load and generation is being affected for load disturbances and RES variations. For the instants after a disturbance ($t = 0$), $\Delta P_{bal}(t)$ is:

$$\Delta P_{bal}(t) = 2H_{tot,i}\frac{d\Delta f_i(t)}{dt}, \tag{4-10}$$

and consequently,

$$\frac{d\Delta f_i(t)}{dt} = \frac{\Delta P_{bal}(t)}{2H_{tot,i}}. \tag{4-11}$$

Equation (4-11) evidences that frequency changes are inversely proportional to the system inertia $H_{tot,i}$. However, many of the most widely employed generation systems based on RES directly lack inertia or contribute in a drastically smaller rate than conventional units [88]. Therefore, equation (4-1) would depend almost exclusively on the conventional units; and most of the times it will result in a power system area with less inertia than the same system with purely conventional generation.

4.1.2. Quantifying Inertia Variation with RES

Let $H_{base,i}$ denote the inertia of area i with only conventional generation units. Let define r_{RES} as the fraction of inertia from RES and r_r as the fraction of conventional generation inertia that is reduced in the presence of RES. We need to acknowledge that power replacement is different than inertia reduction [21]. In this case:

$$H_{tot,i} = H_{base,i}(1 + r_{RES} - r_r) \tag{4-12}$$

Clearly, equation (4-12) shows how the value of $H_{tot,i}$ depends on the relationship $r_{RES} - r_r$:

- If $(r_{RES} - r_r) > 0$, then $H_{tot,i} > H_{base,i}$. This is the unlikely case where RES sources actually contribute to system inertia and this parameter actually increases. In this case, performance of frequency regulation would be improved.
- If $(r_{RES} - r_r) = 0$, then $H_{tot,i} = H_{base,i}$. Inertia contribution from RES actually matches the reduced inertia from conventional sources.
- If $(r_{RES} - r_r) < 0$, then $H_{tot,i} < H_{base,i}$. This is the most common case, and it actually illustrates the inertia reduction produced in the area when RES sources are integrated.

Inertia variations also affect system parameters such as speed droop R and frequency bias coefficient B. Denoting by subindex *base* and *new* the parameters of area i with only conventional generation units and with RES integration, respectively, the following equations express the updated parameter values:

$$R_{new,i} = \frac{R_{base,i}}{1 + r_{RES} - r_r} \tag{4-13}$$

$$B_{new,i} = \frac{1}{R_{base,i}}(1 + r_{RES} - r_r) + D_i \tag{4-14}$$

For the sake of simulation, the effects described here are illustrated using the same system studied in Chapter 3. A 20 % of conventional generation is replaced by wind farms with zero inertia contribution: $r_{RES} = 0$ and $r_r = 0{,}2$. System parameters are updated using equations (4-12) to (4-14), and then Control Sensitivity Functions are extracted and analyzed (see Figure **4-2**).

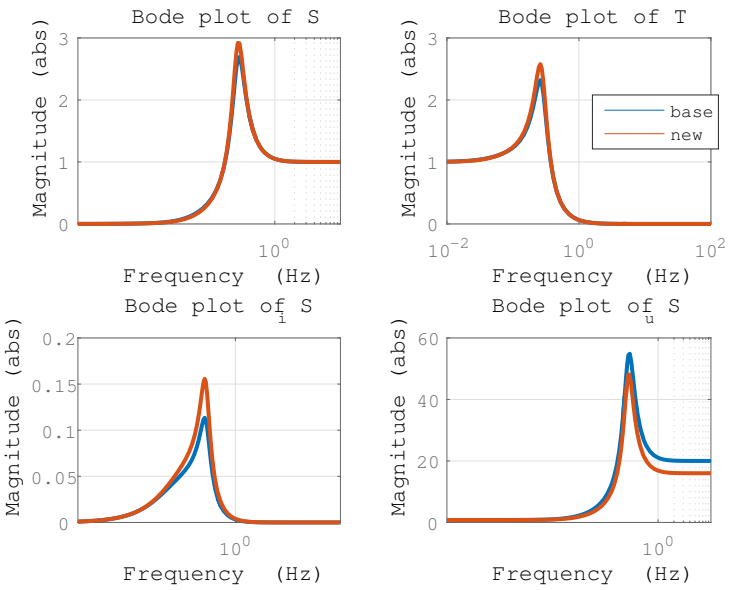

Figure 4-2: Sensitivity functions for a system with pure conventional generation (red) and after a 20 % RES penetration with inertia reduction (blue).

Despite the adjustments in system parameters due to RES sources, Bode plots of Control Sensitivity Functions show similar behavior to the case of inertia variations presented in Chapter 3. Figure **4-2** shows almost identical performances from Sensitivity S and Complementary Sensitivity T, with slightly worse conditions for the system with diminished inertia.

An increased region of influence to input disturbances can be observed from the plot of disturbance sensitivity S_i. Additionally, the performance curve for Control Sensitivity S_u indicates a reduced impact of the control actions when the inertia decreases due to RES integration. In consequence, Control Sensitivity Functions confirm that consideration of the RES sources as disturbances to LFC without contributing to system inertia degrades the performance of the control system.

The analysis of Control Sensitivity Functions is verified after the integration of a wind farm to the power system, representing a 20 % inertia reduction. Figure **4-3** presents frequency deviations after wind integration for both the base case and the new case with reduced inertia. Although both curves show the same behavioral trend, the reduced inertia case reaches larger peaks than the base system with purely conventional generation. Despite the adjusted system parameters for the inertia reduction, the frequency deviations for this case present more peaks outside the operational boundaries. Even if the differences seem pretty slight in absolute units, the system operator may have to face sanctions for frequency peaks over 0.6 in absolute value. As the model presented here suggests, there is a need for inertia contribution from RES sources to maintain the frequency regulation inside the standard operating conditions.

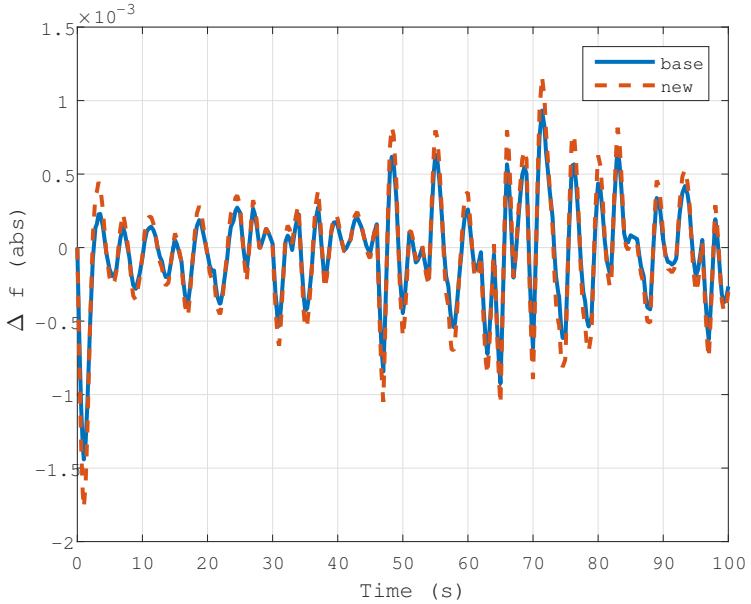

Figure 4-3: Frequency deviations with wind generation as a disturbance for a system with pure conventional generation (blue) and after a 20 % RES penetration and the corresponding inertia reduction and parametric variations (dashed red).

4.2. Inclusion of Variable Speed WT in LFC

This work only considers variable-speed DFIG-WT, as they are the best-suited WT for active participation in grid ancillary services [53]. However, WT units with DFIG do not present a natural inertial response to frequency changes [6]. For enabling frequency response capabilities to the DFIG-WT, a synthetic inertia control strategy [51] was employed. This technique proposes operating the DFIG-WT below the point of maximum power extraction to maintain a reserve of kinetic energy to be used for frequency compensation. The operating point P_o depends on the DFIG angular speed w_r and the so-called operational torque T_o $[N\ m]$, calculated as indicated in equation (4-15):

$$T_{op} = K_{op} v^2. \tag{4-15}$$

for different values of wind speed v. Gain K_{op} is adjusted for operating the WT under the curve formed by the points of maximum withdrawable power from wind at each speed.

For the electromagnetic component of the DFIG, the simplified model proposed in [69, 25] is used and included in the LFC as the *wind-turbine model* block in Figure **4-4**. This representation, denominated as *synthetic-inertia model*, is a reduced induction-machine model of fourth order and only uses the quantities in q-axis, as the d-axis is selected as the reference frame. Figure **4-5** presents both models.

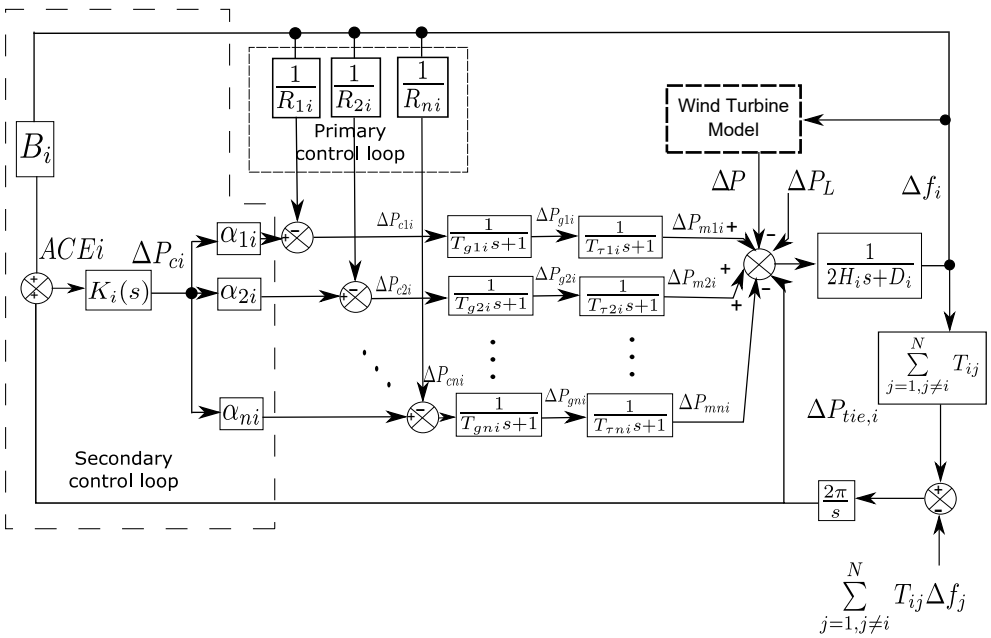

Figure 4-4: LFC scheme for a multi-area (N areas) power system, including primary and secondary control loops [6]. The block "Wind Turbine Model" integrates WT to LFC.

In the scheme of Figure **4-5**, P_{base} is the nominal power of the area, w_r is the angular speed of rotor, n is the quantity of WTs, v_{qr} is the rotor quadrature voltage, i_{qr} is the rotor quadrature current, $iq_{r,r}$ is the reference quadrature current for rotor, PIv_{qr} is the PI controller for v_{qr}, T_e is the electromagnetic torque, T_m is the mechanical torque, β is the blade pitch angle, β_r is the blade pitch angle reference, τ_β denotes the time delay of pitch angle actuator, $w_{r,r}$ is the rotor angular speed reference, PIv_{qr} is the PI controller for w_r, v_r is the rated wind speed of WT, K_1 is the proportional action of primary control, K_2 is the proportional action of secondary control, K_w and T_w are the gain and time delay of secondary control loop, J is the inertia moment of WT, and X_1 X_2, X_3 and T_1 are approximately constant values representing some combinations among DFIG internal generator parameters (see [69, 70] for detailed explanation).

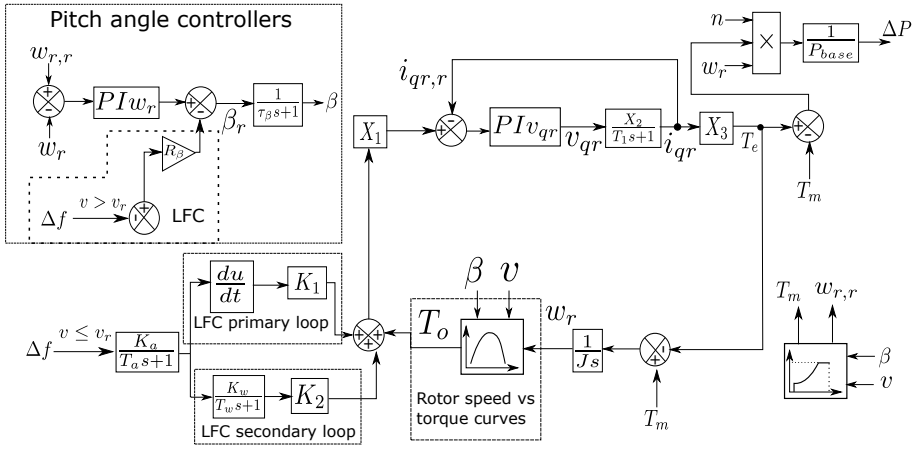

Figure 4-5: Wind turbine model with frequency response and variable wind speed (based on [25]).

As shown in Figure **4-5**, several control loops are added to the simplified turbine model to emulate the behavior of the different control stages of the LFC structure and to keep the stable operation of the DFIG WT after contributing to frequency regulation. These loops are described as follows:

1. A primary response loop for the DFIG labeled as *LFC primary loop* in Figure **4-5**. Proportional gain K_1 is modulating the frequency change rate $\frac{d\omega}{dt}$. Similar to the primary response of conventional units, this loop offers a fast action time.

2. A secondary response loop marked as *LFC secondary loop* in Figure **4-5** operating in the same way as the secondary control of LFC. The power delivered by WT is restored to the nominal operating point after a control of frequency disturbances.

3. The *pitch-angle controller* loop in Figure **4-5**, tasked with maintaining the angular speed of the WT at nominal operating wind speed values equal or over the rated ones.

Under the pitch control action, in case of a frequency disturbance occurring, an additional control loop is required for modulating pitch angle with a gain R_β proportional to the frequency deviation.

The area deviation frequency signal is filtered (through a filter with gain K_a and time delay T_a, see Figure **4-5**) before being applied to the primary and secondary control loops. Here, we compare the mentioned loops for two different secondary controllers in frequency regulation. The following subsections describe the PI and linear quadratic regulator (LQR) secondary controllers (see $K_i(s)$ block in Figure **4-4**), and their interaction with the WT control scheme.

4.2.1. Considerations for system with secondary PI controller

PI controllers constitute the traditional strategy for secondary regulation in LFC system. Starting from a simple Single-Input Single-Output (SISO) loop [27], the transfer function $C_{PI}(s)$ of the PI controller is $C_{PI}(s) = K_p(1 + (T_r s)^(- 1)$. The term K_p is the Proportional gain, T_r is known as the reset time [27], and the relationship $K_p(T_r)^(- 1)$ is called the integral gain. Here, additional PI controllers regulate quadrature rotor current (PIi_{qr}) and the pitch angle (PIw_r), as shown in Figure **4-5**.

4.2.2. Considerations for LFC system with secondary LQR controller

Criterion-based synthesis of controllers is a design technique driven by the complexity of multi-variable systems. A commonly employed set of criteria is formed by cost functions related to quadratic forms of control effort and error signals [27]. For linear case, the so-called Linear Quadratic Regulator expresses the problem as the feasible solving of the dynamic Riccati equation in continuous time, leading to a time-variable state feedback [27].

For this configuration, secondary controller $K_i(s)$ requires a state-space representation of the whole LFC. Equations (4-16) to (4-25) describe the complete non-linear state-space model for a multi-area power system with integration of WT to the LFC scheme, adapted from [49]. This representation includes the transferred power between areas ΔP_{tie} as a state, with an additional state equation for WT pitch-angle β (see equation (4-22)) as a parameter with high influence in the contribution of WT to LFC [9].

$$\Delta \dot{f} = \frac{\Delta P_m - D\Delta f - \Delta P_L}{2H} - \frac{\Delta P_{tie}}{2\pi} + \left(\frac{X_3 w_r i q_r n - P_{ref}}{P_{base}} \right) \frac{\Delta f}{2H} \tag{4-16}$$

$$\Delta \dot{P}_{tie} = 2\pi \sum_{j=1}^{N} T_{i,j} \Delta f + \frac{\Delta P_c}{T_g} - 2\pi v_i \tag{4-17}$$

$$\Delta\dot{P}_m = \frac{-\Delta P_m}{T_\tau} - \frac{\Delta P_g}{T_g} \tag{4-18}$$

$$\Delta\dot{P}_g = \frac{-\Delta f}{RT_g} - \frac{\Delta P_g}{T_g} + \frac{\Delta P_c}{T_g} \tag{4-19}$$

$$\dot{i}_{qr} = \frac{-i_{qr}}{T_1} + \frac{v_{qr}}{T_1} \tag{4-20}$$

$$\dot{w}_r = \frac{-X_3 i_{qr}}{J} + \frac{T_m}{J} \tag{4-21}$$

$$\dot{\beta} = \frac{-\beta}{\tau_\beta} + \frac{\beta_{ref} + R_\beta \Delta f}{\tau_\beta} \tag{4-22}$$

Mechanical torque T_m is calculated from parameters such as air density, length of turbine blades, and WT power coefficient C_p (fraction of available wind power being extracted). Differences with [49] involve the consideration of pitch angle reference β_{ref} as an input, and wind speed v and frequency deviation of neighboring areas Δf_j as outputs. Complete vectors of system inputs U and disturbances W are shown below, with ΔP_L being the deviations in demanded-load.

Mechanical torque is calculated dividing equation (4-23) by the angular rotor speed:

$$P_m = \frac{1}{2}\rho\pi R^2 v^3 C_p. \tag{4-23}$$

where ρ represents air density, R is the length of the turbine blades, and the power coefficient C_p denotes the fraction of available power in the wind that is being harvested. This parameter is a function of the Tip-Speed Ratio (TSR) denoted by $\lambda = \frac{Rw_r}{v}$, and the collective blade pitch β.

$$U^T = \begin{bmatrix} v_{qr} & \Delta P_c & \beta_{ref} \end{bmatrix}, \qquad W^T = \begin{bmatrix} \Delta P_L & \Delta f_j & v \end{bmatrix} \tag{4-24}$$

Finally, vector Y presents system outputs in equation (4-25). The first output is the rotor quadrature current i_{qr}, whose reference is given by $i_{qr,r}$. The second output is the system Area Control Error (ACE), reference signal for the LFC secondary controller ($ACE = \Delta f + \Delta P_{tie}$). The last output is the rotor angular speed, whose reference is defined for a given mechanical torque.

$$y^T = \begin{bmatrix} iq_r & \beta\Delta f + \Delta P_{tie} & w_r \end{bmatrix}. \tag{4-25}$$

4.3. Case of study

4.3.1. Description

A slightly modified version of the WSCC 9-bus power system [3] was employed for simulating the DFIG participation in the LFC for a multi-area power system. This system was partitioned into three areas, as illustrated in Figure **4-6**. The modified system parameters are summarized in Table **4-1**. Consider Generator 1 as hydraulic and Generators 2 and 3 as gas units. For the sake of this work, 50 % of conventional generation in Area III was replaced by a wind farm. The wind farm was formed by 32 DFIG WT of 2 MW each, whose model parameters are shown in Table **4-2**. Wind speed was simulated from a normally distributed random signal with a period of 50 s, mean value of 12,5 m/s and variance of 2,8 m/s. Finally, load disturbances were applied as follows: an increment of 0.06 $[p.u]$ at 30 seconds of operation in area III; a variation of magnitude 0.08 $[p.u]$ at 60 seconds in area II; and another disturbance of 0.01 $[p.u]$ at 90 seconds for area I. The Power Base was set at 100 MVA.

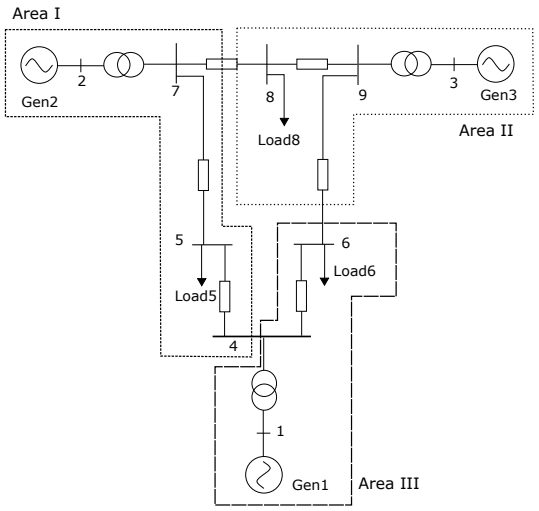

Figure 4-6: WSCC 9-bus system multi-area partitioning. System parameters can be found in [3].

4.3.2. Tuning of PI controllers

PI controllers for secondary frequency regulation in each area were tuned using the Gradient Descent method, along with PI controllers of rotor angular speed w_r and rotor quadrature voltage v_{qr}. Table **4-3** presents their parameters.

Table 4-1: WSCC 9 bus system parameters [3].

Parameter	Value	Parameter	Value	Parameter	Value
H_1	23.64 s	T_{12}	2.064 p.u.	R_1	2 p.u.
H_2	6.4 s	T_{13}	6.1191 p.u.	R_2	10 p.u.
H_3	1.505 s	T_{23}	14.4353 p.u.	R_3	7.5019 p.u.
MVA_{nom1}	247.5	$D1, D2, D3$	0.8	B_1	2.8 s
MVA_{nom2}	192	$Tg1, Tg2, Tg3$	0.2	B_2	10.8 s
MVA_{nom3}	128	$T_{\tau}1, T\tau 2, T\tau 3$	0.3	B_3	8.3 s

Table 4-2: Wind-turbine model simulation parameters [51].

Parameter	Value	Parameter	Value
P_{nom}	2 MW	R_s	0.00491 p.u.
V_{nom}	966 V	X_{ls}	0.09273 p.u.
K_1	5000 Nm	X_m	3.96545 p.u.
K_2	2000 Nm	R_r	0.00552 p.u
T_w	1	X_{lr}	0.1 p.u.
K_a	500	H	4.5 s
T_a	20	J	506.6059 Kgm^2.

Table 4-3: Parameter values for the different PI controllers in simulation for the case of study.

Controller	Proportional Gain k_P	Integral Gain k_I
PI Area I	0	-0.05
PI Area II	0	-0.05
PI Area III	0	-0.28
PI v_{qr}	0	2.70
PI w_r	7.19	0.53

4.3.3. Tuning of LQR controller

To calculate the gains of LQR controller with reference tracking, a linearization must be performed in the non-linear state-space model described by equations (4-16) to (4-22). This process results in the operating point vectors $U_{op}^T = [27{,}97\ 0{,}08\ 9]$ for the inputs and $W_{op}^T = [0{,}2\ 0\ 12]$ for disturbance signals. Design of LQR controllers for secondary LFC implies the tuning of the positive definite matrices Q_{area} and R_{area} for each area. The adjusted matrix elements are listed in Table **4-4**.

Table 4-4: Parameter values for the different PI controllers in simulation for the case of study. Matrix dimensions for area III are different due to the presence of wind generation.

Parameter	Value
Q_{area1}	$diag([1, 1, 10^{-1}, 10^{-1}, 10^{3}])$
Q_{area2}	$diag([1, 1, 10^{-1}, 10^{-1}, 10^{3}])$
Q_{area3}	$diag([10^{2}, 10^{2}, 5, 5, 10^{-2}, 10^{-2}, 10^{-2}, 1, 10^{6}, 10^{2}])$
R_{area1}	10^{7}
R_{area2}	10^{2}
R_{area3}	$diag([10^{2}, 10^{6}, 10^{9}])$

4.3.4. Comparison between PI and LQR controlled LFC

Simulations were performed on the selected benchmark with models and conditions previously described. Figures **4-7** and **4-8** depict frequency deviations for areas II and III respectively, as they present more significant variations than area I. Load disturbance in area III at 30 s causes the most notorious effects, not only in the local frequency deviation but also in the other areas as well. This behavior could be attributed to the inertia reduction in area III and some latency in the operation of WT control loops: power transferred to area III increases as WT contributions in frequency regulation start.

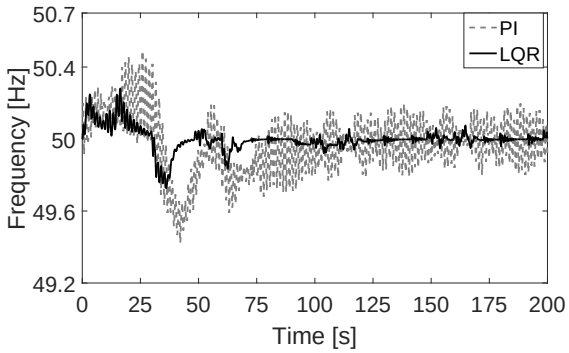

Figure 4-7: Frequency deviation in area II. LQR achieved a reduction of 0.32 Hz over PI response in maximum value.

On the other hand, the overall magnitude of the frequency deviations over the total simulation time is smaller for the LQR controller in each area. Fewer variations would mean less stress in the regulation systems, a key factor as RES penetration increases. Additionally, longer recovery and settling times can be seen for PI controllers at each area, giving the LQR a better overall performance for secondary control design in the studied case.

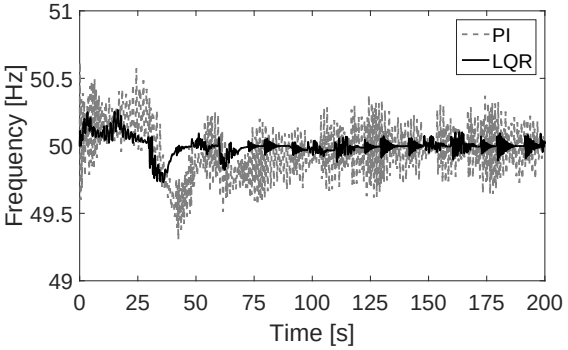

Figure 4-8: Frequency deviation in area III. Peak deviation value for PI was 0.17 Hz larger than LQR.

Figure **4-9** shows the exchanged powers between area III and the other areas. In this case, LQR reduces the power exchanged with other areas when compared with PI response. However, a continued oscillation in power is observed, due to wind variability causing fluctuations in WT generation. This variation makes area III more sensitive to sudden changes in load, as confirmed when the most significant power deviations appear at the same time as the load disturbances occur. With a load disturbance in area III at 30 s, LFC system requires an increase in power transference from the other areas to mitigate frequency fluctuations. However, the exchanged power in area III stabilizes as WT start contributing to frequency regulation. Figure **4-10** shows the power generated by the wind farm in area III.

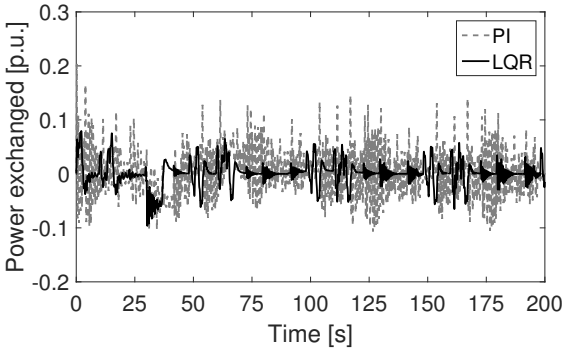

Figure 4-9: Inter-area power exchange deviation for area III.

Focusing on DFIG-WT performance, an analysis of the control efforts for both LQR and PI strategies in area III is required. Control actions for the pitch-angle β_{ref} are smaller for LQR than for PI controller, as seen in Figure **4-11**. This behavior seems to indicate that WTs are less stressed with the LQR controller. However, the total control effort of the secondary control ΔP_c is higher for the LQR than for the PI scheme, as shown in Figure **4-12**. LQR is imposing an aggressive control action in the conventional unit of area III, diminishing

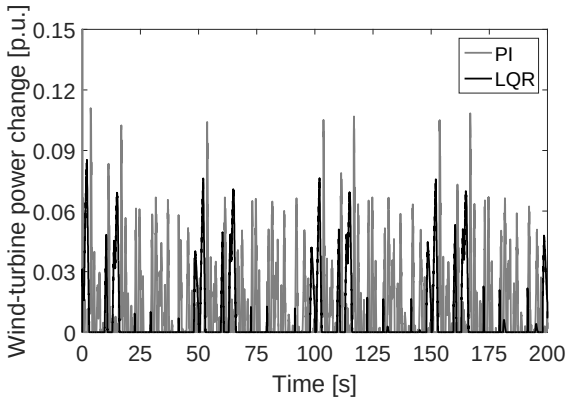

Figure 4-10: Variations in power generated by the wind farm in area III.

the stress in WT contributions to frequency regulation. This, in turn, reduces frequency fluctuations due to wind variability for the LQR in this area.

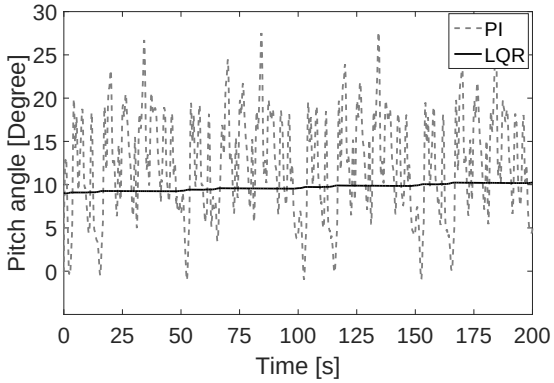

Figure 4-11: figure
Magnitude of control action for variable β_{ref} in area III

4.4. Summary

This chapter examined the integration of the renewable sources to LFC. Starting with the consideration of RES units as disturbances to frequency regulation tasks, the effects on system inertia were highlighted. The expressions from the studied model showed the consequences of the reduced inertia in frequency control. The analysis through Control Sensitivity Functions and the time-response of the system has shown the need for some inertia contribution from the RES-based units to maintain the operational conditions of the power system.

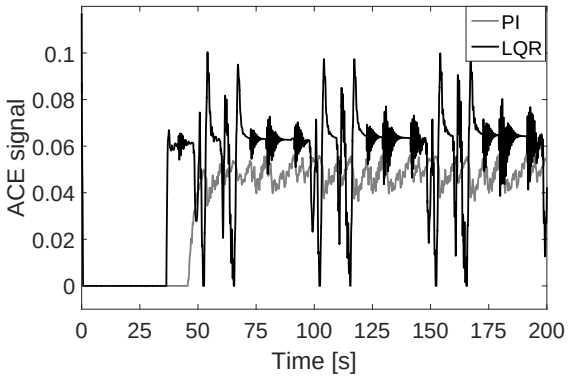

Figure 4-12: figure
Magnitude of control action for variable ΔP_c in area III.

In this sense, we also studied the performance of variable-speed wind turbines integration to the LFC structure of power systems. With inertial response emulation methodology, DFIG-WT were included in the primary regulation stage of the LFC. Two controllers were compared for secondary regulation in the test system, using PI and LQR structures. The LQR presented a better overall performance than the PI controller. For every explored case, frequency deviations under LQR strategy were smaller and the settling times of the output variables were also lower than the PI-controlled results. Furthermore, LQR operation diminished control efforts of WT. LQR controller is based on the system model, and it achieved acceptable performances despite the mandatory requirement for linearization of the state-space representation. An unwanted overshoot in area III frequency appeared for both strategies with sudden wind variations. This reaction occurs because the operating point of the system is changing with every value of wind speed. This effect was more notorious for LQR configuration, as the model implemented included wind speed as a disturbance. When the operating point changed, linearization might have led to the inadequate representation of the nonlinear system. Neither PI nor LQR presented a total disturbance rejection, and wind variability may require the pairing of WT with "continuous" generation to reduce operational uncertainty.

Usually, system inertia is calculated empirically. However, the actual value of inertia could differ from the estimated value. This effect could be accentuated by contributions of renewable energy sources, as evidenced by the analysis of this chapter. In consequence, a sensitivity analysis is required to assess the impacts of parametric variations in inertia when RES sources are integrated to frequency regulation.

5 Sensitivity Analysis of Frequency Regulation in Power Systems with Wind Units

In power systems, frequency constitutes a parameter indicating the equilibrium between power demanded by load and energy produced by generation systems [3]. When this relationship is unbalanced, control structures are in place to return the system frequency to operational values in the so-called Load Frequency Control (LFC) of power systems. However, traditional frequency control strategies were developed for a power system with almost complete reliance on conventional energy sources, and penetration of Renewable Energy Sources (RES) may require the participation of these new units in the control tasks [16].

Wind is the fastest rising and most widely deployed renewable energy source around the world [71]. Variable Speed Wind Turbine Generators (VSWTG) are the most popular devices for extracting electrical power from wind. VSWTG operation requires the action of electronic power converters for effectively decouple the rotor angular speed of the wind generating unit from the electrical frequency of the grid. Consequently, VSWTG does not contribute directly to the natural inertial response of the system under frequency disturbances and other operational events [94].

However, the increment of wind generators and the unpredictability and variability associated with the resource increase the difficulty level of the frequency regulation tasks in power systems. In future grid operating normative, the participation of wind turbine generators in system frequency regulation might become mandatory. Hence, several studies have been proposed about control strategies for the active inclusion of VSWTG in LFC loops. Complete reviews can be found in [17, 21, 94]. Among many other techniques, the required primary reserves for frequency regulation contributions from Wind Turbine Generators can be supplied through de-loaded operation (under the point of maximum power extraction) of the WTG and the addition of control loops, emulating the response of conventional units (inertia and droop controllers) [94, 67].

This chapter focuses on analyzing the effects of parameter variations in the frequency regula-

tion structure of power systems involving wind generation. Sensitivity functions with respect to inertia are established using linearized models and transfer function representations for the system components.

Sensitivity analysis has been previously employed in the assessment of the dynamic performance of power systems. Nanda and Kaul [55] explored the optimal tuning of automatic generation controllers in a multi-area power system with conventional steam generation units. The role of inertia was studied through sensitivity tests in the development of a composite load model for Western Systems Coordinating Council with conventional machines [65]. For scenarios considering renewable energy sources, the impacts of damping and inertia in the dynamic performance of grid frequency were studied in [7], looking for the best locations to provide emulated inertia. Additionally, the behavior of DFIG wind units in power systems was studied using eigenvalue sensitivities with relation to inertia [26]. However, these works do not consider an explicit function for the sensitivities of the system, basing their results in different simulation scenarios. In this regard, transfer functions for power systems frequency regulation elements are developed in [33, 34] for conventional-only scenarios, and extended in [67] for assessing the effects of load damping including wind farms.

Amidst this context, this chapter studies the effects of varying different system parameters on the overall performance of the traditional LFC system when including contributions of renewable energy systems such as VSWTG. Through both theoretical analysis and performance simulations, the impact of an inaccurate representation of system parameters such as inertia H is established.

5.1. Linearization of the Wind Turbine Model

In Chapter 4, the integration of RES to the LFC was presented using a non-linear wind turbine model. Now, a linearized version of that wind turbine model is required to extract the sensitivity expressions of the LFC parameters in presence of wind generation. If wind turbines are contributing to frequency regulation, the linearized representation must include changes of the area frequency Δf and wind speed variations v. In the same way as the LFC, frequency regulation contributions can come from the variation of mechanical or electrical power in response to grid frequency changes.

Frequency contribution from wind turbines is possible due to so called de-loaded operation [94]. In this mode, the wind turbine operates under the point of maximum power extraction (MPP) to generate the active power reserve employed to contribute to frequency control tasks. This active power reserve P_{cont} (p.u) is:

$$P_{cont} = P_{MPP} - P_{und} = (1 - X_u)\, K_{wind}\, \omega^3 \tag{5-1}$$

where ω denotes the rotor speed, $X_u \in (0,1)$ is a weighting factor expressing the fraction of maximum power at de-loaded operation point [67], P_{und} is the de-loaded power, P_{MPP} is the maximum power extracted at the operating speed, and K_{wind} is a constant parameter depending on the characteristics of the wind turbine [87]. In operation, ω_{MPP} and ω_{und} are the rotor angular speeds at P_{MPP} and P_{und} respectively. According to [15], the power P_{uref} and torque τ_{uref} for operation at determined wind speed are:

$$P_{uref} = P_{und} + (P_{MPP} - P_{und})\frac{(\omega_{und} - \omega)}{(\omega_{und} - \omega_{MPP})} \tag{5-2}$$

$$= X_u\ K_{wind}\,\omega^3 + K_{wind}\,\omega^3 \frac{(1 - X_u)\ (\omega_{und} - \omega)}{(\omega_{und} - \omega_{MPP})} \tag{5-3}$$

$$\tau_{uref} = X_u\ K_{wind}\,\omega^2 + K_{wind}\,\omega^2\ \ \frac{(1 - X_u)\ (\omega_{und} - \omega)}{(\omega_{und} - \omega_{MPP})} \tag{5-4}$$

Figure **5-1** illustrates the model of WT with the control loops for frequency contribution from wind turbines. According to this figure, variations in electrical torque $\Delta\tau_{e,cont}$ can be expressed as:

$$\Delta\tau_{e,cont}(s) = \frac{\Delta P_{e,cont}(s)}{\omega_0} = (-1)\left[\frac{1/R_w + K_n s}{\omega_0}\right]\Delta f(s) \tag{5-5}$$

In equation 5-5, $\Delta P_{e,cont}$ denotes electrical power variations related to changes in frequency,

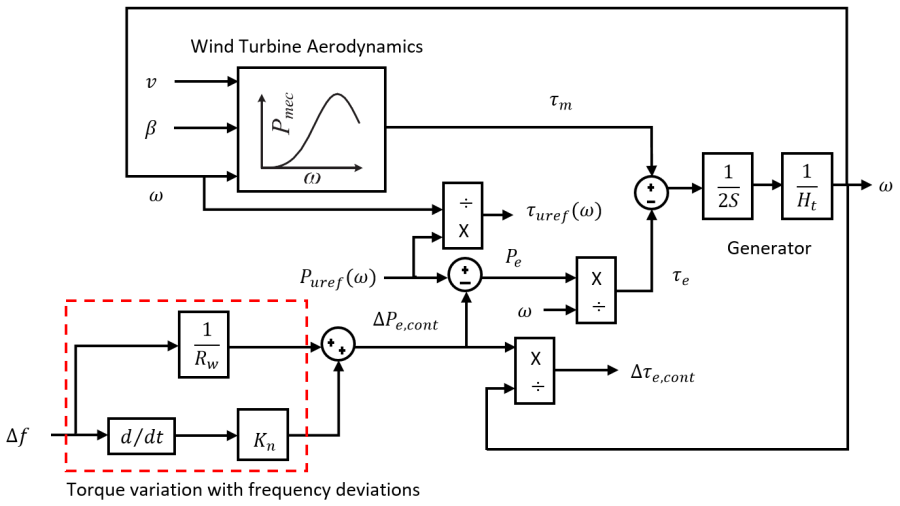

Figure 5-1: Model of variable speed WT for LFC support

ω_0 is the current angular speed of the rotor, K_n is a parameter weighting the inertia control loop, and R_w is a parameter similar to the speed droop R of the LFC regulation. The latter parameters are responsible for inertial emulation from WT, with dynamic performance

improving with both low values of R_w and high values of K_n [15]. Let the linearized dynamic operating electrical torque be:

$$\Delta\tau_{uref}(s) = \frac{\partial\tau_{uref}}{\partial\omega}\Delta\omega(s) \tag{5-6}$$
$$= \left[2K_{wind}\,\omega_0\,X_u + 2K_{wind}\,\omega_0(1-X_u)\cdot\frac{(\omega_{und}-\omega_0)}{(\omega_{und}-\omega_{MPP})} - \frac{K_{wind}\,\omega_0^2\,(1-X_u)}{(\omega_{und}-\omega_{MPP})}\right]\Delta\omega(s).$$

The total variation in electrical torque ($\Delta\tau_e$) can be presented in terms of $\Delta f(s)$ and $\Delta\omega(s)$ as follows:

$$\Delta\tau_e(s) = \Delta\tau_{e,cont}(s) + \Delta\tau_{uref}(s) = (-1)\left[\frac{1/R_w + K_n s}{\omega_0}\right]\Delta f(s) + \frac{\partial\tau_{uref}}{\partial\omega}\Delta\omega(s). \tag{5-7}$$

Let denote by v_0 the wind speed (p.u) and ω_0 as the initial angular speed of the rotor at deloading operating point, λ_{ref} and $C_{p,ref}$ be the operational values of the tip speed ratio λ, and the performance coefficient $C_p(\lambda,\beta)$ of WT for a reference pitch-angle β_{ref}. The mechanical torque τ_m of the turbine is:

$$\tau_m = \frac{K_{wind}C_p v^3}{\omega} \tag{5-8}$$

From equation 5-8, the linearized mechanical torque $\Delta\tau_m(s)$ can be expressed as:

$$\Delta\tau_m(s) = \frac{\partial\tau_m}{\partial\omega}\cdot\Delta\omega(s) + \frac{\partial\tau_m}{\partial v}\cdot\Delta v(s) + \frac{\partial\tau_m}{\partial f}\cdot\Delta f(s);\ \text{with} \tag{5-9}$$
$$\frac{\partial\tau_m}{\partial\omega} = \left(\frac{K_{wind}\,\varsigma\,{v_0}^2}{\omega_0} - \frac{K_{wind}\,C_{p,\mathrm{ref}}\,{v_0}^3}{{\omega_0}^2}\right)$$
$$\frac{\partial\tau_m}{\partial v} = \left(\frac{3K_{wind}\,C_{p,\mathrm{ref}}\,{v_0}^2}{\omega_0} + \frac{K_{wind}\,\varsigma\,\lambda_{\mathrm{ref}}\,{v_0}^2}{\omega_0}\right)$$
$$\frac{\partial\tau_m}{\partial f} = \left(\frac{\varepsilon\,K_{wind}\,K_b\,{v_0}^3}{\omega_0}\right).$$

The expressions for $\varepsilon = \frac{\partial C_p}{\partial\beta}|_{op}$ and $\varsigma = \frac{\partial C_p}{\partial\lambda}|_{op}$ should be calculated depending on the operational conditions λ_{ref} and $C_{p,ref}$. Also, $K_b = \frac{\Delta\beta}{\Delta f} = \frac{\partial\beta}{\partial f}$.

For a wind turbine with a inertia H_w, the swing equation can be employed to obtain and expression for the variations in rotor angular speed $\Delta\omega$ in terms of the grid frequency variations Δf and wind speed changes Δv. Using the functions for $\Delta\tau_e(s)$ and $\Delta\tau_m(s)$, the power swing equation becomes:

$$\Delta\omega(s) = \frac{\Delta\tau_m(s) - \Delta\tau_e(s)}{2H_w\,s}. \tag{5-10}$$

As illustrated in [42], the actual parameter values related with active power production in WT can be obtained with small-signal analysis. Denote by ΔP_e, $\Delta\tau$ and $\Delta\omega$ the small deviations in electrical power P_e, electrical torque τ_e and the angular rotor speed ω respectively. Then,

$$\omega = \omega_0 + \Delta\omega; \tag{5-11}$$

$$\tau_e = \tau_{e0} + \Delta\tau_e; \tag{5-12}$$

$$P_e = P_{e0} + \Delta P_e = \tau_e\,\omega = (\tau_{e0} + \Delta\tau_e)\,(\omega_0 + \Delta\omega)\,, \tag{5-13}$$

where P_{e0}, τ_{e0}, and ω_0 are the initial values for the corresponding parameters previously mentioned. After the expansion of equation (5-13) and neglecting the terms of superior order, ΔP_e can be expressed in terms of the angular speed and electrical torque deviations as:

$$\Delta P_e = \omega_0\,\Delta\tau_e + \tau_{e0}\,\Delta\omega. \tag{5-14}$$

In this context, the initial operating electrical torque τ_{e0} equates the de-loaded torque T_{uref} presented in equation 5-4. Using the previously developed expressions for $\Delta\omega$, $\Delta\tau_e$, and τ_{e0}, the linearized electrical power ΔP_e for a wind turbine in terms of the grid frequency variations Δf and wind speed changes Δv is:

$$\Delta P_e(s) = (\frac{-1}{s+r})\left(\frac{as^2+bs+c}{qs+1}\right)\Delta f(s) + \left(\frac{g}{qs+1}\right)\Delta v(s),\ with \tag{5-15}$$

$$G_{wf}(s) = (\frac{-1}{s+r})\left(\frac{as^2+bs+c}{qs+1}\right) \tag{5-16}$$

$$G_{wv}(s) = \left(\frac{g}{qs+1}\right). \tag{5-17}$$

Parameters g, q, r, a, b, and c are constant terms omitted because of its extension.

5.2. Sensitivity Analysis of LFC to Inertia Coefficient with Wind Turbines

Figure **5-2** illustrates the complete system representation for m_1 conventional units and an aggregated with contribution from m_2 wind generation systems. Note that wind speed variations Δv_j are acting as input parameters, just as the load variations (ΔP_L). The remaining system elements have already been defined in previous sections. The total inertia H_{tot} represents the inertia of conventional units and wind turbines, as in equation (4-12). Usually, this parameter is calculated empirically, but the analysis of previous sections has shown the impact of inertia in frequency regulation. The sensitivity analysis in this section shows the impacts on frequency regulation when the measured value of H is different from the a-priori

calculated one. This is also justified as the emulation inertial from wind turbines could lead to inertia variations (see Chapter 3). Speed droop R and frequency bias coefficient B are also calculated using equations (4-13) and (4-14) respectively.

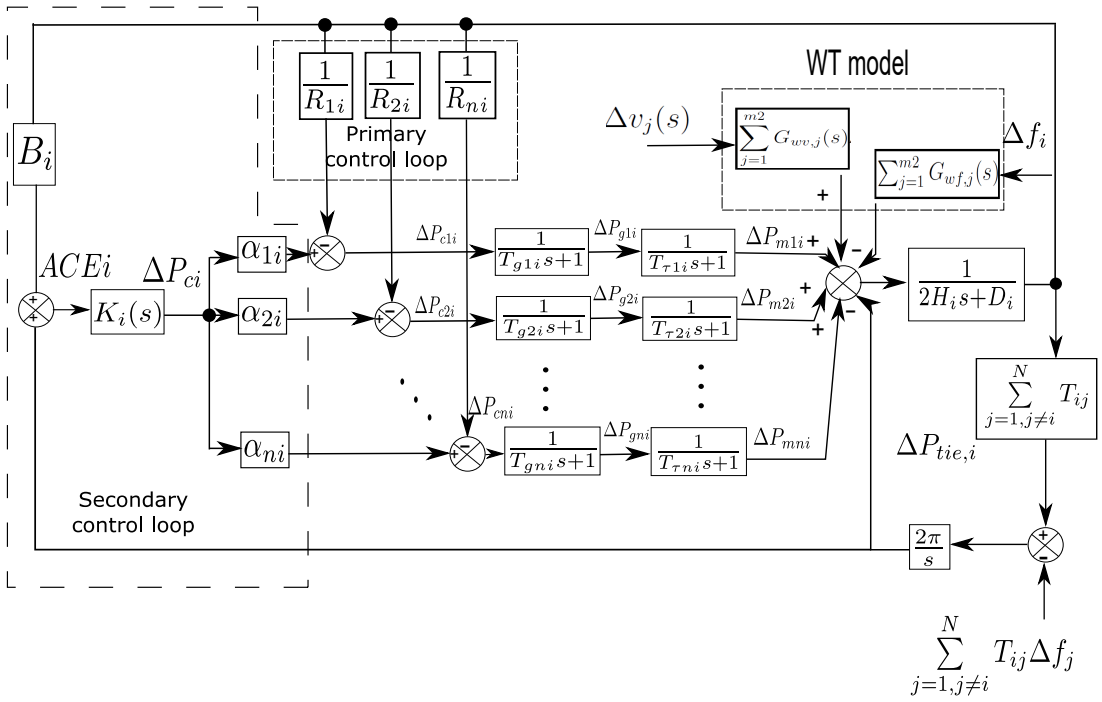

Figure 5-2: Load frequency regulation system with linearized WT model for RES power contributions

From Figure 5.1, the total variations on system frequency Δf can be obtained as the linear composition of the individual responses to each input signal. Let denote with Δf_L the variations in system frequency with respect to load changes ΔP_L. Making $\Delta v_j = 0$, Δf_L is given by:

$$\Delta f_L(s) = \frac{\frac{1}{2H_{tot}s+D}\left\{-\Delta P_L(s)\right\}}{1+\frac{1}{2H_{tot}s+D}\left\{K(s)+\sum_{i=1}^{m_1} M_i(s)+\sum_{j=1}^{m_2} G_{wf,j}(s)\right\}} \tag{5-18}$$

In the same way, denoting with Δf_v the variations in system frequency with respect to wind speed changes Δv_j and making $\Delta P_L = 0$, the following expression is obtained:

$$\Delta f_v(s) = \frac{\frac{1}{2H_{tot}s+D}\left\{\sum_{j=1}^{m_2} G_{wv,j}(s)\Delta v_j(s)\right\}}{1+\frac{1}{2H_{tot}s+D}\left\{K(s)+\sum_{i=1}^{m_1} M_i(s)+\sum_{j=1}^{m_2} G_{wf,j}(s)\right\}} \tag{5-19}$$

The total variations on system frequency $\Delta f(s)$ can be expressed from equations (5-18) and

(5-19), as:

$$\begin{aligned}\Delta f(s) &= \Delta f_L(s) + \Delta f_v(s) \\ &= \frac{\left\{-\Delta P_L(s) + \sum_{j=1}^{m_2} G_{wv,j}(s)\Delta v_j(s)\right\}}{2H_{tot}s + D + \left\{K(s) + \sum_{i=1}^{m_1} M_i(s) + \sum_{j=1}^{m_2} G_{wf,j}(s)\right\}}\end{aligned} \tag{5-20}$$

5.2.1. Sensitivity to inertia H

To represent the effects of inertia variations in frequency regulation, the calculation of $\frac{\partial \Delta f(s)}{\partial H_{tot}}$ is required. Extracting the partial derivative of Δf with respect to H_{tot}, the following expression is obtained from equation (5-20):

$$\begin{aligned}\frac{\partial \Delta f(s)}{\partial H_{tot}} &= \frac{2s\left[\Delta P_L(s) - \sum_{j=1}^{m_2} G_{wv,j}(s)\Delta v_j(s)\right]}{\left[2H_{tot}s + D + \left\{K(s) + \sum_{i=1}^{m_1} M_i(s) + \sum_{j=1}^{m_2} G_{wf,j}(s)\right\}\right]^2} \\ &= \{2s\}\left[\frac{\Delta f(s)}{\left\{\Delta P_L(s) - \sum_{j=1}^{m_2} G_{wv,j}(s)\Delta v_j(s)\right\}}\right]^2 \left\{\Delta P_L(s) - \sum_{j=1}^{m_2} G_{wv,j}(s)\Delta v_j(s)\right\}\end{aligned} \tag{5-21}$$

The unit-less sensitivity function S_H with respect to total inertia H_{tot} can be also calculated by definition as:

$$\begin{aligned}S_H &= \frac{d\Delta f(s)}{\Delta f(s)} \Big/ \frac{dH_{tot}}{H_{tot}} = \frac{\partial \Delta f(s)}{\partial H_{tot}} \cdot \frac{H_{tot}}{\Delta f(s)} \\ &= \frac{\Delta f(s)}{\left\{\Delta P_L(s) - \sum_{j=1}^{m_2} G_{wv,j}(s)\Delta v_j(s)\right\}} \cdot \{2sH_{tot}\}\end{aligned} \tag{5-22}$$

In the work of Huang and Li [34], a similar sensitivity analysis was performed for a power system but only with conventional hydraulic machines. From those results and returning to the "base" case definition of Chapter 4, frequency variations Δf_{base} for a purely conventional system can be obtained. In this sense, the sensitivity expression Δf_{base} with respect to to inertia for conventional power systems is

$$\frac{\partial \Delta f_{base}(s)}{\partial H} = \left[\frac{\Delta f_{base}(s)}{\Delta P_L(s)}\right]^2 \cdot \Delta P_L(s) \cdot 2s. \tag{5-23}$$

Similarly, the aforementioned unit-less sensitivity expression $S_{H,base}$ of Δf_{base} with respect to H_{base} for a completely conventional power system is [33]:

$$S_{H,base} = \frac{d\Delta f(s)}{\Delta f(s)} \Big/ \frac{dH_{base}}{H_{base}} = \frac{\partial \Delta f(s)}{\partial H_{base}} \cdot \frac{H_{base}}{\Delta f(s)} = \frac{\Delta f_{base}(s)}{\Delta P_L(s)} 2H_{base}s. \tag{5-24}$$

The comparison among sensitivities with respect to inertia for power systems with and without wind turbine contributions to frequency variations can be established from equations (5-21) to (5-24). As expected, the inclusion of wind turbines means the consideration of wind velocity in frequency sensitivity through the term $\sum_{j=1}^{m_2} G_{wv,j}(s)\Delta v_j(s)$ (see equations (5-21) and (5-22)). From Chapter 4, the influence of wind contributions in system inertia was established. It is expected that the intrinsic unpredictable and variable nature of the wind resource impacts the power generated from generation units. In consequence, the dynamic characteristics of the frequency regulation are being modified according to the wind profile for a determined inertia value. This will be illustrated through simulation in subsequent sections.

5.3. Stability Analysis of Inertia Sensitivity of LFC with WT

Traditionally, grid frequency variations $\Delta f(s)$ have been exclusively analyzed under the influence of load disturbances $\Delta P_L(s)$ [42, 3, 6]. This approximation was developed for systems involving only conventional generation, resulting in the following expression:

$$d\Delta f(s) = \frac{\partial \Delta f(s)}{\partial \Delta P_L(s)} \cdot d\Delta P_L(s). \tag{5-25}$$

For systems with contribution of wind turbines to frequency regulation, wind speed variations Δv_j need to be considered in the analysis of frequency deviation. Therefore, for a system with frequency regulation contributions from m_2 wind turbines, equation (5-25) becomes:

$$d\Delta f(s) = \frac{\partial \Delta f(s)}{\partial \Delta P_L(s)} \cdot d\Delta P_L(s) + \sum_{j=1}^{m_2} \frac{\partial \Delta f(s)}{\partial \Delta v_j(s)} \cdot d\Delta v_j(s). \tag{5-26}$$

Nevertheless, the impacts of the system inertia coefficient are not considered neither in equation (5-25) nor equation (5-26). This omission could offer incomplete information, because a loss of generation or an interruption event may result in a variation of the inertia coefficient for a given machine, affecting the aggregated system inertia [32]. These events have an high probability of occurrence in an environment with variable and unpredictable renewable energy sources, where resource intermittence or generation drops may result in changes from the initial calculation of inertia [88]. Additionally, inertia could have been estimated form an outdated generation profile. All these phenomena suggest that frequency deviation Δf should consider the effects of generator inertia coefficient rather than being function of the external disturbances ΔP_L and Δv_j exclusively. In consequence, the impact of inertia coefficient in the performance of grid frequency regulation must be determined.

5.3.1. Extraction of differential equation of frequency deviation

Assuming mutual independence among ΔP_L, Δv_j, and inertia coefficient H_{tot}, equation 5-26 is modified by adding variations with respect to H_{tot}, as follows:

$$d\Delta f(s) = \frac{\partial \Delta f(s)}{\partial \Delta P_L(s)} \cdot d\Delta P_L(s) + \sum_{j=1}^{m_2} \frac{\partial \Delta f(s)}{\partial \Delta v_j(s)} \cdot d\Delta v_j(s) + \frac{\partial \Delta f(s)}{\partial \Delta H_{tot}} d\Delta H_{tot}. \tag{5-27}$$

From equation (5-21),

$$\frac{\partial \Delta f(s)}{\partial H_{tot}} dH_{tot} = 2s(dH_{tot}) \left[\frac{\Delta f(s)}{\Delta P_L(s) - \sum_{j=1}^{m_2} G_{wv,j}(s)\Delta v_j(s)} \right]^2 \left\{ \Delta P_L(s) - \sum_{j=1}^{m_2} G_{wv,j}(s)\Delta v_j(s) \right\} \tag{5-28}$$

Additionally, taking partial derivatives with respect to ΔP_L and Δv_j from equation 5-20, we can show that:

$$\frac{\partial \Delta f(s)}{\partial \Delta P_L(s)} = \frac{\Delta f(s)}{\Delta P_L(s)}; \qquad \frac{\partial \Delta f(s)}{\partial \Delta v_j(s)} = \frac{\Delta f(s)}{\Delta v_j(s)} \tag{5-29}$$

Replacing equations (5-28) and (5-29) in equation (5-27), we get:

$$\begin{aligned} d\Delta f(s) =& \frac{\Delta f(s)}{\Delta P_L(s)} \cdot d\Delta P_L(s) + \sum_{j=1}^{m_2} \frac{\Delta f(s)}{\Delta v_j(s)} \cdot d\Delta v_j(s) \\ &+ 2s(dH_{tot}) \left[\frac{\Delta f(s)}{\Delta P_L(s) - \sum_{j=1}^{m_2} G_{wv,j}(s)\Delta v_j(s)} \right]^2 \left\{ \Delta P_L(s) - \sum_{j=1}^{m_2} G_{wv,j}(s)\Delta v_j(s) \right\} \end{aligned} \tag{5-30}$$

Laplace inverse transformation is employed to get the time domain representation of equation (5-30), resulting in:

$$\begin{aligned} d\Delta f(t) =& L^{-1}\left[\frac{\Delta f(s)}{\Delta P_L(s)} \cdot d\Delta P_L(s) \right] + L^{-1}\left[\sum_{j=1}^{N} \frac{\partial \Delta f(s)}{\partial \Delta v_j(s)} \cdot d\Delta v_j(s) \right] + \dots \\ \dots & L^{-1}\left\{ \left[\frac{\Delta f(s)}{\Delta P_L(s) - \sum_{j=1}^{m_2} G_{wv,j}(s)\Delta v_j(s)} \right]^2 \left[\Delta P_L(s) - \sum_{j=1}^{m_2} G_{wv,j}(s)\Delta v_j(s) \right] \cdot 2sdH_{tot} \right\}. \end{aligned} \tag{5-31}$$

Further, taking integration of equation (5-31), we get $\Delta f(t)$ as

$$\int d\Delta f(t) = \Delta f(t) = \int L^{-1}\left[\frac{\Delta f(s)}{\Delta P_L(s)} \cdot d\Delta P_L(s)\right] + \int L^{-1}\left[\sum_{j=1}^{N} \frac{\partial \Delta f(s)}{\partial \Delta v_j(s)} \cdot d\Delta v_j(s)\right] + \cdots \tag{5-32}$$

$$\cdots L^{-1}\left\{\left[\frac{\Delta f(s)}{\Delta P_L(s) - \sum_{j=1}^{m_2} G_{wv,j}(s)\Delta v_j(s)}\right]^2 \left[\Delta P_L(s) - \sum_{j=1}^{m_2} G_{wv,j}(s)\Delta v_j(s)\right] \cdot 2sdH_{tot}\right\}.$$

Equation 5-32 presents the total differential equation of frequency deviation $\Delta f(t)$ in time domain considering inertia effects. In order to determine the impacts of inertia coefficient, the stability analysis of $\Delta f(t)$ is presented in the following subsection.

5.3.2. Stability Analysis

After a disturbance, all the characteristic poles of the transfer function of a power system are located on the left half-plane in the s-domain if the system is stable. In this case, the finite time-domain input signals $\Delta v_j(t)$ and $\Delta P_L(t)$ would not be producing infinite time-domain responses on system output $\Delta f(t)$. As established in control systems theory, that is equivalent to show that the norm of the transfer function of the system is bounded. From equation 5-32, this would represent that the transfer functions listed in equation 5-33 are already bounded:

$$\begin{cases} \left\| \Delta f(s) \Big/ \left[\Delta P_L(s) - \sum_{j=1}^{m_2} G_{wv,j}(s)\Delta v_j(s)\right] \right\| \\ \left\| \Delta f(s) \Big/ \Delta P_L(s) \right\| \\ \left\| \sum_{j=1}^{N} \Delta f(s) \Big/ \Delta v_j(s) \right\| \end{cases} < \infty \text{ for } \forall_t \in (0, \infty) \tag{5-33}$$

Moreover, frequency regulation in power systems is designed to keep $\Delta f(t)$ inside a determined finite band despite variations in Δv_j and ΔP_L. Assuming the stability of the system, the bounds of frequency variations should be determined. Considering both Δv_j and ΔP_L as step functions, and using triangle inequality properties in the expression of equation 5-32

we get:

$$
\begin{aligned}
\|\Delta f(t)\| \leq & \left\| \int L^{-1}\left[\frac{\Delta f(s)}{\Delta P_L(s)} \cdot d\Delta P_L(s)\right] + \int L^{-1}\left[\sum_{j=1}^{m_2} \frac{\Delta f(s)}{\Delta v_j(s)} \cdot d\Delta v_j(s)\right] + \cdots \right. \\
& \left. \cdots \int L^{-1}\left\{ \left[\frac{\Delta f(s)}{\Delta P_L(s) - \sum_{j=1}^{m_2} G_{wv,j}(s)\Delta v_j(s)}\right]^2 \cdot \left[\Delta P_L(s) - \sum_{j=1}^{m_2} G_{wv,j}\Delta v_j(s)\right] \cdot 2sdH_{tot} \right\} \right\| \\
& \leq \left\| \int L^{-1}\left\{ \left\| \frac{\Delta f(s)}{\Delta P_L(s)} \right\| d\Delta P_L(s) \right\} \right\| + \left\| \int L^{-1}\left\{ \left\| \sum_{j=1}^{m_2} \frac{\Delta f(s)}{\Delta v_j(s)} \right\| \left\| \sum_{j=1}^{m_2} d\Delta v_i(s) \right\} \right\| + \cdots \right. \\
& \left. \cdots \left\| \int L^{-1}\left\{ \left\| \left[\frac{\Delta f(s)}{\Delta P_L(s) - \sum_{j=1}^{m_2} G_{wv,j}\Delta v_j(s)}\right]^2 \right\| \left[\Delta P_L(s) - \sum_{j=1}^{m_2} G_{wv,j}\Delta v_j(s)\right] \cdot 2sdH_{tot} \right\} \right\| \\
& \leq \left\| \int L^{-1}\left[\kappa\, d\Delta P_L(s)\right] \right\| + \left\| \int L^{-1}\left[\eta \sum_{j=1}^{m_2} d\Delta v_j(s)\right] \right\| + \cdots \\
& \cdots \left\| \int L^{-1}\left\{ \varrho^2 \left[\Delta P_L(s) - \sum_{j=1}^{m_2} G_{wv,j}\Delta v_j(s)\right] \cdot 2sdH_{tot} \right\} \right\| \\
& \leq \left\| \int \kappa \cdot 1(t-t_0) d\Delta P_L \right\| + \left\| \int \eta \cdot 1(t-t_0) \sum_{j=1}^{m_2} d\Delta v_j \right\| + \cdots \\
& \cdots \left\| \int \varrho^2 . \left[1(t-t_0)\Delta P_L - \sum_{j=1}^{m_2} \left(\frac{g_j}{q_j}\right) \cdot e^{-\left(\frac{1}{q_j}\right)t} \Delta v_j \right] 2sdH_{tot} \right\| \\
& \leq \kappa \,\|\, \Delta P_L\| + \eta \left\| \sum_{j=1}^{m_2} \Delta v_j \right\| + \varrho^2 \,\|H_{tot}\| \left\| \left[\Delta P_L - \sum_{j=1}^{m_2} \left(\frac{g_j}{q_j}\right) \cdot e^{-\left(\frac{1}{q_j}\right)t} \Delta v_j \right] \right\|
\end{aligned} \tag{5-34}
$$

where $\kappa = \left\| \frac{\Delta f(s)}{\Delta P_L(s)} \right\|$, $\eta = \left\| \sum_{j=1}^{N} \frac{\Delta f(s)}{\Delta v_j(s)} \right\|$ and $\varrho = \left\| \left[\frac{\Delta f(s)}{\Delta P_L(s) - \sum_{j=1}^{N} G_{wv,j}(s)\Delta v_j(s)} \right] \right\|$ represent the respective bounded magnitudes of the transfer functions established in equation 5-33. Also, $L^{-1}[1/s] = 1(t-t_0)$, with $1(t-t_0) = 1$ when $t \geq t_0$. In this way, $||1(t-t_0)|| = 1$.

Therefore, we can see that the system remains stable when the effects of inertia variations are considered.

In the same way, the output frequency deviation Δf of the traditional power system model

without consideration of inertia effects is given as [32]:

$$\|\Delta f_{base}(t)\| \leq \kappa_{base} \|\Delta P_L\| \tag{5-35}$$

The expressions in equations 5-34 and 5-35 show that the frequency deviations in both cases remain bounded in both cases when stable power system is considered. However, it is also evident that the boundaries are different. The limits of the conventional model depend on the boundaries of load disturbance ΔP_L. However, the consideration of inertia effects and wind turbine integration to frequency regulation affects the boundaries of frequency deviations. In this case, the limits depend on factors such as load disturbance, variations in wind speed, system configuration and the specific value of H_{tot}.

5.4. Numerical Simulation

The results of the previous sections are verified through simulation. Just as done in Chapter 3, a slightly modified version of the WSCC 9-bus power system [3] was employed for simulating wind turbine contribution in the LFC for a multi-area power system. The modified system parameters are summarized in Table **4-1**, considering an hydraulic machine and two gas units. In this work, 20 % of conventional generation was replaced by a wind farm. The wind farm was formed by 32 DFIG WT of 2 MW each, whose model parameters were shown in Table **4-2**. Wind speed was simulated from data obtained from the database of Virgin Islands [72]. The Power Base was set at 100 MVA. The system was modeled as indicated in Figure **5-1**, and several case studies were analyzed.

5.4.1. Case 1: Frequency response for a load step change

A step change of 10 % is applied to the simulated system at $t = 0$ s. The system with a reduced inertia was simulated without wind, and with increasing constant wind speed (5 and 10 m/s) as disturbance. Contribution of wind turbines in frequency regulation is not being considered. Figure **5-3** presents the grid frequency deviations for this case. Frequency nadir is lower for the system with reduced inertia and no wind. Despite the wind being considered exclusively as disturbance, the effects of the wind power injections help to improve the frequency characteristic of the system. Wind power production increases with higher speeds. However, higher speeds may lead to a more oscillatory response, as seen from the curve for a speed of 10 m/s.

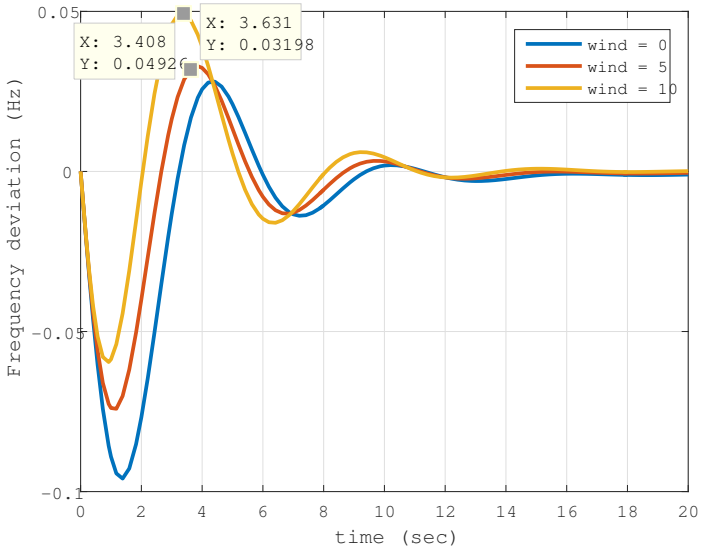

Figure 5-3: Case 1: Frequency response without contribution of WT and increasing wind speed

5.4.2. Case 2: Frequency response for a load step change and WT contribution to LFC

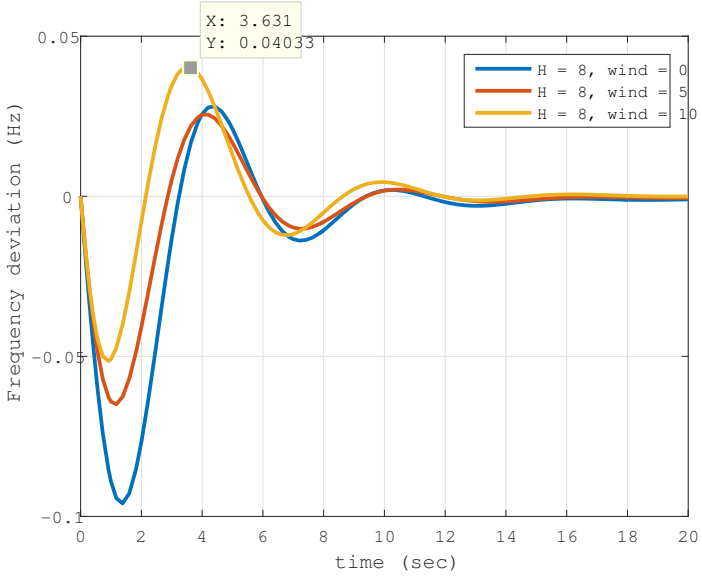

Figure 5-4: Case 2: Frequency response with constant contribution of WT and increasing wind speed

A step change of 10 % is applied to the simulated system at $t = 0\ s$. Contribution of wind turbines in frequency regulation is being considered as constant in every case. The system with a reduced inertia was simulated without wind, and with increasing constant wind speed (5 and 10 m/s). Figure **5-4** presents the grid frequency deviations for this case. Again, we can see how the lower frequency nadir is given for the case without active power injections from RES. Response is similar as the one shown in Figure **5-3**; however, the contribution of wind turbines to frequency regulation makes for a smoother response in grid frequency deviation. Again, a higher speed may be cause of concern and oscillatory response even with inertia emulation from wind turbines.

5.4.3. Case 3: Frequency response for a load step change and increasing wind contribution to LFC

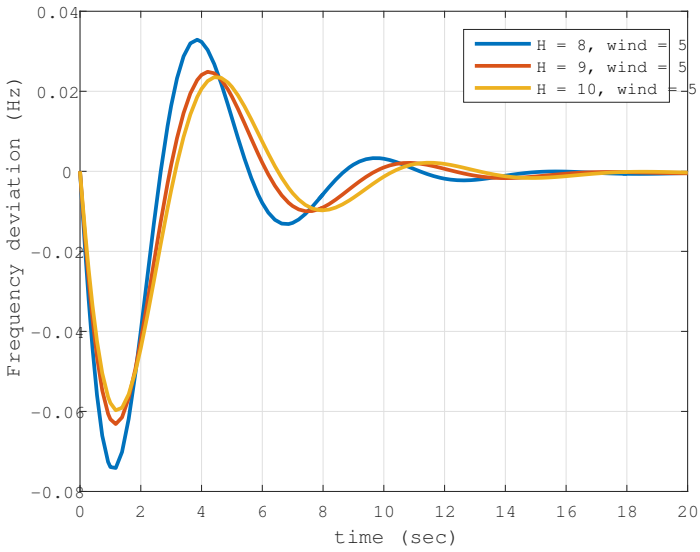

Figure 5-5: Case 3: Frequency response with constant wind speed and increasing contribution of WT

A step change of 10 % is applied to the simulated system at $t = 0\ s$. Contribution of wind turbines in frequency regulation is being increased (0 % to 10 % to 20 %) in every case by modification of the loop parameters. The system with a reduced inertia was simulated with a constant constant wind speed of 5 m/s. Figure **5-5** presents the grid frequency deviations for this case. Here, the effects of the increased inertia with the contribution of wind turbines are evident. However, these effects are being shown with the assumption of constant wind speed.

5.4.4. Case 4: Frequency response with constant wind speed and increasing contribution of WT after unstable conditions

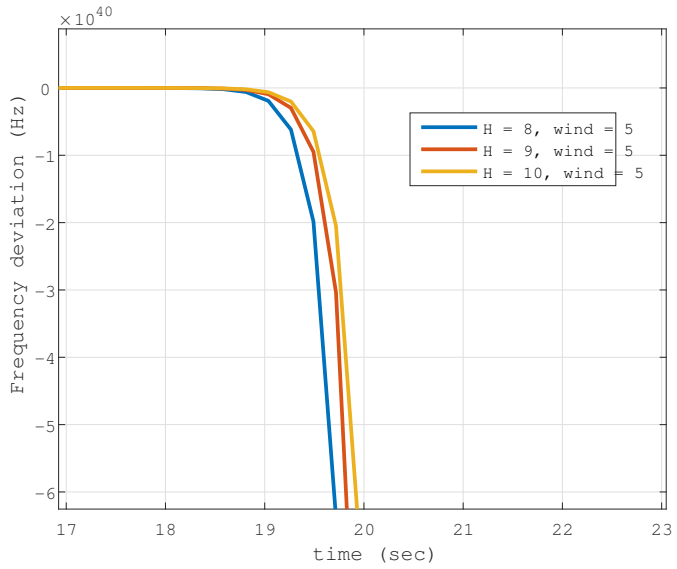

Figure 5-6: Case 4: Frequency response with constant wind speed and increasing contribution of WT, starting from unstable case.

For this case, one of the system poles was changed to a value in the right half-plane of the s-domain. This causes an unstable response in frequency deviations. The same conditions of 5.4.3 are applied in this case and the resulting responses are plotted in Figure **5-6**. From Figure **5-6**, the system lasts longer in reaching unstable conditions when wind turbines contribute to grid frequency regulation. Wind speed was kept as constant value of 5 m/s. Variability in wind speed may lead to unstable mode faster.

5.4.5. Case 5:Frequency response with a simulated wind profile and increasing contribution of WT

The power generation in wind units depends on the wind profile. Wind speed is highly variable and unpredictable, and then the wind power production also fluctuates. The variation in wind power produces frequency deviations. A wind speed profile was simulated from data obtained from the database of Virgin Islands [72]. Load disturbance was not considered, just wind speed. The resulting responses are plotted in Figure **5-7**, while contribution of wind turbines in frequency regulation is increased (0 % to 10 % to 20 %). According to Figure **5-7**, the curves with higher inertia contributions from wind turbines present smaller

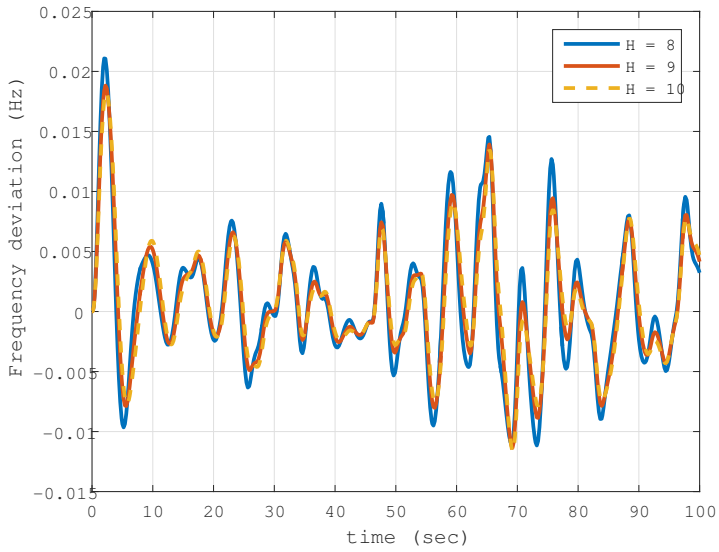

Figure 5-7: Case 5: Frequency response with a simulated wind profile and increasing contribution of WT

peaks than the purely conventional system. In consequence, frequency deviation has a better performance with contribution of RES despite the inherent variability of the wind speed.

5.4.6. Case 6: Frequency response with a simulated wind profile and load disturbance

The same conditions of the immediately previous case were replicated, but a step load disturbance of 10 % was applied at $t = 50s$. The contributions of wind turbines make the system more robust to disturbance action, even under the effects of variable wind speed. Starting from an stable case, the consideration of inertia variations maintains the stability of the system. This is expected from the Equation 5-32, and the analysis in section 5.3.2. The dynamic characteristics of grid frequency deviations can actually improve with a higher value of inertia coefficient.

5.5. Summary

This chapter addressed the effects of inertia variations for power system under the integration of wind units. The transfer functions of the system were obtained starting from a linearized wind turbine model. The mathematical relationships were formulated to analyze

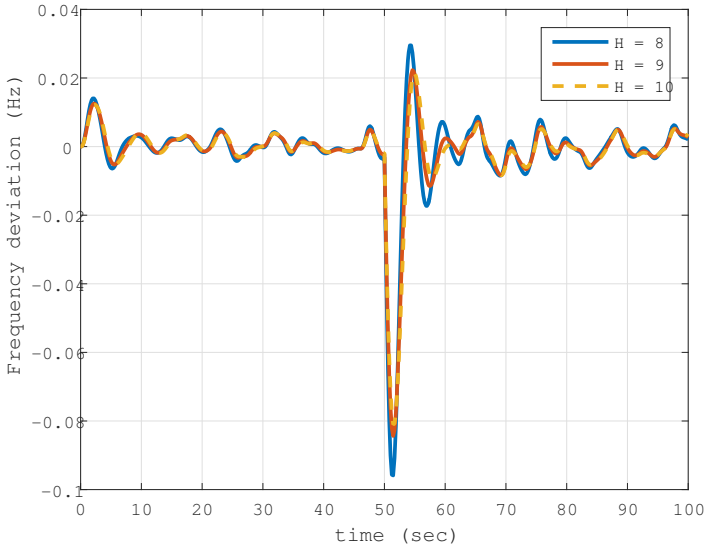

Figure 5-8: Case 6: Frequency response with a simulated wind profile and increasing contribution of WT, and load disturbance $\Delta P_L = 0{,}1$ at $t = 50s$

the sensitivity and stability regarding inertia coefficient H. These expressions were verified through simulation of several cases under different stability conditions and disturbances in wind speed and load.

Simulations have shown a better and smoother response of frequency deviations for the cases with contributions of wind turbines in comparison with the basic case of the purely conventional system. These improvements on frequency response characteristic makes for a better power quality. The impacts of different values of H were studied. The results indicate the better performance of the frequency response for higher contributions of wind turbines to system inertia. Results suggests more robustness to parameter variations for systems that include wind turbine participation. However, frequency deviation rate increases when the uncertainty in system parameters grows. This behavior would lead to instability scenarios under frequency disturbances for the power system.

6 Conclusions and Recommendations

6.1. Conclusions

The need to have a better environment, now and in the future, manifests itself as an inexcusable obligation to present and future generations. Our worries go beyond respecting the environment for a better quality of life in the present because it is increasingly necessary to preserve the environment for future generations so that their development possibilities are not limited by the environmental deterioration or the depletion of natural resources. In this sense, a reflection is imposed on the ways of generating electricity, especially as regards the ingredients of a generation mix that should be anchored in sustainability. Of course, this sustainability must be manifested in its environmental, technical and economic aspects.

Renewable energy sources arise as a logical alternative for improving the energy generation around the world. But unfortunately, a large part of these energies are not manageable, understanding the manageability as the capacity to face the very variable and unknown in terms of power production. This question is not trivial, as the success of the operation of an electrical system resides in the ability to guarantee the electrical supply in secure conditions to cover the demand. This goal is achieved with the anticipated programming of the required generation satisfying that demand. Regrettably, there is uncertainty about the possibility of offering this energy time after the real-time, since this type of plant can not guarantee the existence of a resource primary (wind or sun) that makes them work. In consequence, the variability and difficulty of their production are limiting factors of the manageability of renewable energies.

Additionally, the natural variability of demand opposes to a generation that losses manageability with the growing penetration of renewable energies. This fact significantly complicates the operation of the electrical system. Therefore, to be able to integrate a high contingent of non-manageable renewable energies securely, it will be necessary to provide the service of the electrical system of a range of tools that make possible its secure integration in the system. Some of these tools have to do with the own technologies for the use of renewable energies that are usually asynchronous machines that do not facilitate the ancillary functions provided by conventional generation. In addition to producing electricity, generation units

contribute to voltage gaps, Short circuit currents, voltage control, tracking of the power frequency binomial, inertia coefficient in the system, etc.

All these considerations are valid for the particular analysis of one of those ancillary services of the power system: Load Frequency Regulation. This a significant control subsystem of power grid that facing changes related to the growing penetration of Renewable Energy Sources. From the dynamic analysis of these situation, the following contributions were produced from this thesis work:

- **On the use of Control Sensitivity Functions for Frequency-Domain Analysis of Frequency Regulation in Power Systems**. The so-called Control Sensitivity Functions were used for determination of the dynamical characteristics of the traditional regulation structure for frequency control in power systems. Through the simulation of a one-area power system and using Bode plots for response visualization, the analysis of these sensitivities led to the description of some key features of control systems such as disturbance rejection, control action effects, and reference tracking. These analyses could be useful for assessing the effects of alternative energy systems such as renewable sources in power system frequency regulation.

- **On the effects of wind turbines in frequency regulation systems**. The use of Bode plots as an analysis tool for the determination of the impacts of load disturbances in frequency regulation schemes shows that there are regions of significant implications according to the disturbance spectral characteristics. The previous knowledge of these sensible zones will allow the identification of severe disturbances, and the development of compensation techniques that attenuate the adverse effects in advance. This will come in handy for the accommodation of renewable energy sources into the power systems, and for the involvement of this kind of generation in frequency regulation tasks. Starting with the consideration of RES units as disturbances to frequency regulation tasks, the effects on system inertia were highlighted. The expressions from the studied model showed the consequences of the reduced inertia in frequency control. The analysis through Control Sensitivity Functions and the time-response of the system has shown the need for some inertia contribution from the RES-based units to maintain the operational conditions of the power system.

- **On the Sensitivity Analysis of Frequency Regulation in Power Systems with Wind Generation**. With the growing development of intermittent renewable energy sources and its integration of the electrical grid, renewable energy will take more responsibility for frequency regulation tasks in the foreseeable future. Although the impact may not be clear, this gives enough motivation to investigate the effect of the changes in generator inertia coefficient H on the power system frequency regulation based on the typical Load Frequency Control model with the integration of wind turbines

for inertia emulation. Both theoretic and simulation analysis shows that the impact of an inaccurate generator inertia coefficient H is relatively small and bounded when the power system is inherently stable; while the system frequency deviation may be accelerated when the power system is indeed unstable after disturbance.

6.2. Recommendations

- **Extension of results with inclusion of additional power injection elements and power system variables**. Inertial emulation techniques apply for a wide set of generation sources in power systems, such as photovoltaic units, batteries and other Energy Storage Systems. Also, the consideration of other stages for power systems operation like economic dispatch could lead to interesting research avenues from the results presented here.

- **Combination of sensitivity functions of frequency regulation**. The analysis of the impacts of the combination of the frequency sensitivities with respect to the main system parameters should be explored. This would include the generator inertia coefficient H, the governor speed coefficient R and load-damping coefficient D on the regulation of power system frequency response and stability studies with the basis on the Load Frequency Control model rather than considering them individually as done in Chapters 3 and 5.

- **Improvement of robustness of frequency regulation systems**. The development of a robust load shedding scheme for a power system with integration of renewable sources would be useful. This scheme would consider the effects of system parameters in the frequency regulation systems. Also, this strategy may involve the changes in system parameters such as the load-damping coefficient D, the generator inertia coefficient H, and the governor speed coefficient R and the effects of renewable sources.

- **Consideration of the market effects in the generation with renewable energies**. Renewable energies generate uncertainties about the recovery of investments in conventional technology, since investors do not perceive signals economic conditions that allow them to rely on the return of their investments. It is necessary to review the implications of changing the mix of generation (betting on renewable energies) with a substantial impact on the formation of prices in the market and the induction of specific costs (guarantee of power) out of it.

Bibliografía

[1] Grid integration of large-capacity Renewable Energy sources and use of large-capacity Electrical Energy Storage. White paper, International Electrotechnical Commission Market Strategy Board, October 2012.

[2] A. Abiri-Jahromi and F. Bouffard. Characterizing statistical bounds on aggregated demand-based primary frequency control. In *Power and Energy Society General Meeting (PES), 2013 IEEE*, pages 1–5, July 2013.

[3] Paul M. Anderson and A. A. Fouad. *Power System Control and Stability (IEEE Press Power Engineering Series)*. Wiley-IEEE Press, 2002.

[4] Goran Andersson. Dynamics and Control of Electric Power Systems, February 2012.

[5] H. Banakar, Changling Luo, and B.T. Ooi. Impacts of Wind Power Minute-to-Minute Variations on Power System Operation. *Power Systems, IEEE Transactions on*, 23(1):150–160, February 2008.

[6] Hassan Bevrani. *Robust Power System Frequency Control*. Power Electronics and Power Systems. Springer, 2 edition, 2014.

[7] T. S. Borsche, T. Liu, and D. J. Hill. Effects of rotational Inertia on power system damping and frequency transients. In *2015 54th IEEE Conference on Decision and Control (CDC)*, pages 5940–5946, December 2015.

[8] H. Camblong, G. Tapia, and M. Rodriguez. Robust digital control of a wind turbine for rated-speed and variable-power operation regime. *IEE Proceedings - Control Theory and Applications*, 153(1):81–91, January 2006.

[9] Haritza Camblong, Ionel Vechiu, Xavier Guillaud, Aitor Etxeberria, and Stéphane Kreckelbergh. Wind turbine controller comparison on an island grid in terms of frequency control and mechanical stress. *Renewable Energy*, 63:37–45, March 2014.

[10] J. Chen, F. Yang, and Q. L. Han. Model-Free Predictive h_∞ Control for Grid-Connected Solar Power Generation Systems. *IEEE Transactions on Control Systems Technology*,

22(5):2039–2047, September 2014.

[11] B.-I. Craciun, T. Kerekes, D. Sera, and R. Teodorescu. Frequency Support Functions in Large PV Power Plants With Active Power Reserves. *Emerging and Selected Topics in Power Electronics, IEEE Journal of*, 2(4):849–858, December 2014.

[12] M. Datta, T. Senjyu, A. Yona, and T. Funabashi. A frequency control method for isolated photovoltaic-diesel hybrid power system with use of full renewable energy. In *Power Electronics and Drive Systems, 2009. PEDS 2009. International Conference on*, pages 1283–1288, 2009.

[13] S. Dechanupaprittha, I. Ngamroo, and Y. Mitani. Decentralized design of robust power system stabilizers considering system uncertainties. In *2005 IEEE Russia Power Tech*, pages 1–6, June 2005.

[14] Kaveh Dehghanpour and Saeed Afsharnia. Electrical demand side contribution to frequency control in power systems: a review on technical aspects. *Renewable and Sustainable Energy Reviews*, 41(0):1267 – 1276, 2015.

[15] G. Delille, B. Francois, and G. Malarange. Dynamic Frequency Control Support by Energy Storage to Reduce the Impact of Wind and Solar Generation on Isolated Power System's Inertia. *Sustainable Energy, IEEE Transactions on*, 3(4):931–939, October 2012.

[16] Christopher L. DeMarco and Chaitanya A. Baone. Chapter 29 - Control of Power Systems with High Penetration Variable Generation. In Lawrence E. Jones, editor, *Renewable Energy Integration*, pages 369 – 379. Academic Press, Boston, 2014.

[17] Francisco Díaz-González, Melanie Hau, Andreas Sumper, and Oriol Gomis-Bellmunt. Participation of wind power plants in system frequency control: Review of grid code requirements and control methods. *Renewable and Sustainable Energy Reviews*, 34:551 – 564, 2014.

[18] Francisco Díaz-González, Melanie Hau, Andreas Sumper, and Oriol Gomis-Bellmunt. Coordinated operation of wind turbines and flywheel storage for primary frequency control support. *International Journal of Electrical Power & Energy Systems*, 68(0):313 – 326, 2015.

[19] R. Doherty, A. Mullane, G. Nolan, D.J. Burke, A. Bryson, and M. O'Malley. An Assessment of the Impact of Wind Generation on System Frequency Control. *Power Systems, IEEE Transactions on*, 25(1):452–460, February 2010.

[20] José Luis Domínguez-García, Oriol Gomis-Bellmunt, Fernando D. Bianchi, and Andreas

Sumper. Power oscillation damping supported by wind power: A review. *Renewable and Sustainable Energy Reviews*, 16(7):4994 – 5006, 2012.

[21] Mohammad Dreidy, H. Mokhlis, and Saad Mekhilef. Inertia response and frequency control techniques for renewable energy sources: A review. *Renewable and Sustainable Energy Reviews*, 69:144 – 155, 2017.

[22] E. Duque, J. Patino, and L. Velez. Implementation of the ACM0002 methodology in small hydropower plants in Colombia under the Clean Development Mechanism. *International Journal of Renewable Energy Research*, 6(1):21–33, 2016.

[23] Eduardo Duque and Julian Patino. El mercado de bonos de carbono y su aplicación para proyectos hidroeléctricos. *Revista CINTEX*, 18:131 – 143, 2013.

[24] Eduardo Alexander Duque Grisales, Julian Alberto Patino Murillo, and Luis Diego Velez-Gomez. Aplicación del mercado de carbono en pequeñas centrales hidroeléctricas. *Energética*, 44:19–32, 2014.

[25] Janaka Bandara Ekanayake, Nicholas Jenkins, and G Strbac. Frequency response from wind turbines. *Wind Engineering*, 32(6):573–586, 2008.

[26] D. Gautam, V. Vittal, and T. Harbour. Impact of Increased Penetration of DFIG-Based Wind Turbine Generators on Transient and Small Signal Stability of Power Systems. *IEEE Transactions on Power Systems*, 24(3):1426–1434, August 2009.

[27] G.C. Goodwin, S.F. Graebe, and M.E. Salgado. *Control System Design*. Prentice Hall, 2001.

[28] T. Goya, E. Omine, Y. Kinjyo, T. Senjyu, A. Yona, N. Urasaki, and T. Funabashi. Frequency control in isolated island by using parallel operated battery systems applying H∞; control theory based on droop characteristics. *Renewable Power Generation, IET*, 5(2):160–166, March 2011.

[29] Weng Khuen Ho, Chang Chieh Hang, and Lisheng S. Cao. Tuning of PID controllers based on gain and phase margin specifications. *Automatica*, 31(3):497–502, March 1995.

[30] Hannele Holttinen, Peter Meibom, Antje Orths, Bernhard Lange, Mark O'Malley, John Olav Tande, Ana Estanqueiro, Emilio Gomez, Lennart Soder, Goran Strbac, J Charles Smith, and Frans van Hulle. Impacts of large amounts of wind power on design and operation of power systems, results of IEA collaboration. *Wind Energy*, 14(2):179–192, 2011.

[31] Ricardo Horta, Jairo Espinosa, and Julian Patino. Frequency and voltage control of a

power system with information about grid topology. In *Automatic Control (CCAC), 2015 IEEE 2nd Colombian Conference on*, pages 1–6. IEEE, 2015.

[32] Hao Huang. *Studies of Economics and Stability with Variable Generation and Controllable Load*. PhD, University of Tennessee, 2014.

[33] Hao Huang and Fangxing Li. Sensitivity Analysis of Load-Damping Characteristic in Power System Frequency Regulation. *Power Systems, IEEE Transactions on*, 28(2):1324–1335, May 2013.

[34] Hao Huang and Fangxing Li. Sensitivity analysis of load-damping, generator inertia and governor speed characteristics in hydraulic power system frequency regulation. In *Power Engineering Conference (AUPEC), 2014 Australasian Universities*, pages 1–6, September 2014.

[35] M. Jafarian and A. M. Ranjbar. The impact of wind farms with doubly fed induction generators on power system electromechanical oscillations. *Renewable Energy*, 50(0):780 – 785, 2013.

[36] Alberto Carbajo Josa. *La integración de las energías renovables en el sistema eléctrico*. Fundación Alternativas, 2012.

[37] Naoto Kakimoto, S. Takayama, H. Satoh, and K. Nakamura. Power Modulation of Photovoltaic Generator for Frequency Control of Power System. *Energy Conversion, IEEE Transactions on*, 24(4):943–949, December 2009.

[38] M. Kayikci and J.V. Milanovic. Dynamic Contribution of DFIG-Based Wind Plants to System Frequency Disturbances. *Power Systems, IEEE Transactions on*, 24(2):859–867, 2009.

[39] A. Keyhani and A. Chatterjee. Automatic Generation Control Structure for Smart Power Grids. *Smart Grid, IEEE Transactions on*, 3(3):1310–1316, September 2012.

[40] Brendan Kirby. Frequency Regulation Basics and Trends. Technical report, Oak Ridge National Laboratory, Tennessee, December 2004.

[41] P. Kundur, J. Paserba, V. Ajjarapu, G. Andersson, A. Bose, C. Canizares, N. Hatziargyriou, D. Hill, A. Stankovic, C. Taylor, T. Van Cutsem, and V. Vittal. Definition and classification of power system stability IEEE/CIGRE joint task force on stability terms and definitions. *IEEE Transactions on Power Systems*, 19(3):1387–1401, August 2004.

[42] Prabha Kundur. *Power System Stability and Control*. McGraw-Hill Professional, 1994.

[43] G. Lalor, A. Mullane, and M. O'Malley. Frequency control and wind turbine technologies. *Power Systems, IEEE Transactions on*, 20(4):1905–1913, November 2005.

[44] Wei Li, G. Joos, and C. Abbey. Wind Power Impact on System Frequency Deviation and an ESS based Power Filtering Algorithm Solution. In *Power Systems Conference and Exposition, 2006. PSCE '06. 2006 IEEE PES*, pages 2077–2084, October 2006.

[45] Patrick J. Luickx, Erik D. Delarue, and William D. D'haeseleer. Impact of large amounts of wind power on the operation of an electricity generation system: Belgian case study. *Renewable and Sustainable Energy Reviews*, 14(7):2019 – 2028, 2010.

[46] Changling Luo, H.G. Far, H. Banakar, Ping-Kwan Keung, and Boon-Teck Ooi. Estimation of Wind Penetration as Limited by Frequency Deviation. *Energy Conversion, IEEE Transactions on*, 22(3):783–791, September 2007.

[47] Alejandro Marquez, Julian Patino, and Jairo Espinosa. Min-Max Economic Model Predictive Control. In *Decision and Control (CDC2014), 53rd IEEE Conference on*, pages 1–5, Los Angeles, CA, 2014. IEEE.

[48] M. Milligan, E. Ela, D. Lew, D. Corbus, Yih-huei Wan, and B. Hodge. Assessment of Simulated Wind Data Requirements for Wind Integration Studies. *Sustainable Energy, IEEE Transactions on*, 3(4):620–626, October 2012.

[49] Tarek Hassan Mohamed, Jorge Morel, Hassan Bevrani, and Takashi Hiyama. Model predictive based load frequency control_design concerning wind turbines. *International Journal of Electrical Power & Energy Systems*, 43(1):859 – 867, 2012.

[50] M. El Mokadem, V. Courtecuisse, C. Saudemont, B. Robyns, and J. Deuse. Experimental study of variable speed wind generator contribution to primary frequency control. *Renewable Energy*, 34(3):833 – 844, 2009.

[51] Ian F. Moore. *Inertial Response from Wind Turbines*. Ph.D. thesis, Cardiff University, Cardiff, 2012.

[52] J. Morren, S.W.H. de Haan, W.L. Kling, and J.A. Ferreira. Wind turbines emulating inertia and supporting primary frequency control. *Power Systems, IEEE Transactions on*, 21(1):433–434, February 2006.

[53] A. Mullane and M. O'Malley. The Inertial Response of Induction-Machine-Based Wind Turbines. *Power Systems, IEEE Transactions on*, 20(3):1496–1503, August 2005.

[54] S.M. Muyeen, R. Takahashi, T. Murata, and J. Tamura. Integration of an Energy Capacitor System With a Variable-Speed Wind Generator. *Energy Conversion, IEEE*

Transactions on, 24(3):740–749, September 2009.

[55] J. Nanda and B. L. Kaul. Automatic generation control of an interconnected power system. *Proceedings of the Institution of Electrical Engineers*, 125(5):385–390(5), May 1978.

[56] Majid Nayeripour, Mohammad Hoseintabar, and Taher Niknam. Frequency deviation control by coordination control of {FC} and double-layer capacitor in an autonomous hybrid renewable energy power generation system. *Renewable Energy*, 36(6):1741 – 1746, 2011.

[57] Micheal O'Flaherty, Niall Riordan, Noel O'Neill, and Ciara Ahern. A Quantitative Analysis of the Impact of Wind Energy Penetration on Electricity Prices in Ireland. *Energy Procedia*, 58(0):103 – 110, 2014. Renewable Energy Research Conference, {RERC} 2014.

[58] Fabrizio Padula and Antonio Visioli. Tuning rules for optimal PID and fractional-order PID controllers. *Journal of Process Control*, 21(1):69 – 81, 2011.

[59] Shashi Kant Pandey, Soumya R. Mohanty, and Nand Kishor. A literature survey on load-frequency control for conventional and distribution generation power systems. *Renewable and Sustainable Energy Reviews*, 25(0):318 – 334, 2013.

[60] Julian Patiño, José David López, and Jairo Espinosa. Analysis of Control Sensitivity Functions for Power System Frequency Regulation. In Juan Carlos Figueroa-García, Eduyn Ramiro López-Santana, and José Ignacio Rodriguez-Molano, editors, *Applied Computer Sciences in Engineering*, volume 915 of *Communications in Computer and Information Science*, pages 606–617. Springer International Publishing, Cham, 2018.

[61] Julian Patiño, José David López, and Jairo Espinosa. *Sensitivity Analysis of Frequency Regulation Parameters in Power Systems with Wind Generation*, pages 67–87. Springer Singapore, Singapore, 2019.

[62] J. Patino and J. Espinosa. Control sensitivity functions of frequency regulation for a one-area power system. In *2017 IEEE 3rd Colombian Conference on Automatic Control (CCAC)*, pages 1–6, October 2017.

[63] J. Patino, F. Valencia, and J. Espinosa. Sensitivity analysis for frequency regulation in a two-area power system. *International Journal of Renewable Energy Research*, 7(2):700–706, 2017.

[64] Julián Patino, Alejandro Marquez, and Jairo Espinosa. An economic MPC approach for a microgrid energy management system. In *Conference and Exposition (T&D-LA*

2014), 2014 IEEE PES Transmission & Distribution, pages 1–5, Medellín, Colombia, September 2014. IEEE.

[65] L. Pereira, D. Kosterev, P. Mackin, D. Davies, J. Undrill, and Wenchun Zhu. An interim dynamic induction motor model for stability studies in the WSCC. *IEEE Transactions on Power Systems*, 17(4):1108–1115, November 2002.

[66] Ignacio J. Perez-Arriaga. Managing large scale penetration of intermittent renewables. Framework paper, MIT Energy Initiative Annual Symposium, 2011.

[67] C. Pradhan and C. N. Bhende. Frequency Sensitivity Analysis of Load Damping Coefficient in Wind Farm-Integrated Power System. *IEEE Transactions on Power Systems*, 32(2):1016–1029, March 2017.

[68] Elyas Rakhshani. *Analysis and control of multi-area HVDC interconnected power systems by using virtual inertia*. Doctor of Philosophy, Universitat Politécnica de Catalunya, Barcelona, 2016.

[69] G. Ramtharan, J.B. Ekanayake, and N. Jenkins. Frequency support from doubly fed induction generator wind turbines. *IET Renewable Power Generation*, 1(1):3–9, March 2007.

[70] Gnanasambandapillai Ramtharan, Nicholas Jenkins, and Olimpo Anaya-Lara. Modelling and control of synchronous generators for wide-range variable-speed wind turbines. *Wind Energy*, 10(3):231–246, 2007.

[71] REN21, editor. *Renewables 2017 Global Status Report*. REN21 Secretariat, Paris, 2017.

[72] Roberts, O. and Andreas, A. United States Virgin Islands: St. Thomas (Bovoni) &; St. Croix (Longford), 1997.

[73] J.L. Rodriguez-Amenedo, S. Arnalte, and J.C. Burgos. Automatic generation control of a wind farm with variable speed wind turbines. *Energy Conversion, IEEE Transactions on*, 17(2):279–284, June 2002.

[74] Pedro Rosas. *Dynamic Influences of Wind Power On the Power System*. Ph.D. thesis, Technical University of Denmark, 2003.

[75] Mark Rothleder and Clyde Loutan. Chapter 6 - case study-renewable integration: Flexibility requirement, potential overgeneration, and frequency response challenges. In Lawrence E. Jones, editor, *Renewable Energy Integration (Second Edition)*, pages 69 – 81. Academic Press, Boston, second edition edition, 2017.

[76] Semaria Ruiz, Julián Patiño, and Jairo Espinosa. Load Frequency Control of a Multi-area Power System Incorporating Variable-speed Wind Turbines. In *Conference Proceedings of XVII LATIN AMERICAN CONFERENCE IN AUTOMATIC CONTROL*, pages 447–452, Medellín, Colombia, 2016.

[77] Semaria Ruiz, Julian Patino, and Jairo Espinosa. PI and LQR controllers for Frequency Regulation including Wind Generation. *International Journal of Electrical and Computer Engineering (IJECE)*, 8(6), 2018.

[78] Semaria Ruiz, Julian Patino, Alejandro Marquez, and Jairo Espinosa. Optimal design for an electrical hybrid microgrid in Colombia under fuel price variation. *International Journal of Renewable Energy Research*, 7(24):1535–1545, 2017.

[79] Hadi Saadat. *Power system analysis*. PSA Pub, United States, 2010.

[80] Peter W Sauer and M. A Pai. *Power system dynamics and stability*. Stipes Publishing L.L.C., Champaign, IL., 2006.

[81] Hamed Shakouri G. and Hamid Reza Radmanesh. Identification of a continuous time nonlinear state space model for the external power system dynamic equivalent by neural networks. *International Journal of Electrical Power & Energy Systems*, 31(7-8):334–344, September 2009.

[82] Jae Woong Shim, Youngho Cho, Seog-Joo Kim, Sang Won Min, and Kyeon Hur. Synergistic Control of SMES and Battery Energy Storage for Enabling Dispatchability of Renewable Energy Sources. *Applied Superconductivity, IEEE Transactions on*, 23(3):5701205–5701205, June 2013.

[83] Sigurd Skogestad. *Multivariable feedback control : analysis and design*. John Wiley, Chichester, England Hoboken, NJ, 2005.

[84] Peter Sorknaes, Anders N. Andersen, Jens Tang, and Sune Strom. Market integration of wind power in electricity system balancing. *Energy Strategy Reviews*, 1(3):174 – 180, 2013. Future Energy Systems and Market Integration of Wind Power.

[85] T. Strasser, F. Andren, J. Kathan, C. Cecati, C. Buccella, P. Siano, P. Leitao, G. Zhabelova, V. Vyatkin, P. Vrba, and V. Marik. A Review of Architectures and Concepts for Intelligence in Future Electric Energy Systems. *Industrial Electronics, IEEE Transactions on*, 62(4):2424–2438, April 2015.

[86] Goran Strbac, Anser Shakoor, Mary Black, Danny Pudjianto, and Thomas Bopp. Impact of wind generation on the operation and development of the {UK} electricity systems. *Electric Power Systems Research*, 77(9):1214 – 1227, 2007. Distributed Gene-

ration.

[87] Sven Creutz Thomsen. *Nonlinear control of a wind turbine, ME Thesis*. PhD thesis, Technical University of Denmark, 2006.

[88] Pieter Tielens and Dirk Van Hertem. The relevance of inertia in power systems. *Renewable and Sustainable Energy Reviews*, 55:999 – 1009, 2016.

[89] N.R. Ullah, T. Thiringer, and D. Karlsson. Temporary Primary Frequency Control Support by Variable Speed Wind Turbines -Potential and Applications. *Power Systems, IEEE Transactions on*, 23(2):601–612, May 2008.

[90] F. Valencia, J.D. López, J.A. Patiño, and J.J. Espinosa. Bargaining Game Based Distributed MPC. In Jose M. Maestre and Rudy R. Negenborn, editors, *Distributed Model Predictive Control Made Easy*, volume 69 of *Intelligent Systems, Control and Automation: Science and Engineering*, pages 41–56. Springer Netherlands, 2014.

[91] F. Valencia, J. Patino, and J. Espinosa. A performance comparison for wind power integration into the grid system. In *Alternative Energies and Energy Quality (SIFAE), 2012 IEEE International Symposium on*, pages 1–5, Barranquilla, Colombia, October 2012.

[92] Felipe Valencia, Julian Patino, Jose David Lopez, and Jairo Espinosa. Game Theory Based Distributed Model Predictive Control for a Hydro-Power Valley Control. In *13th IFAC Symposium on Large Scale Complex Systems: Theory and Applications 2013*, pages 538–544, Shanghai, China, July 2013. Xi, Yugeng.

[93] S. Vesti, J. A. Oliver, R. Prieto, J. A. Cobos, and T. Suntio. Simplified small-signal stability analysis for optimized power system architecture. In *2013 Twenty-Eighth Annual IEEE Applied Power Electronics Conference and Exposition (APEC)*, pages 1702–1708, March 2013.

[94] K. V. Vidyanandan and N. Senroy. Primary frequency regulation by deloaded wind turbines using variable droop. *IEEE Transactions on Power Systems*, 28(2):837–846, May 2013.

[95] Hao Wang, Zhenlin Xu, Zhijie Li, Zhe Shang, and Haihua Zhang. Analysis of electric power steering control based on S/T method. In *Fifth World Congress on Intelligent Control and Automation (IEEE Cat. No.04EX788)*, volume 1, pages 582–585 Vol.1, June 2004.

[96] Huanhai Xin, Yun Liu, Zhen Wang, Deqiang Gan, and Taicheng Yang. A New Frequency Regulation Strategy for Photovoltaic Systems Without Energy Storage. *Sustainable*

Energy, IEEE Transactions on, 4(4):985–993, October 2013.